FACULTY OF TECHNOLOGY

THE VALIDATION AND USE OF A PREDICTIVE GEOMETALLURGICAL MODEL IN PLANT PROCESS DESIGN

Danish Bilal

MASTER'S PROGRAM IN GEOSCIENCES

Master's thesis

July 2021

ABSTRACT

The validation and use of a predictive geometallurgical model in plant process design

Danish Bilal

University of Oulu, Mineral Resources and Sustainable Mining

Master's thesis, July 2021

Maria Sinche Gonzalez

Geometallurgy is more often used for a concentrator plant design. Geometallurgy determines the metallurgical response of ore before the ore is feed to a plant. In a processing plant, the feed keeps changing due to the heterogeneity of ore deposits. There is ore variability in different parts of a deposit, so the optimum blending is critical to provide a constant feed. The study of different blends enables to predict the plant performance.

The thesis' main objective is to study the effect of ore variations and blends on flotation performance. The productivity of HSC Chemistry ®'s flowsheet simulation module for the prediction of flotation kinetics for blends, is studied. The second objective is the investigation of the effect of ore pre-sorting on flotation kinetics.

This thesis work is conducted using four samples from Sotkamo Silver Oy: malmi, sorter feed, sorter product, and ore 60. The experimental part includes crushing, grinding, sample splitting, grinding calibration tests, flotation tests for each sample, simulation of flotation tests, blends preparation, blend flotation tests and simulation of blend flotation.

In terms of grindability, the sorter feed and sorter product samples are similar. The specific grinding energy of the malmi is 10% less than the sorter feed and sorter product. Ore 60 is the softest in terms of grindability. Both galena and sphalerite in the Malmi sample are oxidized, while Ore 60 has oxidized more completely as compared to the malmi. Sorter product is least oxidized while sorter feed is slightly higher oxidized than sorter product. Sorter feed and sorter product are similar in terms of flotation kinetics, having similar recoveries. Malmi sample also has good recoveries of galena and dyscrasite. Ore 60 has the lowest recovery of galena and the highest recovery of pyrite.

The flotation in ore 60 is complex due to oxidation and the presence of slimes. The experimental and simulated recoveries of blends are close to each other. The blend of malmi and sorter product resulted in higher experimental grades of valuable minerals and lower grades of gangue than the simulated grades. The blends of ore 60 with malmi and sorter product have a higher experimental grade of gangue and lower experimental grade of ore minerals than simulated grades. The predictivity of simulation is close to the experimental results; hence HSC's simulation module tool is productive to predict the kinetics of blends.

Keywords: Geometallurgy model, simulation, blends, flotation, Taivaljärvi deposit, Plant design

FOREWORD

This thesis was carried out under the supervision of Metso Outotec, from February 2021 to July 2021. The experimental work was carried out at Metso Outotec Research Center Pori from February 2021 to May 2021.

First of all, I would like to thank my supervisors: Maria Sinche Gonzalez, PhD from the University of Oulu, and Jussi Liipo PhD from Metso Outotec, for supervision, support, and guidance throughout the whole thesis work. I want to thank Kaisa Kaski, Senior Process Metallurgist from Metso Outotec, for sharing her advice throughout the thesis work. I want to thank Erdem Ozdemir, Metallurgist from Metso Outotec Research Center, for supporting and guiding the experimental part of the thesis. I want to pay special thanks to Hannu Heiskari, Research, and Process Support Engineer at Metso Outotec Research Center Pori, for his support and guidance for mergan grindability tests. I want to thank Caroline Izart, Specialist, Modeling and Simulation from Metso Outotec, for HSC simulation training. The advice and support for simulation from Rodrigo Grau DSc (Tech) are appreciated. The lab technicians at Metso Outotec Research Center Pori are thanked for their support during the experimental part.

I want to thank my family and friends for their support and motivation during this thesis.

Finally, I want to thank Eine Pöllänen, Jarmo Huuskonen and Erkki Kuronen from Sotkamo Silver Oy for providing the samples and process information for this study

Oulu, 28.06.2019 Danish Bilal

TABLE OF CONTENTS

LIST OF ABBREVIATIONS

Ag	silver
Au	Gold
AWi	Macpherson autogenous work index
BWi	Bond ball mill work index
CaO	calcium oxide
Ccp	chalcopyrite
Cu	copper
Dys	dyscrasite
Fe	iron
GCT	geometallurgical comminution test
Gn	galena
ICP	Inductively coupled plasma
ICP-MS	Inductively coupled plasma mass spectroscopy
ICP-OES	Inductively coupled plasma optical emission spectroscopy
K_{max}	maximum flotation rate constant
NaCN	Sodium cyanide
NSG	non-sulfide gangue
P80	80% passing particle size
Pb	lead
pH	hydrogen potential
Py	pyrite
RC	rougher concentrate
RF	rougher flotation
R_{inf}	infinity recovery
RPM	revolutions per minute
RT	rougher tailings
RWi	bond rod mill work index
S	sulfur
Sp	sphalerite
SPI	sag power index
XRD	x-ray diffraction
Zn	zinc

ZnSO4 Zinc sulfate

1 INTRODUCTION:

Geometallurgy combines geological and metallurgical information to create a predictive geometallurgical model for a mineral processing plant (Lamberg, 2011). It is critical for the effective utilization of mineral reserves/resources and risk management. The use of geometallurgy for the design of process plants is becoming more and more common. Due to lower grades and more complexity of the new ore deposits, there is no room for errors in a process chain, and more efficient utilization of the ore body is critical. It provides comprehensive knowledge of the ore body, including the metallurgical response. It also enables effective utilization of the ore body. Forecasted metallurgical performance helps to tune the process plant accordingly. Comprehensive knowledge of the ore body enables controlled mining and better-controlled mineral processing. Geometallurgy makes room for implementing new technologies and helps in economic optimization and lower risk in the process chain.

A geometallurgical program contains the following steps shown in Figure 1. Lamberg, (2011) modified the steps after (Bulled & McInnes, 2005, David, 2007 and Dobby et al., 2004). A geometallurgical program starts with the collection of geological data. Geological data contains drilling, outcrop study, drill core logging, chemical analysis, and other analysis. The second step is the collection of metallurgical samples with the help of geological data. In the third step, the metallurgical samples are tested in the laboratory to get metallurgical performances. In the fourth step, the geological data and metallurgical data are used to develop geometallurgical domains. The fifth step is the development of miasmatical relationships to derive metallurgical parameters over the geometallurgical domains. The sixth step is developing a process model in which the models for unit operation are derived using metallurgical parameters. In the seventh step, the plant simulation models are generated based on the process model. The last step is the calibration of the models.

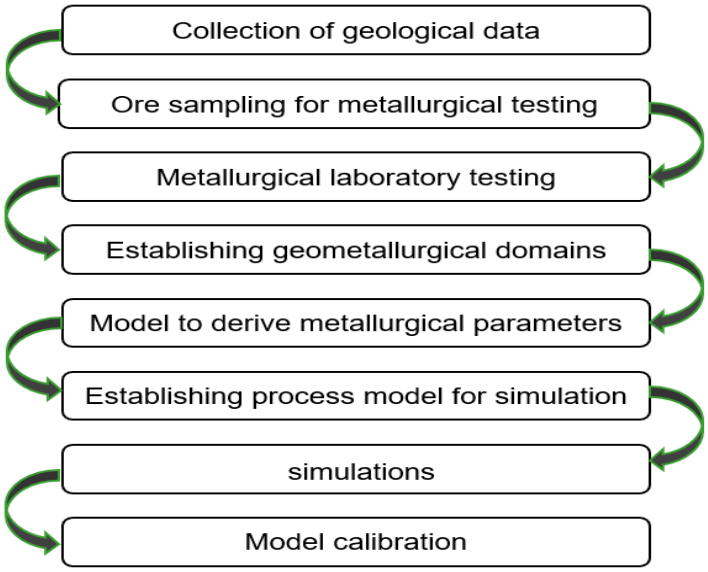

Figure 1 Steps of a geometallurgical program, modified from (Lamberg, 2011)

Lamberg, (2011) proposed a particle-based geometallurgical model which considered particles and minerals from beginning to end, shown in Figure 2. This particle-based model contains a geological model, particle breakage model, and unit process models. The geological model provides quantitative mineralogy of ore blocks. A particle breakage model describes the type of particles generated during the breakage of different ore blocks. While the unit process models forecast the behavior of particles and minerals under other unit processes.

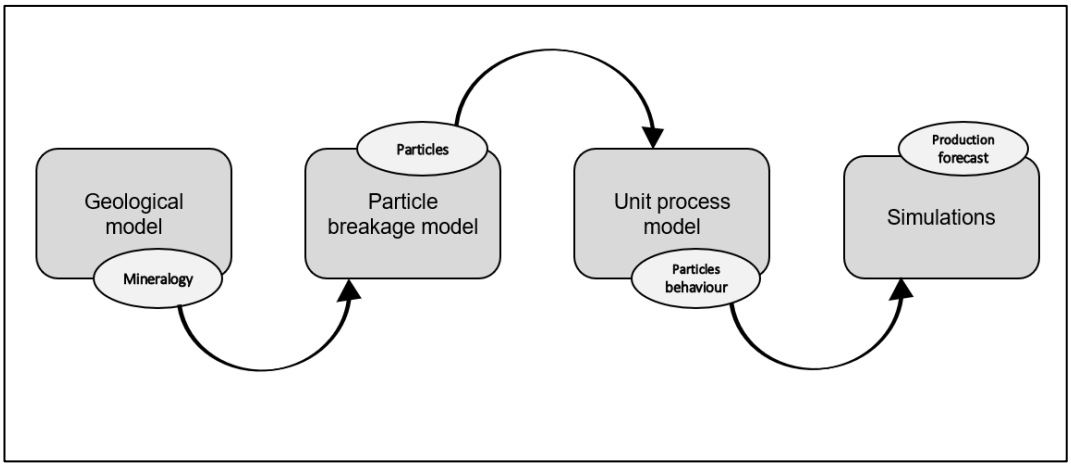

Figure 2 Particle-based geometallurgical model (Lamberg, 2011)

This thesis is focused on the effect of ore variations and ore blends on metallurgical performance by using experimental test work and HSC simulations. The main research questions are:

- Effect of ore variations and blends on flotation performance, can be simulated?
- May the product of sorting before flotation bank affect flotation kinetics?

This thesis work is conducted using four samples and their blends from Sotkamo Silver Oy. These four samples include main ore, sorter feed, sorter product, and oxidized ore60. The Sotkamo Silver's rougher and scavenger of Pb/Ag flotation circuit are targeted for this study.

The objective of the thesis is to know the effect of ore variation and ore blends on a processing plant. The feed to a processing plant is not uniform due to variation in an orebody. The low-grade ore is usually processed with a high-grade ore in the form of blends. It may affect comminution and separation processes. So, it is critical to know the metallurgical response to ore variation and ore blends. In this thesis, the flotation response is studied for different ore types and blends.

The experimental and simulation work is validated. The grinding calibration curves are validated by conducting one extra grinding test. The experimental P80 of the additional grinding test is compared to modeled P80. Flotation results are validated by comparing back-calculated grades of elements and minerals with analyzed feed analysis. Blend flotation results are validated similarly. Simulation results are validated by comparing with the experiment blends flotation results.

The experiment work of this thesis started with sample preparation. Grinding calibration tests are conducted to find grinding time for the required P80. In addition, each ore type's grindability tests were conducted using mergan grindability test method (Niitti, 1973). The mergan test method is based on wet batch grinding and measurement of energy consumption and mill revolution. The mergan test can be used to calculate the operating work index and approximation to the bond work index (Heiskari et al., 2019). Reference flotation tests are conducted for each ore type and their blends. The concentrate and tailings are analyzed using Inductively coupled plasma (ICP) analysis. Inductively coupled plasma optical emission spectroscopy (ICP-OES) was used to analyze the main elements and inductively coupled plasma mass spectroscopy (ICP-MS) and ICP-OES are

used for Ag analysis, depending on the silver content in the sample. The elemental data from ICP analysis is converted into modal mineralogy using HSC-Geo module, and HSC-Sim module is used for the simulation of reference flotation and blends flotation results.

2 LITERATURE REVIEW:

2.1 Taivaljärvi Zn-Pb-Ag-Au ore

2.1.1 Regional Geology

The Taivaljärvi Zn-Pb-Ag-Au ore is located in the Archean area of eastern Finland and the southern part of the greenstone belt. Greenstone belt is divided into Suomussalmi, Kuhmo and Tipasjärvi belts. The Taivaljärvi area is the part if Tipasjärvi belt (Papunen et al., 1989). The Geological map of Tipasjärvi is shown in Figure 3.

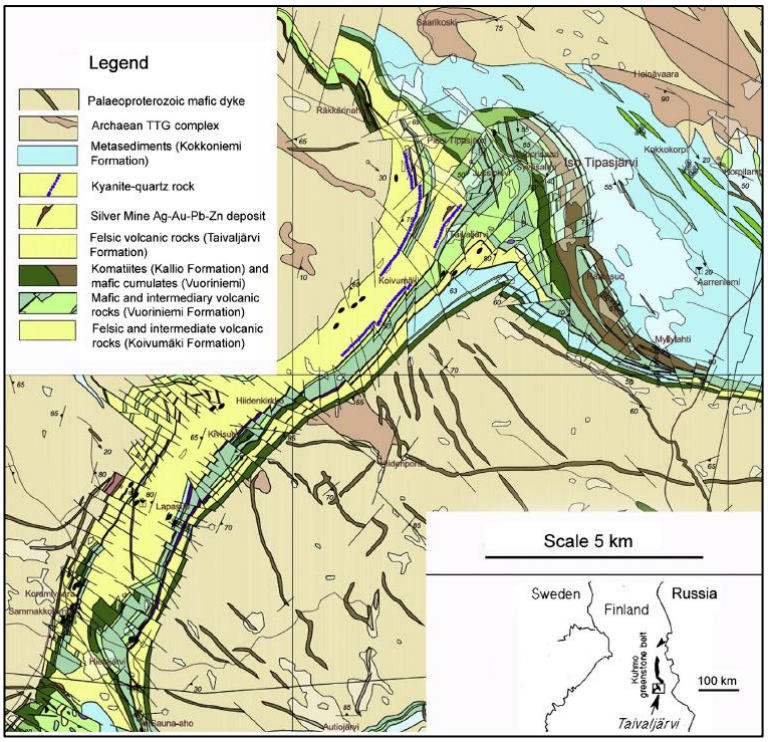

Figure 3 Geology of Tipasjärvi and location of the Taivaljärvi area (Lindborg et al., 2015)

The Archean granitoid area around the greenstone belt is quite heterogenous. This area varies from stromatic and nebulitic migmatitic gneisses to discrete felsic plutons. The granodiorite-granite associations and tonalite-trondhjemite-gneiss surround the Tipasjärvi area and are considered the basement of greenstone belt, shown in Figure 4. It is observed that the bulk of granitoids is younger than the greenstone belt. The study shows short crustal residence time for granitoids. The greenstone area was deformed and metamorphosed in many phases, having Proterozoic as the younger phase. Due to

metamorphism, the rock-forming minerals are metamorphic, but the primary textures are still preserved and can be observed. The greenstone belt is composed of 80% of mafic, ultramafic, and felsic volcanic rocks. The remaining 20% include mica gneisses, metasedimentary rocks, black schist, banded iron formation, and mafic-ultramafic intrusive rocks.

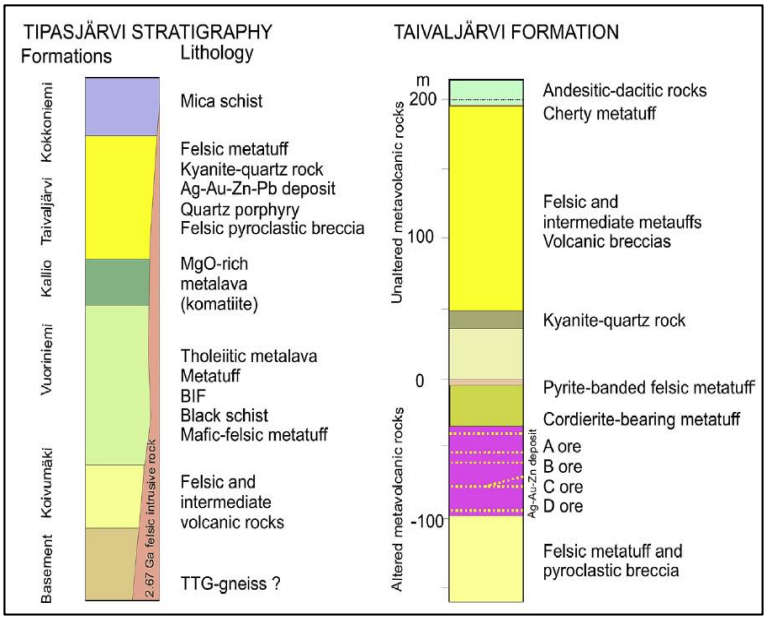

Figure 4 Stratigraphy of Tipasjärvi belt and lithologic succession of Taivaljärvi formation (Lindborg et al., 2015)

The Tipasjärvi belt is subdivided into four lithostratigraphic formations, shown in Figure 4. This scheme is based on field observations and interpretation of successive deformation phases. The Koivumäki formation is the lowermost and composed of felsic metatuffs. The Taivaljärvi felsic volcanics are also included in the Koivumäki formation. The Vuoriniemi formation overlies the Koivumäki formation and varies lithologically from tholeiitic metatuffs and lavas to graphitic black schist, banded iron formation, dacitic metatuffs, and mafic metalavas. The Kallio formation overlies the Vuoriniemi formation and is composed of ultramafic komatiitic lavas. The Kokkoniemi formation is the uppermost and composed of mica schist, weathering product of underlying volcanic rocks. The Koivumäki formation is dated as 2828 ± 3 Ma. The Kokkoniemi sedimentary unit is dated as 2.75Ga.

The Taivaljärvi formation has rocks that vary from massive quartz-porphyries, volcanic breccias, and layered felsic tuffs. The folding sequence of Taivaljärvi is sub-vertical to

steeply dipping east. Drilling data indicated the younger direction eastward. Sotkamo Silver ore is located in the middle of volcanic succession. Several quartz veins characterize the ore zone.

Geochemical and mineralogical studies indicated potassic and magnesian hydrothermal alterations. The mineralized zone has a quartz-kyanite layer about 100m above. K-Mg alteration is found in the felsic rock, which occurs between silver deposit and layer of quartz-kyanite. The intense isoclinal folding and over-thrusting cause the bringing of old greenstone rock into the upper contact zone. The basal contact of TTG gneisses and Taivaljärvi formation is not outcropped, hence studies through drilling data.

2.1.2 The ore deposit

The subcrop is 500m long and 5-110m wide. The dipping of the ore body is 65-degree NE and plunges 60 degrees to S-SW. The depth of the ore body is 600m. The GTK's deep geophysical surveys indicated that the mineralization continues till 2km depth (Niskanen, 2013). The model is demonstrated in Figure 5.

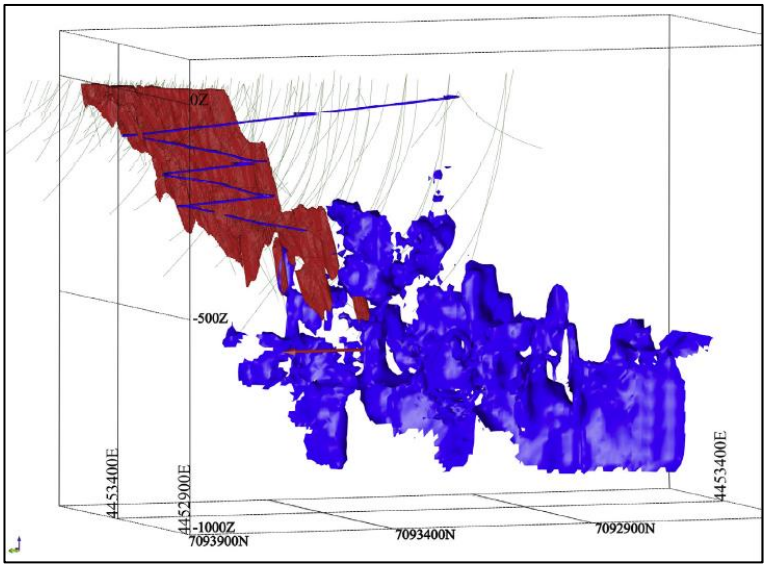

Figure 5 Taivaljärvi Silver mien deposit model, Red=measured, indicated, and inferred resources. Cyan= extension of mineralization. Blue=mine decline and green=drill hole traces (Niskanen, 2012)

Meyer & Davies (2012) completed the feasibility studies in May 2012. Afterward, the mineral resources were updated according to the Australian Code to report exploration results, mineral resources, and ore reserves (JORC-code 2012). The updated mineral resources and reserves on 31st December 2020 are shown in Table 1.

Table 1 Mineral resources and ore reserves of Sotkamo Silver Oy (Sotkamo.com)

Mineral Resources					
	Tons (Kt)	Ag (g/t)	Au (g/t)	Pb (%)	Zn (%)
Measured	2351	79	0,21	0,29	0,63
Indicated	3385	79	0,23	0,29	0,63
Total (Measured + indicated)	5736	79	0,22	0,29	0,63
Inferred	4220	61	0,17	0,2	0,47
Ore Reserves					
Proved	937	109	0,33	0,32	0,67
Probable	922	148	0,55	0,62	1,33
Total (Proved + Probable)	1859	129	0,44	0,47	1

Papunen, et al. (1989) indicated the heterogenous mineralization. It comprises four parallel layers with different composition and metal ratios. These mineralized layers are classified as D, C, B, and A layers, shown in Figure 6. Layer A and B contain mineable ore.

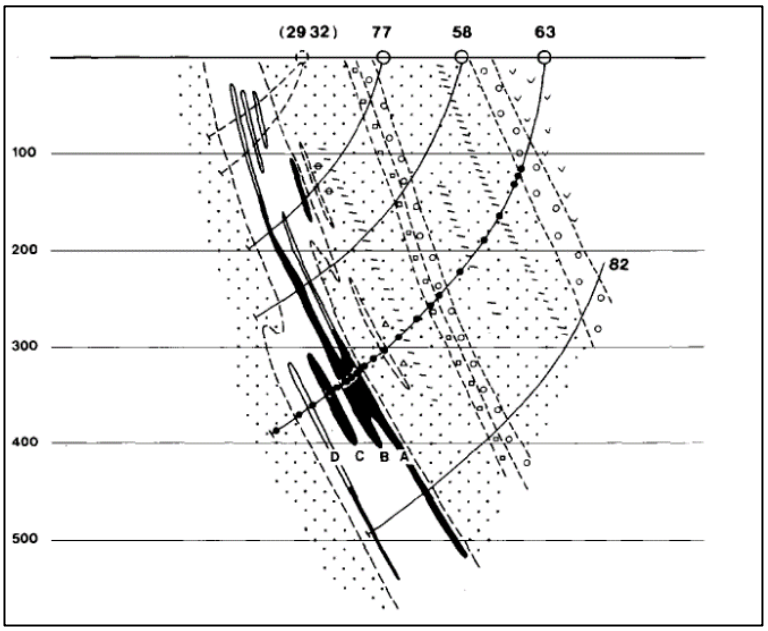

Figure 6 Cross section of the Taivaljärvi deposit (Papunen et al., 1989)

Layer A is the uppermost layer with 4-8m thickness. At a depth of 150-200m, there is a discontinuity in layer A. This layer contains an abundant amount of ankerite and quartz veins. The texture of the body is banded, Pb-Zn rich, and has a high amount of iron

sulfides. This body is rich in silver but has a lower amount of Pb and Zn than other ore bodies.

Layer B is relatively continuous and has a depth of up to 500m. The thickness varies between 4-8m. Galena and sphalerite occur as banded dissemination together with pyrite, pyrrhotite in quartz ankerite veins. The host rock is composed of banded quartz-sericite schist with a higher amount of quartz-carbonate veins.

Layer C is not widespread and has an average of 5m thickness. The sulfides have a texture of thin bands. Layer D has 5m thickness as well and is the lowermost layer and abundant in sulfide minerals. (Papunen et al., Tuokko, 1989)

2.1.3 Ore mineralogy

The ore mineralogy of Taivaljärvi is described by Papunen et al. (1989). The ore minerals include dyscrasite, freibergite, pyrargyrite, native silver, gold, galena, sphalerite, and chalcopyrite. The other identified minerals include pyrite, arsenopyrite, pyrrhotite, covellite, cubanite, gudmundite, acanthite, miargyrite, freieslebenite, bournonite, scheelite, native antimony, and native bismuth. The grain size of Ag-bearing minerals varies between 0.01-0.1mm, while the grain size of common sulfide minerals varies between 0.1-0.5mm. The galena and silver minerals occur in quartz-carbonate veins and band and are most abundant in the uppermost ore zone. The ore has a 5-8% sulfide content, and pyrite and pyrrhotite contain more than 50% of the sulfides.

Pyrite, pyrrhotite, and arsenopyrite are the main iron minerals. Pyrite is dominant and occurs in all types of ore in the form of euhedral cubes. Pyrrhotite occurs in quartz-ankerite veins, C and D ores. Arsenopyrite rarely occurs in the form of banded disseminations.

Sphalerite occurs throughout the deposit. It appears as bands with iron sulfide and galena. In ankerite veins, sphalerite occurs together with galena and other ore minerals.

Galena occurs as inclusions in ankerite and as bands in iron sulfides, chalcopyrite, and sphalerite. Galena also contains inclusions of silver minerals, and silver content in galena varies between 0.01-1.7%.

Chalcopyrite also occurs throughout the deposit with a grain size that varies between 0.02-0.1mm. It occurs as intergrowth with silver minerals in a silver-rich part of the ore. Chalcopyrite also occurs together with pyrrhotite, galena, and sphalerite in calc-silicate layers. Chalcopyrite may also include silver up to 6.8%.

Freibergite and dyscrasite are the two most common silver minerals. Freibergite occurs together with galena and dyscrasite as disseminated and intergrowth in the quartz ankerite veins. The grain size varies between 0.03-0.06mm. Silver replaces copper in the freibergite tetrahedrite series. Dyscrasite occurs together with freibergite, galena, chalcopyrite, and native antimony in quartz ankerite veins. Grain size varies between 0.01-0.1mm, and it appears throughout the deposit.

Freieslebenite is a trace mineral found in A and B ores as inclusions in galena. Silver-copper replacement is also found in this mineral.

Pyrargyrite occurs as a thin coating on the fractures of galena ankerite quartz veins. It also appears as inclusions in the galena boundaries. The grain size varies between 0.01 to 0.03mm.

Native silver and alloys with gold and antimony are also found and considered as accessories. Alloys exist together with galena and other silver minerals. These alloys also occur as fracture fillings of other minerals. The grain size varies between 0.01-0.05mm. (Papunen et al., 1989).

2.1.4 History of the mining

This Zn-Pb-Ag-Au mineralization was indicated in 1980 by researchers from the University of Oulu. The research group found several Ag-Au-Zn boulders along the lakeside. They conducted percussion drilling and bedrock sampling. The drilling results indicated a 500m mineralization up ice direction. Kajaani Oy secured the mineral rights in 1980. A diamond drilling campaign started during 1981-1989. This drilling covers the ore body 40-100m wide, 500m long, and 650m below the surface. A joint venture of Kajaani Oy and Outokumpu Oy resulted in the construction of a 2,6km long and a 350m long ventilation shaft between 1988-1990. The feasibility study was completed in 1991, and due to lower commodities prices, the project was put down. Sotkamo silver applied for the claim reservation in 2005. Sotkamo Silver Oy also applied for the claims over the

silver deposit in 2006, and the claims were issued in 2007. Since 2006 the Sotkamo Silver Oy brought this deposit to production in 2019 (Lindborg et al., 2015).

2.1.5 Mineral processing and metallurgy

Lab-scale processing tests were conducted during the 1980s at GTK MinTek, former Outokumpu laboratory. Metallurgical research and mineral processing tests were conducted during the feasibility studies in 1991. It has been reported that the ore is amenable to using standard flotation techniques. In early 2007 GTK conducted other processing tests to upgrade metallurgical tests and to make processing flowcharts for Sotkamo Silver Oy. Additional pilot plants tests were conducted by GTK in 2011 (Lindborg et al., 2015)

The test results revealed that the ore is amenable to flotation. Pb-Ag and Zn concentrate can achieve acceptable recoveries and grades. These tests were performed at P80 (80% passing) of 75 µm. It was concluded that gravity processing has no benefits over flotation. In a locked cycle, the achieved Ag and Au recoveries were 76.2 and 90%. About 7% silver was recovered in zinc concentrate. The recovery of Zn in zinc concentrate was 90.8% at a grade of 51% Zn. Pyrite concentrate aimed to reduce the sulfur content in the tailing for beneficial tailings disposal. The pyrite concentrate has a 6% Ag recovery. These processing details were updated in the feasibility studies. The final processing flowsheet is based on crushing, grinding, flotation, filtration scheme. The suggested mining method was sublevel stopping and backfill (Lindborg et al., 2015).

2.2 Comminution

Comminution is the process of particle size reduction by blasting, crushing, and grinding. Comminution is used to liberate ore minerals from gangue minerals and reduce the particle size to make them suitable for downstream separation processes. Each separation technique has an optimum particle size for efficient work, shown in Figure 7 (Drzymala, 2007).

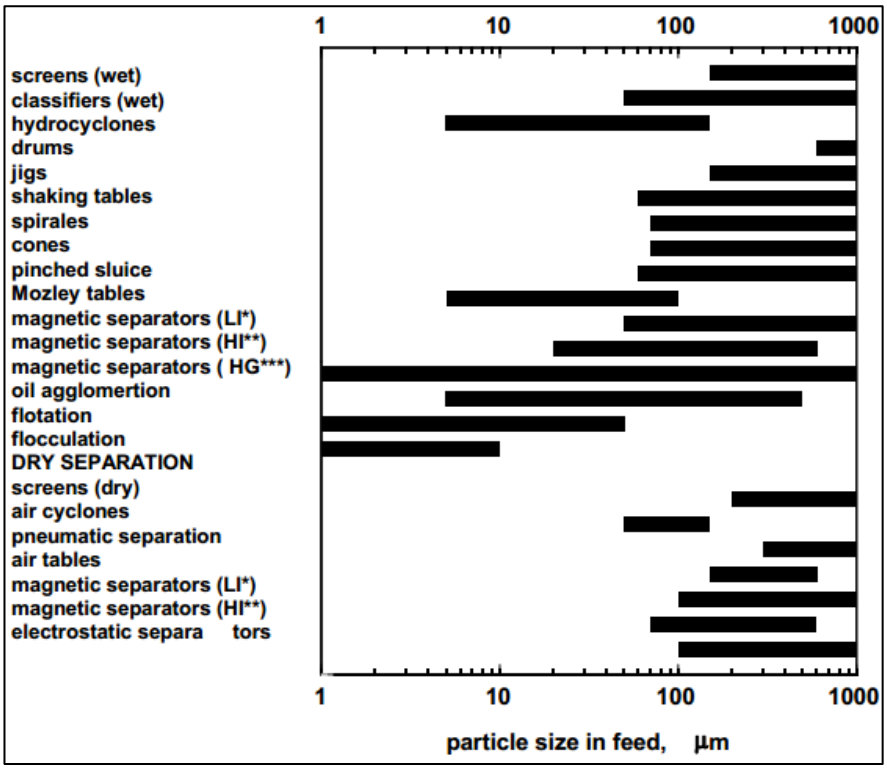

Figure 7 Size ranges for optimum processing for each separation technique (Drzymala, 2007)

The comminution process can be challenging for low-grade and complex ores. The typical interlocking types are shown in Figure 8 (Kelly, 1982). Under-grinding causes liberation issues while over-grinding causes more energy consumption and production of slimes which can cause difficulties in downstream processes. There is always a requirement for optimum grinding to keep a balance between liberation, energy, and particle size.

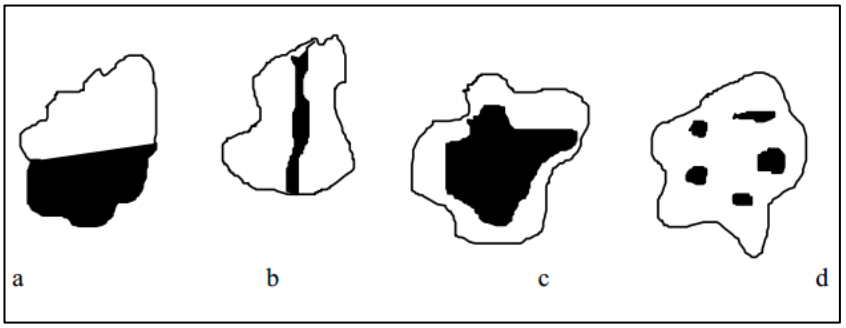

Figure 8 Types of interlocking of ore minerals in gangue minerals, Black=ore mineral, White= gangue mineral (Kelly, 1982)

The particle size P80 (80% passing) can be achieved using comminution tests. A comparison between multiple comminution test methods was made by (Mwanga et al.,

2015), based on geometallurgical approach, shown in Table 2. He also concluded that for a geometallurgical program, none of the previous comminution tests fulfill all the requirements. He used a small lab ball mill and different coefficients to downscale the Bond ball mill process, technique names as geometallurgical comminution test. Bond ball mill tests are widely used due to their repeatability. The bond work index helps in the simulation, modeling, and designing of new grinding circuits.

Table 2 Comparison of comminution test methods based on geometallugical approach, (1) Simplicity, (2) repeatability, (3) sample preparation, (4) time exposure and cost, (5) sample amount, (6) parameters can be used in modelling and simulation, (7) can be extended to mineral liberation (Mwanga et al., 2015)

Fracture Test Method	Suitable Criteria for Geometallurgical test (-=adverse, +=acceptable, +=advantage						
	1	2	3	4	5	6	7
Unconfined compressive strength test	+	0	-	0	+	-	-
Point load test	+	0	0	0	+	-	-
Brazilian test	+	0	-	0	+	-	-
Drop weight test	0	0	-	-	-	+	0
Ultra Fast load cell test	-	0	0	0	-	+	0
Twin pendulum test	-	-	0	0	0	+	0
Split Hopkinson test	-	0	-	-	-	0	0
Rotary breakage test	-	+	0	0	0	+	0
Bond ball mill test	0	+	0	0	-	+	+
Bond rod mill test	0	+	0	0	-	+	+
Single pass test e.g. Mergan mill	+	+	0	-	-	+	+

2.2.1 Comminution indices

Comminution indices are the outcome of the comminution tests and can be used quantitatively in simulation and modeling. There are four most common indices e.g., bond ball mill work index, bond ball mill work index, sag power index, and Macpherson autogenous work index.

Bond ball mill work index (BWi) provides the measure of energy (kWh) used in a ball mill to grind one ton of material. The unit is kWh/t, and it can be calculated using the bond ball mill test (Bond, 1961). Bond work index can be used in simulation, modeling, and designing of grinding circuits. The bond work index values all around the word (ARMC database) show an average of 14.6 kWh/t and a median of 14.8 kWh/t (Mcken & Williams, 2005).

The bond rod mill work index (RWi) provides the energy consumed to grind one ton of material in a rod mill. Bond (1961) referred to bond rod mill work index as resistance to crushing and grinding. Mcken & Williams (2005) state that the average and median values are 14.8 kWh/t for previous bond rod mill tests conducted (ARMC database). The Bond rod work index can also be used to simulate, model, and design rod mills.

Sag power index (SPI) measures the time required for sample reduction from P80 of 12.7mm to P80 of 1.7mm, developed by John Starkey (Starkey & Dobby, 1996). High values of SPI indicated harder ore and lower values indicate a softer ore. The Spi was transformed to kWh/t and used by MinnovEX for designing (Dobby et al., 2001).

Macpherson autogenous work index (AWi) is measured from Macpherson autogenous grindability test, developed by MacPherson & Turner (1978). This grindability test is based on a small-scale AG/SAG steady-state mill. AWi is calculated by using power draw, particle size distribution, and throughput. The typical values for AWi are in the range of 3-7 (Mcken & Williams, 2005).

2.2.2 Mergan Grindability test method

Mergan test method was developed by Niitti (1973) in Outokumpu. The mergan test method is a wet batch grinding test method. There are aspects of the mergan tests to follow: (Niitti, 1973)

- The energy consumption is measurable
- The test is performed till the final fineness as required by the industrial need.
- The test procedure is simple and fast.

In this method, the mill size is 268 x 268 mm. The speed can vary between a wide range. The energy consumed by the mill is constantly measured through torque measurements. The mill revolution speed is also continuously measured. The optimum mill charge includes 22Kg of steel balls. He also concluded that the efficient ball charge comprises 15 and 40mm balls. The pulp density is between 60-70% solids. The mill speed is 70% to the critical speed. (Niitti, 1973)

The mergan test requires a crushed feed of size -4mm. The particle size distribution is calculated using sieving, and surface area is calculated using rapid permeability analysis.

The energy is calculated directly from the mill. The material is then ground to the required fineness, and mill revolutions are noted. The grinding energy measured can be used to calculate the mergan work Index (W-Wi). The mergan work index can be calculated using the Equation below. (Niitti, 1973)

$$\boldsymbol{M - Wi = E_0\left(\frac{\sqrt{F80}}{\sqrt{F80}-\sqrt{P80}}\right)\sqrt{\frac{P80}{100}}}$$

Where M - Wi is mergan work index (kWh/t)

E_0 is Energy consumption (kWh/t)

The energy consumption during the mill revolution is found variable. At the start, the energy consumption is increased by up to 10% to the original value. The energy consumption tends to decrease after a couple of hundred revolutions, and after 2500 revolutions, the mill energy consumption levels to 20-35% lower than the original value. The variation in energy consumption is due to the friction condition inside the mill (Niitti, 1973).

The grinding energy is also dependent on the material ground. Wet grinding is 30-50% more efficient than dry grinding. It is also concluded that it is impossible to determine the wet grindability based on a dry grinding test. The mergan test should be carried out to the same grinding fineness as actual fineness required in the process (Heiskari et al., 2019).

2.3 Flotation

Flotation is a most versatile and vital separation technique that enabled the processing of complex, low-grade, and large tonnage ores. It is considered an improvement of the modern metallurgical era (Wills & Finch, 2016). Flotation is a physico-chemical process that uses the surface chemistry of the valuable and gangue mineral. The previous uncomical deposits became feasible due to flotation technology (Wills & Napier-Munn, 2005). In direct flotation, the valuable hydrophobic minerals are attached with air bubbles and rise to the top and collected in the froth, while hydrophilic minerals stay at the bottom. In a reverse-flotation, the unwanted gangue is floated while valuable mineral is depressed and stay at the bottom. Flotation was patented in 1906 and developed for the flotation of sulfide minerals. The scope is expended for the flotation of oxides and low-grade sulfide ores (Napier-Munn & Wills, 2005).

Flotation utilizes the difference in surface properties of the minerals. Reagents are used to modify the surface properties. Flotation involves solid, liquid, and gas phases. The particles float the top by attachment with the air bubbles, entrainment in the water, and entrainment between the particles. The recovery of flotation is dependent on the attachment of valuable minerals to the air bubble. The principle of flotation is shown in Figure 9. The air bubbles are released at the bottom of the container. The hydrophobic particles are attached with bubbles and rise to the top and collected in the froth during bubbles rise. The hydrophilic gangue stays at the bottom and is collected separately (Napier-Munn & Wills, 2005).

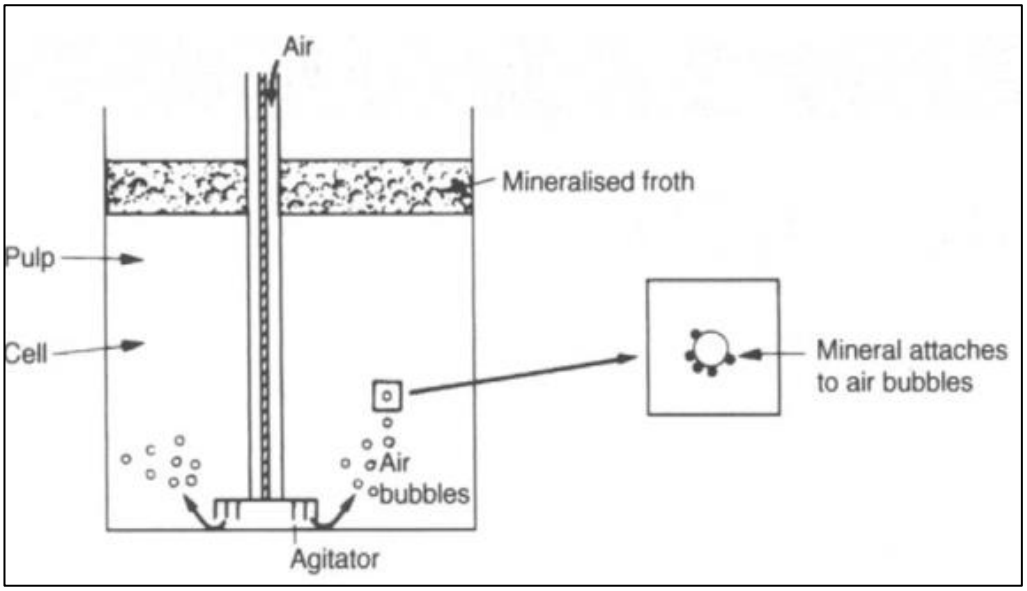

Figure 9 Principle of flotation (Napier-Munn & Wills, 2005)

All minerals do not have ideal surface properties; hence, flotation reagents modify the surface properties. The collectors are essential and widely used. The collectors are adsorbed to the mineral surface and make it hydrophobic. The frothers are used to create a stable froth. The regulators are used to control the pH and control the flotation process (Napier-Munn & Wills, 2005).

The collectors are used to achieve the required hydrophobicity of the minerals. The collectors are organic compounds and contain polar and non-polar parts. The polar part attaches to the mineral surface, and the non-polar part improves the hydrophobicity of the mineral, shown in Figure 10. The collectors are either ionizing or non-ionizing compounds. Ionizing collectors dissociate into ions in the water, while non-ionizing collectors are insoluble in water and cover the surface of minerals to make it hydrophobic.

The ionizing collectors are further classified into cationic and anionic collectors, depending on the ions produced. Cations produce a water repellent effect in the water and the polar group is based on pentavalent nitrogen (amines). Anionic collectors are further classified into oxyhydryl and sulphydryl. The polar group of oxyhydryl collectors contains organic and sulpho-acid anions. The sulphydryl collectors are widely used and contain bivalent sulfur in the polar group. The xanthates-sulphydryl collectors are famous for sulfide flotation. The classification of collectors is shown in Figure 11. The collector's concentration should be optimum for maximum recovery. Excessive concentration of a collector causes the formation of multilayers on the mineral surface, and hence the hydrophobicity and the mineral recovery decreased. The lower concentration does not make particles hydrophobic enough to be attached and recovered by the air bubbles (Napier-Munn & Wills, 2005).

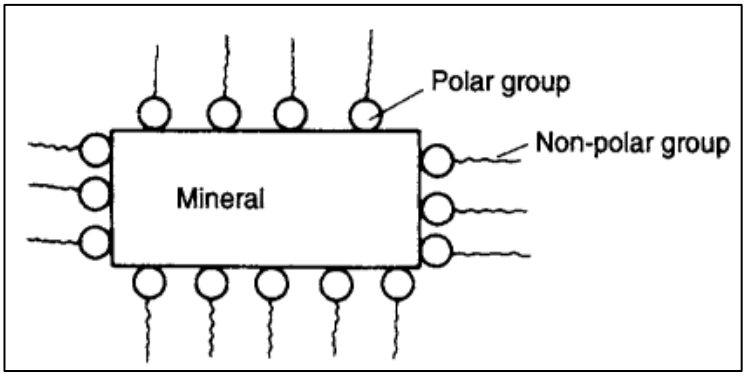

Figure 10 Adsorption of collect on a mineral surface (Napier-Munn & Wills, 2005)

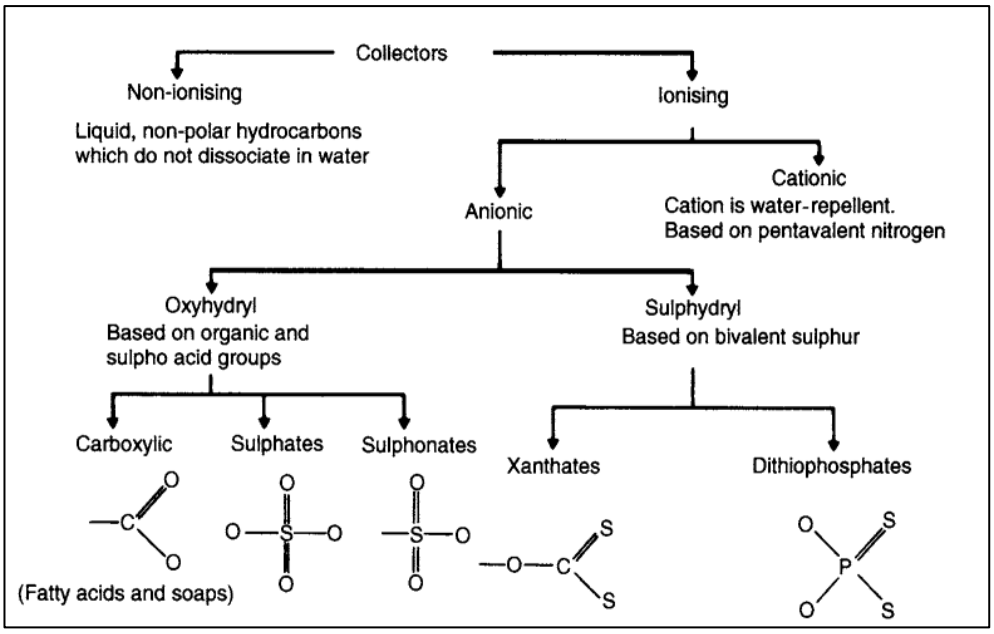

Figure 11 Classification of collectors (Napier-Munn & Wills, 2005)

The frothers are used for the stability of air bubbles and to make a stable froth. Stable froth is essential to reduce the entrainment of gangue minerals and to improve flotation kinetics. A frother should have enough stability to carry floated particles to a collecting launder. Frothers and ionic collectors are similar chemically, and some collectors also have a frothing effect, e.g., oleates are powerful frothers. The frothers are heteropolar organic reagents which are adsorbed at the air-water interface to stabilize air bubble. The non-polar part of the frothers is oriented towards air and the polar part towards the water, shown in Figure 12A. The frothers include one of the groups shown in Figure 12B. Natural frothers like pine oil are effective frothers, while many synthetic frothers are common in use due to their high stability (Napier-Munn & Wills, 2005).

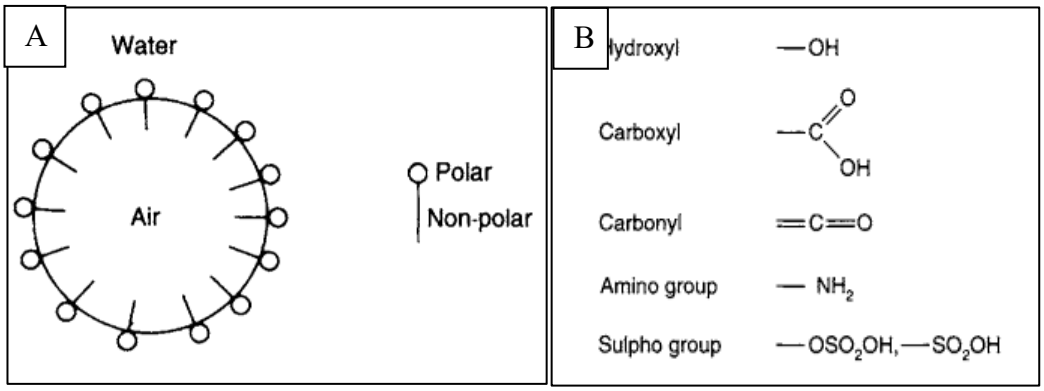

Figure 12 A = action of frother, B = Frother groups (Napier-Munn & Wills, 2005)

The modifiers are also called regulators, used to modify the action of a collector in a selective flotation. The modifiers include activators, depressants, and pH modifiers.

Activators are used to modify the mineral surface to ease the action of a collector. The activators are water-soluble and produce ions in water which alter the surface of the minerals. A typical example is the activation of zinc by copper in sphalerite flotation. Copper sulfate is used as an activating in sphalerite flotation. Copper sulfate is soluble in water and generates copper ions. The copper sulfate deposit on the mineral surface and then xanthates can efficiently react with copper, make sphalerite hydrophobic, and easily float. Depressants are used to create certain minerals hydrophilic and depress during a flotation. A natural depressant is very fine particles called slimes. Slimes cover the surface of a mineral and prevent the action of a collector and flotation. There are many types of depressants, e.g., inorganic and polymeric depressants. Zinc sulfate and cyanides are

more commonly used. Cyanide is toxic, expensive, and challenging in handling (Napier-Munn & Wills, 2005).

The pH plays a significant role during flotation. The stability of reagents and is pH-dependent. In a selective flotation, pH and reagent concentration play an important role together. An alkaline medium is the most suitable for flotation due to the stability of most collectors and the minimal corrosion effect to the flotation cells. pH regulators are cheaper and hence used in a significant amount to lower the concentration of collectors. A relationship between the concentration of the collector and pH value is shown in Figure 13 (Napier-Munn & Wills, 2005).

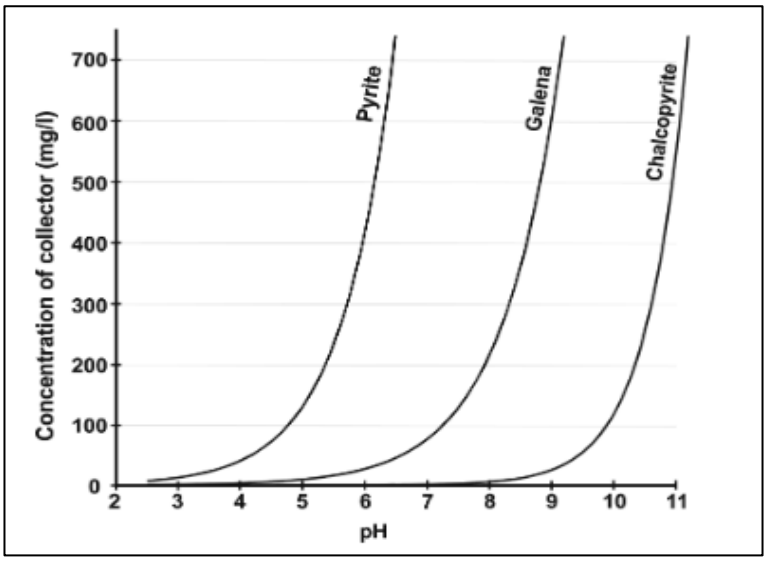

Figure 13 Relationship between the concentration of collector and pH for pyrite, galena, and chalcopyrite at constant [DTP−]/[OH−] (Zanin et al., 2019)

Lime is an effective and economic pH modifier used in selective flotation *(Zanin et al., 2019)*. Sodium cyanide (NaCN) is a commonly used depressant. Cyanide is toxic and effective; hence the concentration of cyanide used in flotation is significant for the economy and environment. A relationship between the concentration of NaCN and pH for different minerals is shown in Figure 14. Hence there should be an optimum balance between pH, reagents concentration, and flotation kinetics (Zanin et al., 2019).

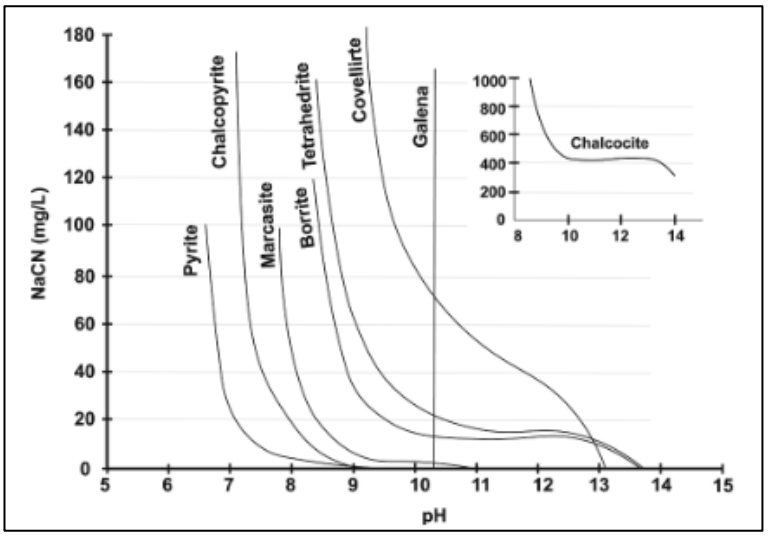

Figure 14 Relationship between NaCN and pH at 25 mg/L potassium ethyl-xanthate (Zanin et al., 2019)

2.4 Flotation of lead-zinc ores

Most of the world's lead-zinc deposits contain finely disseminated bands of galena and sphalerite with varying pyrite amounts (Bulatovic, 2007). Galena and sphalerite are the major ore minerals despite some trace minerals (cerussite, anglesite, marmatite, and smithsonite). Two-stage selective flotation is widely used to separate galena from sphalerite. As usually sphalerite is found in a significant percentage, the zinc and iron minerals are depressed in the first stage, and lead minerals are floated. In the second stage, sphalerite is activated by adding heavy metal ions in the lead tailings and floated. The metal ions replace zinc at the sphalerite surface. Then the activated surface reacts with collectors and makes sphalerite water repellent.

The flotation of galena usually takes place at a pH of 9-12. Lime as a cheaper and effective pH modifier, is used to control the alkalinity of the solution and maintain pH between 10-12. Lime helps to depress pyrite. The most effective depressants for the sphalerite are sodium cyanide and zinc sulfate. Sodium cyanide has a higher selectivity and depresses pyrite and sphalerite. Sodium cyanide and zinc sulfate can be used alone or together and usually added to the grinding circuit. Being toxic and able to dissolve silver and gold, sodium cyanide is replaced by zinc sulfate in many plants. Xanthates are most widely used for the flotation of lead-zinc ores. After the first stage of galena flotation, the tailings are treated with copper sulfate to activate the surface of sphalerite. Isopropyl xanthate is the more effective collector for the activated sphalerite flotation (Napier-Munn & Wills, 2005).

An example of an Ag-Pb-Zn processing flowsheet is shown in Figure 15 (Silver, 2021). In Sotkamo Silver, the ore is crushed and ground. After grinding, Ag-Pb flotation takes place, and sphalerite and pyrite are depressed during this step. In the second step, the sphalerite is activated and floated from lead tailings. After sphalerite flotation, the tailings are used to float pyrite to reduce the environmental effect of the final tailings. This plant produces Ag/Pb, Zn, and pyrite concentrate.

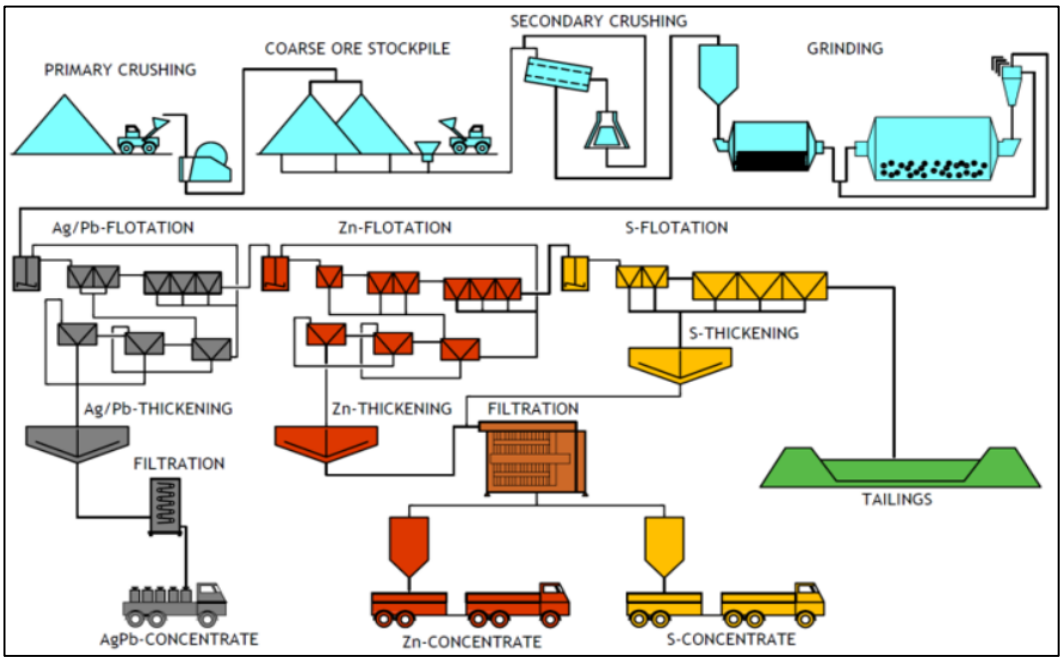

Figure 15 Sotkamo Silver mineral processing flowsheet (Silver, 2021)

A study was conducted by Singh et al. (2004) about the effect of different parameters on the selective flotation of lead-zinc ore. It is concluded that the particle size affects the recovery of lead and zinc minerals, shown in Figure 16A. Sodium cyanide and zinc sulfate together are depressants for the zinc minerals during lead floatation. It is concluded that at the beginning, the increase in depressant dosage caused higher lead recovery and grade. Further increase in depressant -dosage cause depression of lead, shown in Figure 16B. The effect of collector dosage on zinc grade and recovery is also studied. It is concluded that the increase in dosage of a collector caused higher zinc recovery while further increase in dosage caused a sharp decrease in the zinc recovery, shown in Figure 16C. The effect of pH on zinc recovery is also studied. It is concluded that the increase in pH causes higher zinc recovery. Further increase in pH caused a sharp decrease in the zinc recovery, shown in Figure 16D (Singh et al., 2004).

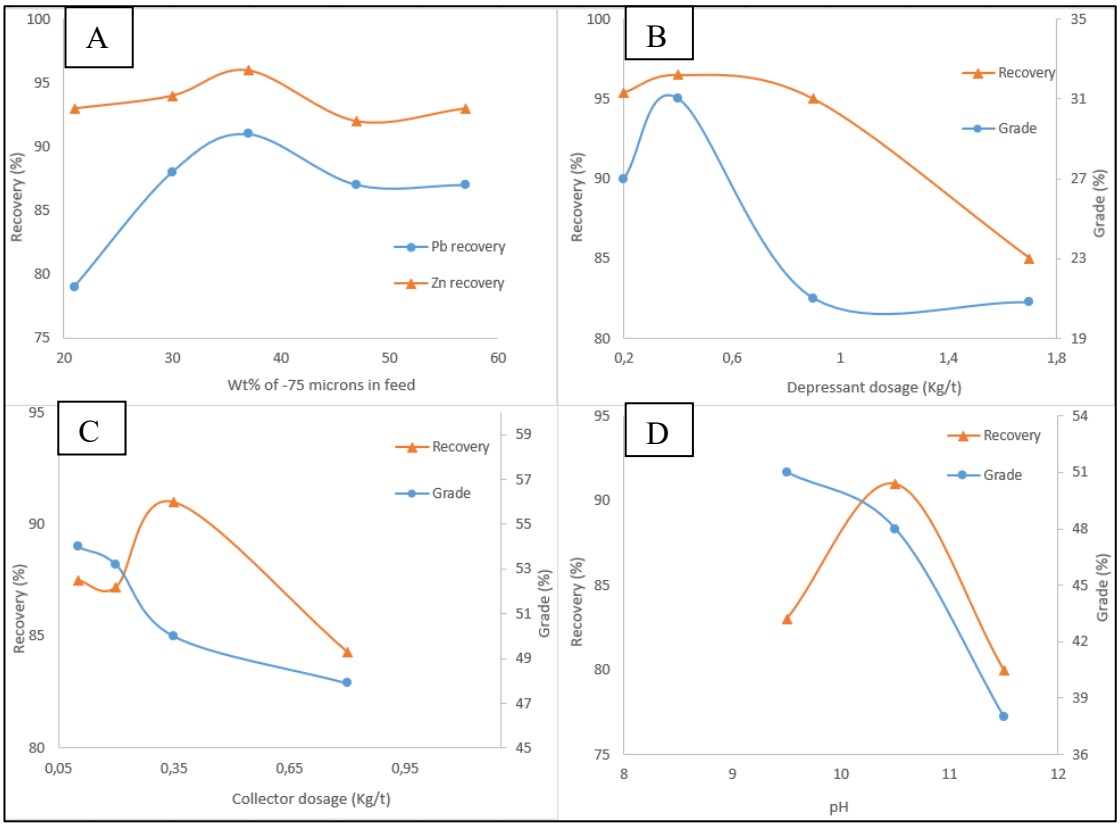

Figure 16 A= effect of particle size on recovery of lead and zinc, B= effect of dosage of depressant on the flotation of lead minerals, C= effect of collector dosage on zinc flotation, D= effect of pH on zinc flotation, regenerated from Singh et al., (2004)

2.5 Flotation Reagents used

2.5.1 Aerophine 3418A

Aerophine 3418A is used as a collector in the flotation tests. Aerophone 3418A is an aqueous solution of sodium-diisobutyl dithiophosphinate. It is phosphine-based collector and developed for copper and activated zinc flotation. Due to its higher selectivity is used for complex ores, polymetallic, and massive sulfide ore (Pecina-Treviño et al., 2003).

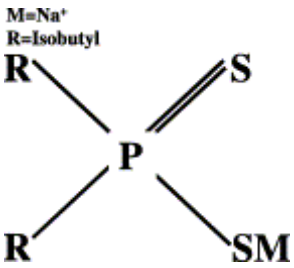

Figure 17 Chemical structure of sodium-diisobutyl dithiophosphinate (Pecina-Treviño et al., 2003)

Aerophone 3418A can be used as a sole collector or as a staged addition for optimum selectivity and control. It has no frothing properties and gives advantages to some plants. Mingione P., (1991) conducted lab-scale flotation tests of Cu-Zn ore using Xanthate and Aerophone 3418A. He concluded that due to the higher selectivity of Aerophone 3418A, improved grade/recovery of Cu was obtained.

During the Taivaljärvi mine feasibility study, it was concluded that the aerophone 3418A shows better flotation performance for rougher flotation (Meyer & Davies, 2012).

2.5.2 MIBC (Methyl Isobutyl Carbinol)

MIBC is used commonly as a frother in flotation, hence used as a frother in the flotation work.
Veras et al. (2014) conducted a study related to comparing three frothers: MIBC, Pine oil, and Polyglycolic ether. He concluded that the MIBC has greater frothing power and efficient in the prevention of coalescence between bubbles. He also concluded that the MIBC has the highest selectivity potential as compared to pine oil and polyglycolic ether. According to the Taivaljärvi mine feasibility study, the MIBC was selected as a frother for lead and zinc flotation circuit (Meyer & Davies, 2012).

2.5.3 Zinc sulfate

Zinc sulfate is used as a depressant for sphalerite. Zinc sulfate makes the sphalerite surface more hydrophilic and depresses it during the galena flotation (CUI et al., 2020).

2.5.4 Calcium oxide (CaO)

CaO is used as a pH modifier to increase and adjust pH during flotation to keep pH under the recommended limit of 11.5 to 12. The pH is essential for selective flotation. The pH indicates the surface charge and reagents adsorptions on the mineral surface. Hence pH should be adjusted in the optimum range to get the required flotation kinetics (Foroutan et al., 2021).

2.5.5 Ore blends

The metallurgical properties of the ore may vary significantly within the deposit. It is always challenging to feed the plant with an optimum blend. Processing plants require a constant feed (grade) to obtain maximum grades and recoveries. The variations in the

feed of a plant may lead to excessive adjustments to the plant and lower throughputs, grades, and recoveries. The ore variations may affect circuits' communication regarding throughputs and mineral separation circuits in terms of grades and recoveries. Since comminution is the most energy-consuming part of the process, it consumes around 75% of total energy (States et al., 2004). It is crucial to have reasonable control over feed grades using proper blends. The blends are also used to process low-grade ore with high-grade ore for efficient resource utilization. In the mineral industry, it is essential to know the metallurgical response of different blends of ores (Käyhkö, 2019)(Talikka et al., 2018) (Liipo et al., 2019).

Many researchers studied the effect of ore blends on metallurgical response. Tonder, Deglon, & Napier-munn (2010) studied the impact of ore blends on the mineral processing of platinum ores. The flotation recovery of blends of Salene (x1) and Townlands (x4) ores is shown in Figure 18. Xi is the good ore head grades while x4 was classified as bad ore with lower head grades. A nonlinear trend was obtained between recovery and ore blends. They also concluded that the relationship between grindability and ore blends is linear.

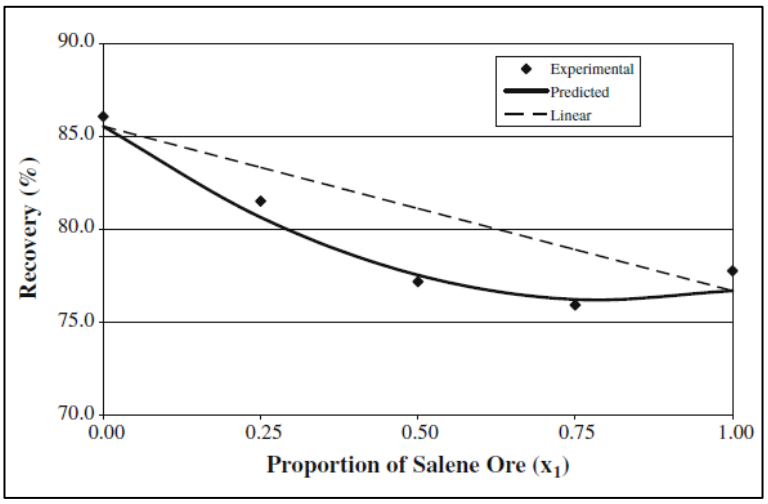

Figure 18 A plot of Recovery vs a mixture of salene (x1) and townlands (x4) ore. The x-axis represents the proportion of x1 ore in the x4 ore.

Marcelo & Kallemback, (2013) studied the effect of ore blends on grindability, shown in Figure 19. It is concluded that there is a relatively linear relationship between the Bond ball mill work index and the blends. It is also concluded that the Bond ball mill work index of blends is usually higher than the weighted Bond ball mill work index of individual ore types.

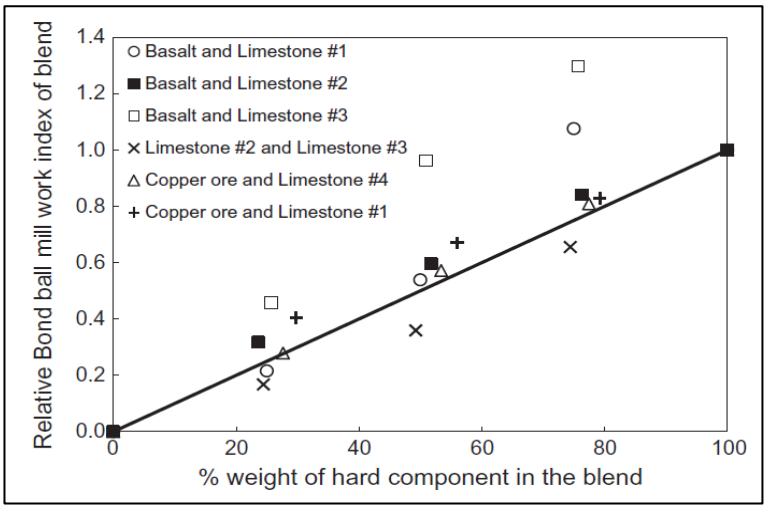

Figure 19 Variation of Bond ball mill work index vs proportion of hard component in the feed.

Wikedzi *et al.* (2018) also conducted a study related to the low-grade sulfide gold ore blends, and their breakage and liberation characteristics. It was concluded that there was a minor effect of blends on liberation. It is also concluded that the grindability is correlated to the quartz content. A linear relationship was found between ore blends and grindability, shown in Figure 20

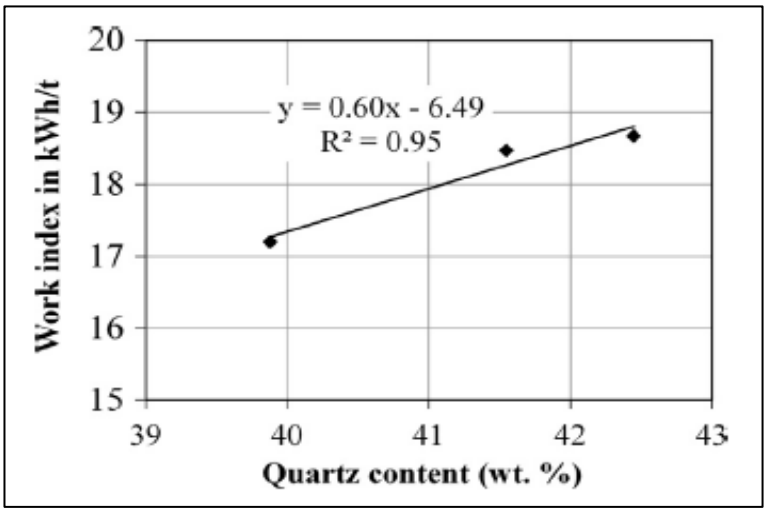

Figure 20 Quartz content vs work index

2.6 Flotation models

The efficiency of different types of separation processes in mineral processing is subjected to their capabilities of distinguishing desired microscopic particles from the

bulk. Some prominent industrial floating practices include floatation deinking, mineral separation, plastics separation, removal of radioactive contaminates, carbon extraction and waste-water treatment, etc. Out of these, water treatment and minerals separation processes are in wider acceptance across the globe. The former one has used dissolved air flotation (DAF) with comparatively smaller bubbles (50-100 µm targeted on 1-10 µm particles) whereas, the later used dispersed air floatation (DAF) with slightly bigger dimension bubbles (500-2500 µm targeted on 150-200 µm particles). However, the operating principles applied to floatation cells, after hydrophobicising the target minerals, are similar in all the above-mentioned processes. Three such generalized sequences of the separation processes are:

I. Aeration (Introduction of air bubbles in a system)
II. Mixing (Optimization of bubble-particle interaction)
III. Separation (Skimming of bubble-particle aggregates from the bulk)

The floating process is often considered an 'intense interactive engineering system' due to the interdependence of the process on various factors and parameters, such as chemical, equipment, operational, reagent dosages, particle sizes, interaction intensity etc. An overview of such dependent factors is shown in Figure 21.

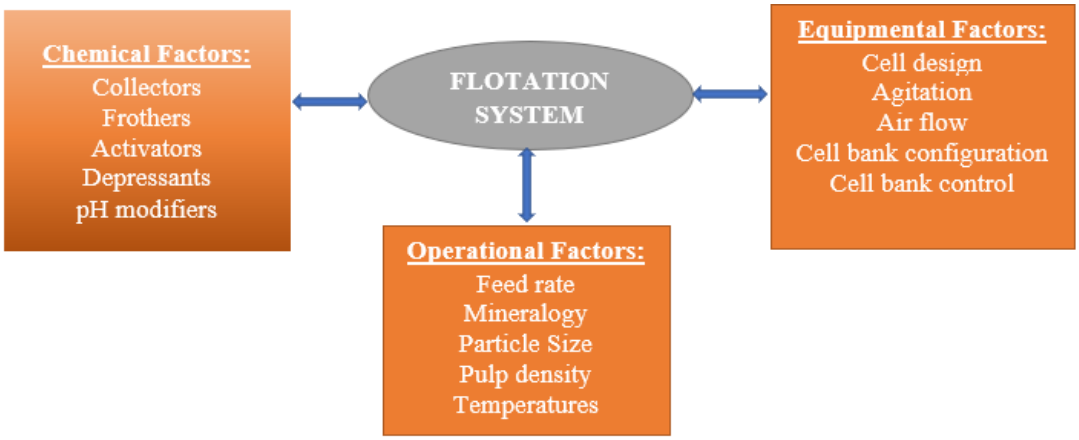

Figure 21. Different Factors contributing to Flotation Process (Gharai & Venugopal, 2016)

Since of beginning of the modern industrial revolution, simulation-based modeling practices are in huge demand. Models prior to the practical implementation provide information about the experiments' performance, efficiency, and reliability. Similarly,

floating models are also beneficial for performance escalation and predictive maintenance of industrial operations (Gharai & Venugopal, 2016).

2.6.1 Modelling Approaches:

The initial floating model was expressed in 'exponential function of time' (like chemical kinetic model) i.e.

$$\frac{dN_1}{dt} = f(k, N_i) = -k_1 N_1^m - k_2 N_2^n$$

Where $\frac{dN_1}{dt}$ is the change in particle concentration w.r.t. time

k_i is the rate constant(s)

m, n are the order of the process

Recoveries of individual species can be calculated using the following equation:

$$R = \frac{k\tau}{1+k\tau}$$

Where k, τ are rate constant & residence time respectively

Based on overall process and sub-processes of flotation, models are broadly categorized into '*macro-scale'* and '*micro-scale'*. A general classification of flotation models is shown in Figure 22 (Gharai & Venugopal, 2016).

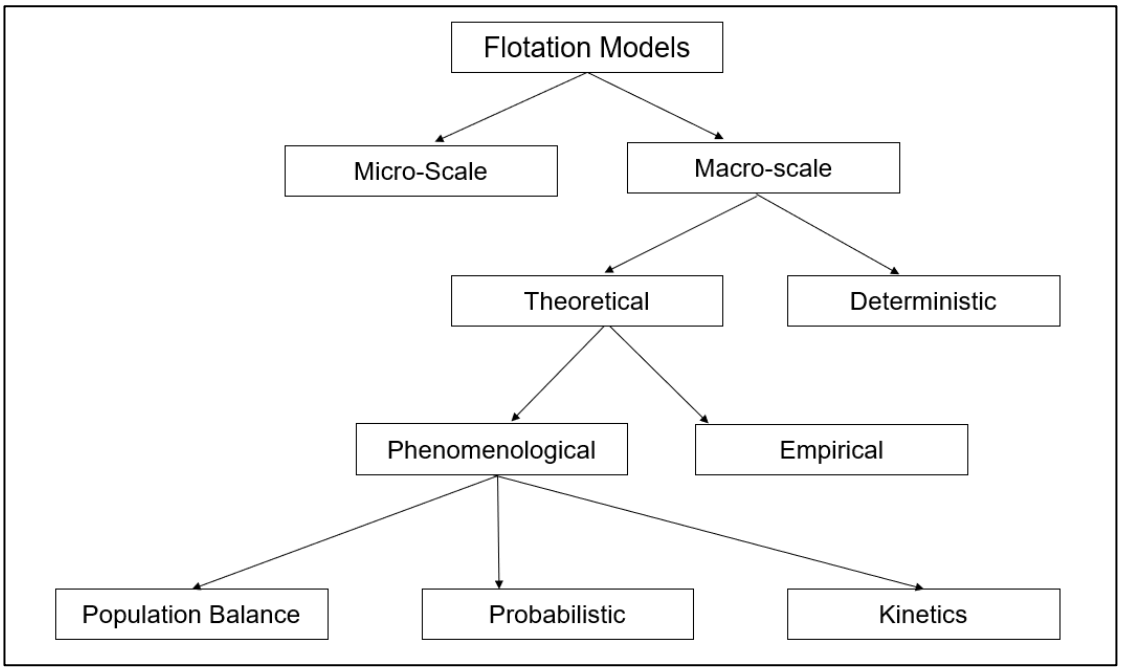

Figure 22. General Classification of Flotation models (Gharai & Venugopal, 2016)

2.6.2 Macro-Scale Models

A. Theoretical models

It involves theoretical assumptions and complex equations to analyze possible events in the flotation process (Gharai & Venugopal, 2016).

1) Phenomenological models

These models are derived from the conservation of mass, momentum, and energy equations. Such models are used to correlate the causes and effects of the flotation process.

i. Population Balance models

It is a 3-phase model that represents mineralogical species and particle size based on their state in the slurry. This model uses kinetic equations and hydrodynamic considerations to simulate the effects i.e. flow-rate, pulp level, agitation. This process is effective for bubble size estimation. The flotation cell is modeled in 2 zones: Impeller zone (where bubble breakage happens) and Bulk zone (bubble coalescence).

ii. Probabilistic models

These models use the rectangular distribution of rate constant as shown in equation 1, also known as 'Klimpel model'.

$$R_t = R\,[1 - \left(\frac{1}{-K_R\,.t}\right)\{1 - e^{-K_R\,.t}\}\,] \quad (1)$$

Where K_R is rectangular rate of coefficient

$R\ is$ recovery after flotation time 't'

It provides information about the relative occurrence of various sub-processes i.e. collision, adhesion, and detachment, which uses probability theory in modelling, as shown in equation 2 (Schuman method).

$$P_x = P_c\,.P_a\,.F.[x].V \quad (2)$$

Where P_x is probability of Success (related to recovery rate of particles).

P_c is probability of particle − bubble collision

$P_a is\ p$robability of particle − adhesion respectively

$F\ is\ f$orth stability factor

$V\ is\ c$ell volume

A modification has done by Tomlinson and Fleming in equation 2 by adding few terms, shown in equation 3.

$$F = P_e\,.P_f \quad (3)$$

Where P_e is probability of levitation to the base of the forth.

$P_f\ is\ p$robability of drainage from the forth

iii. Kinetic models

Intrinsically, Flotation is a rate process and such models use ODEs to define the kinetics of bubble particle collision and coalescence as shown in equation 4.

$$\frac{dC}{dt} = -K_n C^n C_b^m \quad (4)$$

where $C\ is\ c$oncentration of particles $(\frac{M}{V})$

$C_b\ is\ c$oncentration of bubbles

$K\ is\ f$lotation rate constant

$n, m\ are$ respective orders.

There are 3 approaches to define flotation rate constant:

- **First-order kinetics (when *n = 1)***

$$\frac{dC}{dt} = -K_1 C$$

$Where$ K_1 is first order rate constant

Recovery can be calculated using equation 5.

$$R = R_\infty\ (1 - e^{-K_1 t}) \tag{5}$$

Where $R\ is\ c$umulative recovery after time t

R_∞ is maximum recovery after prologed flotation time

Equation 5 can be extended to a 3-component kinetics model (Nguyen & Schulze) with respect to the types of feeds (fast, slow and non-floating components), shown in equation 6.

$$R = 1 - m_f \exp(-K_f t) - m_s \exp(-K_s t) - m_{tail} \tag{6}$$

Where $m_f, m_s\ and\ m_{tail}$ are the mass fractions of fast, slow and non − floating components respectively.

- **Second-order kinetics (when n = 2)**

$$\frac{dC}{dt} = -K_2 C^2 \tag{7}$$

Where K_2 is first order rate constant

Then, the second-order flotation kinetics equation becomes:

$$R = \frac{R_\infty^2 \, K_2 t}{1 + \, R_\infty \, K_2 t}$$

- **Nonintegral-order kinetics**

One of kinetic models by Imauzimi & Inoue, incorporating gauge recovery in the froth (R_g), shown in equation 8.

$$R = \, R_\infty \, (1 - \, e^{-Kt}) + \, \, R_g (1 - \, R_\infty) \tag{8}$$

where R_∞ is recovery at infinite time
R is flotation recovery

Another equation considering the probabilities of occurrences for single-bubble flotation experiment by Nguyen et al. is shown in equation 9.

$$R = 1 - \exp[-P_c P_{at} (1 - P_{det})(1 + \frac{V}{U})] \tag{9}$$

where P_c *is p*robability of collision
P_{at} *is p*robability of attachment
P_{det} *is p*robability of detachment
*V is p*article settling velocity
*U is b*ubble rising velocity

A list of various flotation models based on kinetics is shown in Table 3.

Table 3 Flotation models based on kinetics (Gharai & Venugopal, 2016)

Model 1	1st-order kinetic model	$R = R_\infty(1 - e^{-kt})$
Model 2	1st-order flotation model with rectangular distribution of floatability	$R = R_\infty(\frac{1}{k_2 t}(1 - e^{-kt}))$

Model 3	1st-order 2-stage kinetic model	$R = R_\infty[\left(\frac{k_3}{k_3 + k_3^*}\right)(1 - e^{-k_3^* t}) - \left(\frac{k_3^*}{k_3 + k_3^*}\right)(1 - e^{-k_3 t})]$
Model 4	1st-order reversible kinetic model	$R = \frac{k_4 R_\infty}{(k_4 + k_{-4})}[1 - e^{-(k_4 + k_{-4})t}]$
Model 5	Fully mixed reactor model	$R = R_\infty(1 - \frac{1}{1 + \frac{t}{k_5}}]$
Model 6	*Gas/solid kinetic adsorption model*	$R = \frac{k_6 t}{(1 + k_6 t)^m}$
Model 7	Improved gas/solid adsorption model	$R = R_\infty[\frac{k_7 t}{1 + k_7 t}]$
Model 8	2nd-order kinetic model	$R = [\frac{R_\infty^2 k_\infty t}{1 + R_\infty k t}]$
Model 9	2nd-order kinetic model with rectangular distribution of floatability	$R = R_\infty[1 - \frac{1}{k_9 t}\{\ln(1 - k_9 t)\}]$
Model 10	Three parameters fast and slow floating component	$R = (1 - \emptyset)(1 - e^{-k_{10f} t}) + \emptyset(1 - e^{-k_{10s} t})$
Model 11	Four parameters fast and slow floating component	$R = (R_\infty - \emptyset)(1 - e^{-k_{11f} t}) + \emptyset(1 - e^{-k_{11s} t})$
Model 12	Three parameters kinetic model with particle floatability proportional to sized distribution	$R = R_\infty(1 - \frac{e^{-k_{12s} t} - e^{-k_{12u} t}}{k_{12u} - k_{12s} t})$
Model 13	Three parameter gamma distribution	$R = R_\infty(1 - \left(\frac{\lambda}{\lambda + 1}\right)p)$

- **<u>Multi-phase modeling</u>**

If the rate of constants of the floated particles follow a continuous distribution, then the recovery rate (R) will be given by equation 10.

$$R = R_\infty [1 - \int_0^\infty F(k) \exp(-kt) dk] \quad (10)$$

Where R_∞ is ultimate recovery at infinite time

*F (k) is c*ontinuous distribution function

In a batch flotation process, mineral recovery at any time is given by equation 11.

$$R = R_\infty \left[\int_0^\infty \{1 - \exp(-kt)\} F(k) dk \right] \quad (11)$$

Where $1 - \exp(-kt)$ shows the first order recovery process.

*F (k) is r*ate constant distribution function for mineral species.

In general, for a continuous flotation process, mineral recovery (*R)* follows equation 12.

$$R = R_\infty \left[\iint_0^\infty (1 - e^{-Kt}) F(k) E(t) dk\, dt \right] \quad (12)$$

Where $F(k)\ is\ r$ate constant distribution

$E(t)\ is\ r$esidence time distribution function for continuous processes

According to Woodburn & Loveday, (1965), Gamma distribution (with parameters a, b) can represent different types of processes from exponential decay to normal distribution shown in equation 13.

$$F(k) = \frac{b^{a+1}}{\Gamma(a+1)} . K^a . e^{-bk} \quad (13)$$

Rectangular flotation distribution is given as:

$$F(k) = \frac{1}{k_{max}} , 0 \leq k \leq k_{max}$$

$$F(k) = 0, 0 > k > k_{max}$$

Where k_{max} is the maximum flotation rate constant.

Weibull (Rosin-Rammler) distribution is shown in equation 14.

$$F(k) = \frac{n}{k_m} \left(\frac{k}{k_m}\right)^{n-1} . e^{-\left(\frac{k}{k_m}\right)^n} \quad (14)$$

Where *n is s*hape factor

k_m *is* scale factor of dsitribution

In (Yianatos et al., 2010), rectangular distribution and Gamma distribution of mineral recovery in batch test is given by the equation 15 and 16 respectively. Flotation recovery of continuous process using Gamma distribution is shown in equation 17.

$$R = R_\infty(1 - \frac{1- e^{- k_{max}t}}{k_{max}.t}) \quad (15)$$

$$R = R_\infty[1 - (\frac{b}{b+t})^{a+1}] \quad (16)$$

$$R = R_\infty [1 - \int_0^\infty \{E(t).(\frac{b}{b+t})^{a+1}.dt] \quad (17)$$

2) Empirical models

These models use batch/plant data to relate floatation rate constant values to each component in the system. The model is defined in equation 18 (with assumption that the material has both fast and slow components).

$$R_t = (1 - F_s)\{1 - e^{-k_f t}\} + F_s\{1 - e^{-k_s t}\} \quad (18)$$

Where R_t is fraction of recovery at time t
F_s *is* Fraction of slow floating components
k_f, k_s *is* Rate coefficients for fast and slow floating respectively

$$R(t) = \sum_{i-1}^{n} m_i(1 - e^{-k_i t}) \quad (19)$$

Where $R(t)$ is overall recovery at time t
m_i *is* proportion of a mineral in each component
k_i *is* rate constant of each component

Based on Runge et al., (1998), recovery can be calculated for batch flotation test data and for plant data using equation 19 and 20.

$$R(t) = \sum_{i-1}^{n} m_i(\frac{k_i\tau}{1+k_i\tau}) \quad (20)$$

Where τ *is* residence time for all the cells

Based on Newcombe formula as shown in equation 21, kinetic rate constant *(K)* can be linked within settling zone.

$$K_i = \alpha_i e^{-\beta_i \tau_s} \tag{21}$$

Where τ_s is residence time within the settling zone

α, β are empirical fitted parameters for each size class *i*

In empirical models, froth being the most important factor, can be calculated using equation 22 (Gorain et al.).

$$R_f = e^{-\beta \tau_f} \tag{22}$$

Where τ_f is air retention time in the forth

β is dependent parameter on pulp properties

B. Deterministic models

Surface forces and hydrodynamics

Using the extended DLVO theory, Yoon & Mao, (1996) has proposed a model of two important equations. Equation 23 represents a first order flotation model whereas equation 24 is modified by considering all dominant surface forces.

$$k = 0.25\, S_b \left[1.5 + \frac{4Re^{0.72}}{15} \right] \left(\frac{R_1}{R_2}\right)^2 e^{-\frac{E_1}{E_k}} \text{ X } \left[1 - \exp\left(-\frac{\gamma_{lv}\pi R_1^2(1-cos\theta)^2) + E_1}{E_k'}\right)\right] \tag{23}$$

Where S_b *is s*uperficial surface area rate of bubbles

Re *is r*eynolds number of the bubble

R_1 *is s*ize of the particle

R_2 *is* size of the bubble

E_1 *is e*nergy barrier

E_k is kinetic energies of the macroscopic particles

γ_{lv} *is s*urface free energy at liquid/vapor interface

θ *is c*ontact angle.

E_k' *is k*inetic energy that tears off the bubble surface

$$k = 0.25\, S_b \left[\, 1.5 + \frac{4Re^{0.72}}{15}\right] \left(\frac{R_1}{R_2}\right)^2 e^{-\frac{E_1}{E_k}}\ \mathrm{X}\,[1 - \exp\left(-\frac{W_a + E_1}{E_k'}\right]] \qquad (24)$$

Duan et al., (2003) has proposed a model for chalcopyrite ore considering various efficiencies and frequencies of collision. However, it doesn't account for the effects of the surface forces, shown in equation 25.

$$k = -2.39\, \frac{G_{fr}}{d_b . V_{cell}} \left[\frac{0.33\, \varepsilon^{\frac{4}{9}} d_b^{\frac{7}{9}}}{v^{\frac{1}{3}}} \left(\frac{\Delta\rho_b}{\rho_{fl}}\right) . \frac{1}{v_b}\right] E_c E_a E_{s.} \qquad (25)$$

Where $G_{fr}\ is\ g$as flow rate (cm^3/min)

$\varepsilon\ is\ t$urbulent dissipation rate $\left(\frac{cm^3}{s^2}\right)$

$E_c, E_a, E_s$are efficiencies of collision, attachment and Stability

$v\ is\ f$luid kinematic velocity (cm^2/s)

ρ is density of particle, fluid and bubble

A model by Jameson et al., (1977) and Laskowski & Ralston, (1992) based on no-turbulence environment is shown in equation in 26.

$$K = 1.5\, \frac{G_{fr} . h}{d_b . V_{cell}}\, E_c E_a \qquad (26)$$

Where $h\ is\ h$eight of the flotation cell

Another semi-empirical model by Sherrell, (2004) , considering probability of attachment in turbulent environment, is shown in equation 27.

$$K = \beta N_b P_A (1 - P_D) R_F \qquad (27)$$

Where $\beta\ is\ c$ollision kernel $(m^3 . s^{-1})$

$N_b\ is\ n$umber density of bubbles (per m^{-3})

P_A is probability of Attachment

$P_D\ is\ p$robability of Detachment

$R_F\ is\ f$orth recovery factor

A recent model for flotation rate constant based on CFD simulation by Karimi et al., (2014) is shown in equation 28.

$$k = -\frac{7.5}{\pi}\frac{G_{fr}}{d_b.V_r}\left[\frac{0.33\,\varepsilon^{\frac{4}{9}}d_b^{\frac{7}{9}}}{\nu^{\frac{1}{3}}}\left(\frac{\rho_p-\rho_f}{\rho_f}\right).\frac{1}{u_i}\right]E_cE_aE_{s.} \tag{28}$$

Where V_r *is* reference volume (cm^3)

u_i is turbulent fluid velocity (cm/s)

Entertainment factor

Mathematically, entertainment can be defined as the ratio of free gangue recovery (R_g) to the water recovery (R_w) as shown in equation 29 (Gharai & Venugopal, 2016).

$$R_g = ENT.R_w \tag{29}$$

Recovery equation considering the entertainment factor for true flotation (by Savassi) is given in equation 30. Another model by Savassi, known as compartment model, shown in equation 31, which account for simultaneous contribution of flotation and entertainment factor in a conventional flotation cell.

$$R = \frac{PS_b\tau\,R_f(1-R_w)+ENT.R_w}{(1+PS_b\tau\,R_f)+\,ENT.R_w} \tag{30}$$

$$R = \frac{K_{cz}.\tau_{cz}R_f(1-R_w)+ENT.R_w}{(1+K_{cz}.\tau_{cz}R_f).(1-R_w)+\,ENT.R_w} \tag{31}$$

Veras et al., (2014) has given an expression for froth recovery (R_f) including the mechanical entertainment is shown in equation 32.

$$R_f = \left(1-ENT.R_{wf}\right)\exp\left(-\beta.\tau_f\right)+\,ENT.R_{wf} \tag{32}$$

Where R_{wf} is water recovery in froth

Residence time distribution

There are 2 models to analyze the residence time distribution results. Such distributions are helpful in measuring the gas, liquid, and solid-particle flow patterns in flotation cells (Gharai & Venugopal, 2016).

The axial dispersion model

If the mixing is very minimal, then this model is considered.
Axial dispersion model can be calculated using equation 33. The dimensionless form of the same equation is shown in equation 34.

$$\frac{\partial C}{\partial t} = D\frac{\partial^2 C}{\partial x^2} - u\frac{\partial C}{\partial x} \tag{33}$$

Where $C\ is\ c$oncentration of species
$D\ is\ a$xial dispersion coefficient
$x\ is\ d$istance along which the concentration varies

$$\frac{\partial C}{\partial \theta} = N_d\frac{\partial^2 C}{\partial z^2} - \frac{\partial C}{\partial z}\ ;\ \ N_d = D/\mu L \tag{34}$$

Where $N_d\ is\ d$imensionless dispersion number
$L\ is\ l$ength of the vessel
$z\ is\ d$istance along the linear dimension

The mixed zone model

This model is used for a series of perfectly mixed zones. A theoretical residence time distribution profile for '*N*' cells in series is shown in equation 35 (Gharai & Venugopal, 2016).

$$E(\theta) = \frac{N(N\theta)^{N-1}}{(N-1)!}\exp(-N\theta)\,;N = \frac{\tau^2}{\sigma^2} \tag{35}$$

Where $\sigma^2$is variance of experimental residence time distribution
$\tau\ is\ m$ean residence time

This model estimates the changes in feed properties. Recovery of each mineral phase across the cell (R_{cell}) is shown in equation 36.

$$R_{cell} = R_{attached} \frac{(100 - R_{ent})}{100} + R_{ent} \quad (36)$$

Where $R_{attached}$ *is* recovery of mineral to concentrate

R_{ent} : Recovery of mineral phases by entertainment

2.7 Validation and verification of simulation models

Simulation models are often used nowadays. These are used for problem-solving and to help in decision-making. The simulation model needs to be verified and validated. Verification ensures that the model results are correct, while validation ensures that the results are accurate and consistent. Absolute validation of a model over a complete domain is costly; hence, the model's evaluation is conducted until the results generate sufficient confidence. A confidence model is shown in Figure 23. The value of the model is increased with the increase in the cost. Hence sufficient tests are conducted to get acceptable confidence in the model results (Sargent, 2010).

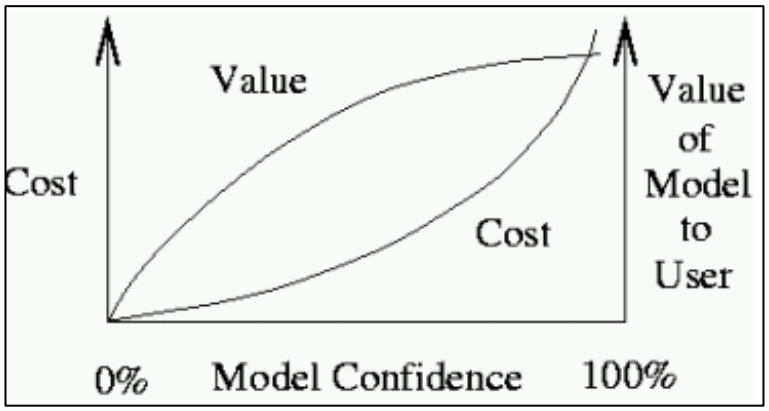

Figure 23 Model confidence, cost, and value relation (Sargent, 2010)

2.7.1 Model development process

There are two common approaches for model development, and one is a simple view while the other uses a complex theory (Sargent, 2010). A simplified version of a model development process is shown in Figure 24 (Sargent, 1981). Problem entity is the prominent phenomenon to be modeled. A conceptual model is the mathematical/logical form of the problem entity, developed by the analysis and modeling phase. The computerized model implements the conceptual model in a computer form, developed by a programming and implementation phase. Conceptual model validation makes sure that the theories and assumptions are correct and the model representation of the problem

entity is accurate. Computerized model verification is essential to ensure that the programming and implementation of the conceptual model are reasonable. Operation validity ensures the reliability of the computer's model outputs. Data validity deals with data validation for each phase of the modeling (Sargent, 2010).

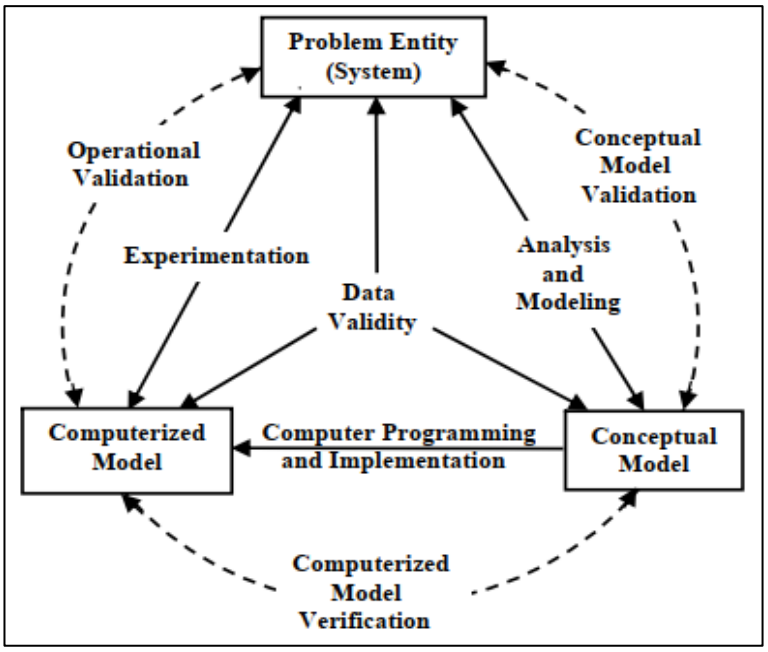

Figure 24 Simple model development process (Sargent, 2010)

2.7.2 Validation techniques

Sargent (2010) states that the following techniques and tests are used to verify and validate a model. This process of validation and verification is repeated till the results are satisfactory. Changes in a model require verification and validation process again.

- Animation
- Comparison
- Degenerate test
- Event validity
- Extreme condition test
- Face validity
- Historical data validation
- Historical methods
- Internal validity
- Multistage validity
- Operational graphics
- Sensitivity analysis
- Predictive validation
- Traces
- Turning tests

In animation, the model is displayed graphically, and operational behavior is motioned. In comparison, the outputs of the model are compared with the previous valid models. During degenerate tests, the model is tested for different parameters and input values. In event validity, the model's output is compared with the actual values. Extreme condition tests are conducted to check the optimum range of the model. In face validity, the model is validated with individual knowledge. Historical data is used to validate the model. Historical validation methods of rationalism, empiricism and positive economics are used to validate the model. Stochastic variability in the model is studied in internal validity. In multistage validation, the previous validation methods are used for the multistage validation. A graphical representation is used to analyze the results of simulation runs. The model's sensitivity analysis is tested with a wide range of input parameters, and the model's response is studied. In predictive validation, the model's outcome is validated using experimental system data. In the trace analysis, the validity of the model is checked for the specific entities. In turning tests, the model is validated by a knowledgeable person based on experimental and model outputs (Sargent, 2010).

3 EXPERIMENTAL WORK:

The experimental test work was carried out at the Metso Outotec Research Center Pori from February to May 2021. The experimental test work includes sample preparation, grinding calibration tests, Flotation tests, blends preparation. Mineral processing laboratory, analytical laboratory, and pilot plant were used for the experimental part of this thesis.

Metso Outotec Research Center Pori can perform laboratory-scale testing, simulate a potential flowsheet, and bench/pilot scale runs. The focused areas are product development, process research, innovations, research services, and research method development.

3.1 Laboratory equipment

3.1.1 Crusher

Primary crushing was done using a bigger-scale crusher in Metso Outotec Pilot Plant, Pori. A jaw crusher was used to reduce the sample to -1mm.

3.1.2 Ball mill

The laboratory ball mill (215 mm height and 205 mm diameter) was used for the grinding test, shown in Figure 25. The grinding was required for grinding calibration tests and the flotation tests. The ball mill and the grinding media are made up of mild steel. The grinding media include 27mm (3337g) and 19mm (8187g) balls.

Figure 25 Laboratory ball mill and ball charge

3.1.3 Slurry divider

The slurry divider was used for the wet sample splitting, as shown in Figure 26. It divides the slurry into two similar portions of 1/12 and one part of 10/12. During grinding calibrations tests, the slurry divider was used to split the ground sample for the sieve analysis.

Figure 26 Slurry divider

3.1.4 Wet-sieve analysis

The wet-sieve analysis machine is used for the sieving tests, shown in Figure 27. It is based on hand sieving in an ultra-sonic bath, made by FinnSonic. The batches (-1mm) were ground using a ball mill, and then sieving was conducted to find the P80 for each

grinding time. Our target P80 was 90μm; hence we used 212, 150, 106, 75, 53, and 20 μm sieves.

Figure 27 Ultrasonic sieving machine

3.1.5 Flotation machine

Outotec GTK LabCell was used for the flotation tests, shown in Figure 28. This machine works automatically, and scrapper rate, impeller speed, airflow, nitrogen flow, and water flow can be adjusted. The cell sizes and related settings are shown in Table 4. The 4L cell is dedicated to the flotation tests to determine the kinetics of flotation. A pH meter was used to measure and adjust the pH of the flotation.

Table 4 GTK LabCell operating parameters

Cell size	Impeller Diameter	Air flowrate	Froth building time
l	mm	l/min	s
2	45	1300	15
4	45	1800	20
8	60	1200	25
12	60	1450	30

Figure 28 Outotec GTK LabCel flotation machine

3.1.6 Rotary sample splitter

A dry rotary sample splitter is used for dry sample splitting, shown in Figure 29. The batches prepared at the crushing plant have masses in the range of 1.6-1.9Kg. Our required batch size was 1.8 Kg; hence we used this splitter to adjust the batch masses and to prepare blends.

Figure 29 Rotary sample splitter

3.1.7 Ring mill

A ring mill was used to pulverize samples for ICP analysis. ICP analysis is used for the flotation concentrates, tailings, and samples for mineralogical studies.

3.1.8 Vacuum and pressure filters

Pressure and vacuum filters were used for dewatering during flotation and grinding tests, shown in Figure 30

Figure 30 Pressure and vacuum filters

3.1.9 Elemental analysis equipment

Inductively coupled plasma optical emission spectroscopy (ICP-OES) was used to analyze Pb, Zn, Cu, and Fe. Inductively coupled plasma mass spectroscopy (ICP-MS) and ICP-OES were used to analyze Ag in the samples. Sulfur was analuzed by combustion method.

3.2 Sample preparation

3.2.1 Ore samples

Four types of ores from Sotkamo were investigated. The weight of each primary sample and the differences of elemental composition is shown in Table 5.

Table 5 Mass and elemental composition of primary samples

Sample Name	Malmi	Sorter Feed	Sorter Product	Ore 60
Sample weight (Kg)	140	130	125	194
Ag (ppm)	43	48	129	170
Pb (%)	0,1	0,22	0,61	0,29
Zn (%)	0,3	0,62	1,72	0,87
Fe (%)	3,69	3	4	3,81
S (%)	2,3	1,9	3,1	1,03

3.2.2 Primary sample preparation

The required batch size is 1.8Kg (-1mm). The sample preparation includes crushing, screening, and sample splitting.

The sample preparation starts with crushing. The crushed material is screened using a 3.35mm screen. The oversize material (+3.35mm) is recirculated to the crusher feed. The undersize material (-3.35mm) is divided into four portions. Two portions are stored for future use, while the third portion is divided into 5Kg batches for mergan grindability tests. The fourth portion is further crushed. The crushed material is screened with a 1mm screen, and oversize material (+1mm) is recirculated to the crusher feed. The under-size material (-1mm) is then further divided into 1.8Kg bathes. The sample preparation flowsheet is shown in Figure 31.

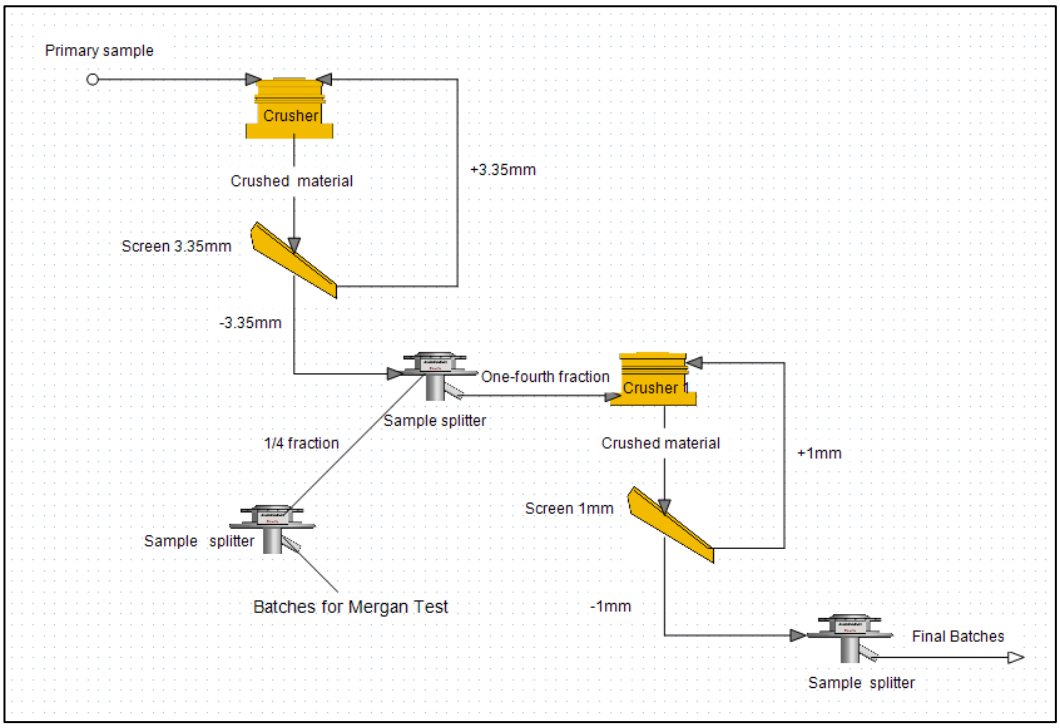

Figure 31 Sample preparation flowsheet

3.2.3 Sample preparation for Mineralogical studies

One batch of mass around 1.8Kg (-1mm) was ground till the P80= 90µm. The grinding conditions are the same as for the flotation test. After grinding, this sample is dried in an oven at 60°C. This dried ground sample is divided into 6 portions, and out of six, two parts are mixed and further divided into 8 portions (about 75g each). One out of 8 parts is ground in the ring mill for sample preparation of ICP analysis. The following analysis took place:

- ICP-OES: Pb, Zn, Cu, Fe, Sb, As, and Ag after total dissolution
- ICP-OES: Fe after bromine-methanol dissolution
- ICP-MS: Au, Ag after total dissolution
- Combustion: S + C
- XRD from bulk samples

Six out of 8 portions are mixed and sieved using 212, 150, 106, 75, 45, and 20 µm sieves. Half sieved products are sent for sample preparation for SEM, and half is ground in the ring mill for the following analysis:

- ICP-OES: Pb, Zn, Cu, Fe, Sb, As after total dissolution
- ICP-OES: Fe after bromine-methanol dissolution
- ICP-MS: Au, Ag after total dissolution

- Combustion: S + C
- XRD from -20µm fraction

The last 1/8 fraction is reserved.

3.3 Grinding calibration test work:

The required P80 for each ore sample is 90µm. To calculate grinding time for the required P80, each sample's grinding calibration test was done. The mild steel laboratory ball mill was used. The ball charge includes 27mm (3337g) and 19mm (8187g) balls. The solids content was 65% solids. The grinding time was 5, 10, 20 minutes. The P80 for each grinding time is plotted and modeled. The grinding residence time for P80=90 µm is calculated using the model obtained from P80 vs grinding time.

The procedure starts with the cleaning of the ball mill by grinding sand for 10 minutes. After mill cleaning, each sample of 1.8Kg is ground under the required grinding condition for 5 minutes. After grinding, the sample is divided into a sub-sample of 20-50g using a slurry divider. This subsample is wet-sieved using 212, 150, 106, 75, 53, and 20 µm sieves. The fraction retained on each sieve is filtered and dried. After drying, the weight of each size fraction is measured, and P80 is calculated. After the first grinding cycle, the size fractions are mixed back to the main sample and then the main sample is filtered using a pressure filter. After filtration, the weight of the filtered cake is measured, and required water is added to obtain the 65% solids for the next grinding cycle of 10 minutes. The same procedure is repeated for the next grinding cycle of 20 minutes. A graph between grinding time and P80 is made and modeled to get an equation having grinding time as an input and P80 as an output. This equation is used to obtain a grinding time for the required P80 of 90µm. The same procedure is repeated for each ore type.

3.4 Flotation Test work:

Kinetic flotation tests were conducted for each type of ore and blend. The 4-liter flotation cell was used with an impeller speed of 1800 rpm, air flowrate of 3 l/min, and scrapper rate every 4 seconds. Tap water was used for grinding and flotation of each sample. The percent of solids in grinding and flotation were 65% and 35%, respectively. The required pH range is 11.5 to 12. The flotation times of RF1, RF2, RF3, RF4, RF5, and RF6 were

1, 2, 3, 6, 6, and 6 minutes respectively, with a total flotation time of 24 minutes. The flotation reagents and dosages are shown in Table 6. The CaO and depressant are added in the grinding stage. The first dosage of collector and frother is added to the conditioning cell, and the second dosage is added after 3 minutes of flotation.

Table 6 Flotation reagents

	pH Adjustment	Depressant	Collector	Frother
Cell	CaO (g/t)	ZnSO4 (g/t)	Aerophine 3418A(g/t)	MIBC (g/t)
Ball Mill	1000	1000		
Conditioner			17,6	4
Third Flotation Cell			3,3	6

The procedure starts with the cleaning of the ball mill. After cleaning each sample of 1.8Kg with 65% solids, 1000g/t of CaO and 1000g/t of ZnSO4 is ground for calculated grinding time. After grinding, the flotation tests start with the conditioning. Before adding reagents, the required tap water is added to get the necessary slurry level in the flotation cell. First, the collector is added and conditioned for two minutes, followed by frother addition with one-minute conditioning. After conditioning, the airflow is started, and 20 seconds are given for froth built up. Then the scrapping of froth is started for one minute in the first cell. The first and second concentrate is collected for one and two minutes of flotation, respectively. After collection of the first two concentrates, the airflow is stopped, and the second dosage of collector and frother is added with a one-minute conditioning time for each. After conditioning, the flotation started again, and further concentrates were collected after 3, 6, 6, and 6 minutes of flotation, respectively. The tap water is added whenever required during flotation. The pH was noted and kept in the range of 11.5 to 12 using CaO. At the end of the flotation, we got six concentrates and one final tailing.

The same procedure is repeated for each ore type and blends. The weighted average grinding time for each blend is used, as shown in Table 8. There are six flotation cells in the flowsheet, as shown in Figure 32, showing the six partial times of flotation.

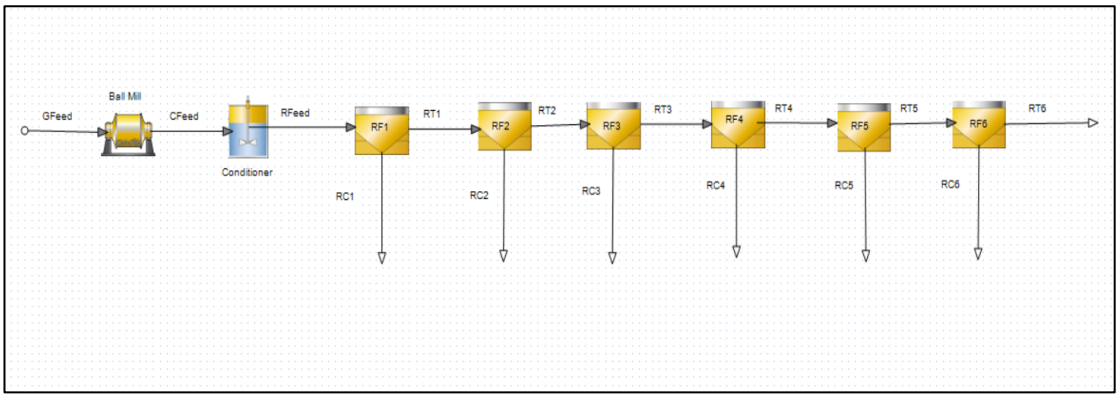

Figure 32 Flotation flowsheet

3.5 Blends Scheme

Various ore blends were prepared to conduct the flotation test. The malmi, sorter product, and Ore 60 were used. Blends are made between two types of ore at 25%, 50%, and 75% portions. The 9 blends obtained and composition in weight percentage are shown in Table 7. The blend I contains 25% malmi and 75% sorter product. However, blend II has 50% malmi and 50% sorter product. The sample mass for grinding and flotation is 1.8Kg hence the subsamples of each ore are prepared using a rotary sample splitter. The actual masses of subsample used for blending are shown in Table 8.

Table 7 Blending plan

Name	Malmi	Sorter product	Ore 60
Blend I	25 %	75 %	
Blend II	50 %	50 %	
Blend III	75 %	25 %	
Blend IV	75 %		25 %
Blend V	50 %		50 %
Blend VI	25 %		75 %
Blend VII		75 %	25 %
Blend VIII		50 %	50 %
Blend IX		25 %	75 %

The grinding times for malmi, sorter product, and ore 60 are 12, 14, and 9 minutes. To find the grinding time of each blend, we took an assumption that the grinding time is proportional to the percentage of each ore type used e.g., the grinding time for blend I is

25% of malmi grinding time (12 minutes) and 75% of grinding time (14 minutes) of sorter product. The weighted average grinding time calculated for each blend is shown in Table 8.

Table 8 Average grinding times and exact masses used

Name	Avg. Grinding time for P80=90µ (min)	Ore (g)	Sorter product (g)	Ore 60 (g)
Blend I	13,50	448,5	1351,6	
Blend II	13,00	898	902,1	
Blend III	12,50	1351,2	448,8	
Blend IV	11,25	1347,6		451,6
Blend V	10,50	904,4		901,4
Blend VI	9,75	449,2		1349,3
Blend VII	12,75		1350,8	448,6
Blend VIII	11,50		901,7	900,5
Blend IX	10,25		450,7	1349,1

Using the blend plan of Table 7 we can make three series, as shown in Table 9. Series 1 contains blends of sorter product sample and malmi sample, including 0-100% of each sample. Series 2 contains blends of malmi and ore 60 samples. While series 3 contains blends of sorter product and ore 60 samples.

Table 9 Series of blends

Series Name	Blend name	Blend structure
Series 1	Sorter product	100% Sorter product + 0% malmi
	Blend I	75% Sorter product + 25% malmi
	Blend II	50% Sorter product + 50% malmi
	Blend III	25% Sorter product + 75% malmi
	Ore	0% Sorter product + 100% malmi
Series 2	Ore	100% malmi + 0% Ore 60
	Blend IV	75% malmi + 25% Ore 60
	Blend V	50% malmi + 50% Ore 60
	Blend VI	25% malmi + 75% Ore 60
	Ore 60	0% malmi + 100% Ore 60
Series 3	Sorter product	100% Sorter product + 0% Ore 60
	Blend VII	75% Sorter product + 25% Ore 60
	Blend VIII	50% Sorter product + 50% Ore 60
	Blend IX	25% Sorter product + 75% Ore 60
	Ore 60	0% Sorter product + 100% Ore 60

3.6 Element to Mineral Conversion:

Elemental analysis was conducted for the flotation concentrates and tailings. Inductively coupled plasma optical emission spectroscopy (ICP-OES) was used to analyze Pb, Zn, Cu, and Fe. Inductively coupled plasma mass spectroscopy (ICP-MS) was used for the analysis of Ag. Sulfur was determined using combustion analysis. After elemental analysis, the elemental data was transformed into minerals using HSC-Geo. Concluding from mineralogical studies, the simplified mineralogy of ore samples is shown in Table 10. There are multiple Ag minerals, and for simplicity, dyscrasite is representing all Ag minerals. Sphalerite is the only mineral containing mainly Zn. At the same time, galena and chalcopyrite include Pb and Cu mainly. Pyrite is calculated based on the remaining S. Quartz represents the group of non-sulfide gangue minerals (NSG). According to previous studies, it is also indicated that pyrite and galena contain traces of Ag, as shown in Table 10.

Table 10 List Minerals and distribution of elements for Sotkamo Silver

Minerals	Si (%)	O (%)	Fe (%)	Cu (%)	Zn (%)	Pb (%)	S (%)	Sb (%)	Ag (%)
Dyscrasite								23,93	74,64
Sphalerite			6,30		61,02		32,68		
Pyrite			46,55				53,45		0,0039
Galena						86,6	13,4		0,092
Chalcopyrite			30,43	34,63			34,94		
Quartz	46,74	53,26							

Two rounds were used for element to mineral conversion, shown in Table 11. First-round contains dyscrasite, galena, sphalerite, pyrite, and chalcopyrite. The elements used in the first round are Ag, Pb, Zn, S, and Cu. In the second round, all the remaining minerals are classified as non-sulfide gangue.

Table 11 Rounds in for element to mineral conversion

Round 1		Round 2	
Minerals	Elements	Minerals	Elements
Dyscrasite	Ag %	Quartz	Sum = 100%
Galena	Pb %		
Sphalerite	Zn %		
Pyrite	S %		
Chalcopyrite	Cu %		

3.7 Simulation of flotation test work

HSC Sim module is used for the simulation of reference flotation tests and blends flotation tests. The flowsheet used for the reference flotation test is shown in Figure 32. First of all, the elemental grades of each stream are converted to simplified mineral groups shown in Table 10, using the recipe shown in Table 11. Since we have experimental data for each concentrate stream and final tailings stream, HSC mass balance module is used to calculate the values of other streams, including the feed stream. After mass balance, the HSC Sim model fit tool is used to calculate the kinetic parameter for each flotation test. The rectangular distribution model is used due to the lower mass pull of the concentrated. The kinetic curves are fitted by adjusting R_{inf} and K_{max} values. The example of fitted curves for galena in the sorter product sample is shown in Figure 33. The kinetic

curves for other main minerals in all samples are shown in appendix D. The kinetic parameters calculated for all samples, including each mineral, are shown in Table 19.

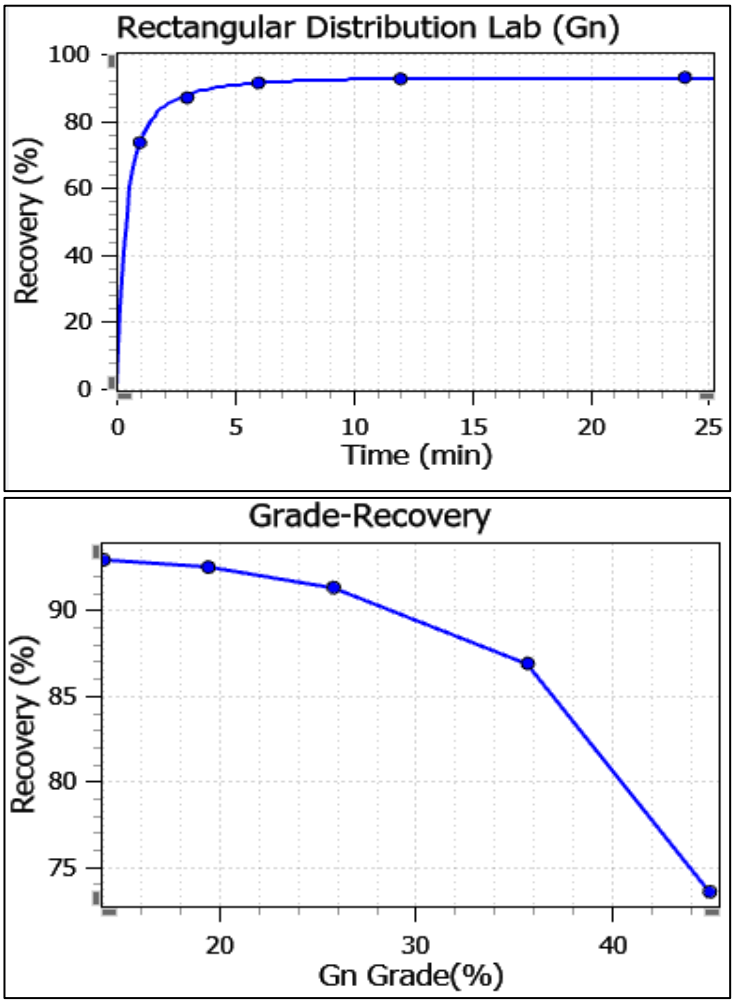

Figure 33 Kinetic curves for galena calculate by HSC Sim model fit tool

After calculating kinetic parameters for each ore type, the simulation is performed using the same flowsheet shown in Figure 32. The input parameters for the feed stream contain solids flowrate, percent solids, mineral distribution, and particle size distribution. The kinetic parameters were used in the conditioner's model. The flotation residence times were defined for each cell parameter.

The flowsheet for blends has few modifications, an example of blend I is shown in Figure 34. The feed of blend I contains 75% sorter feed and 25% malmi sample, as described in Table 7. The two different feeds are connected to a mixing unit before connecting to the conditioner. Since we have different values of kinetic parameters for each feed type, the minerals in each feed type are specified according to the sample type, an example of blend

I is shown in Table 12. The minerals of sorter products are named with (_P) to specify as minerals of the sorter product sample. The minerals of malmi sample are defined with (_M) to identify these minerals as minerals of malmi sample. The names of the minerals in each feed are modified, but the mineral composition is the same. The kinetic parameters are also described according to the minerals of each stream, shown in Table 13.

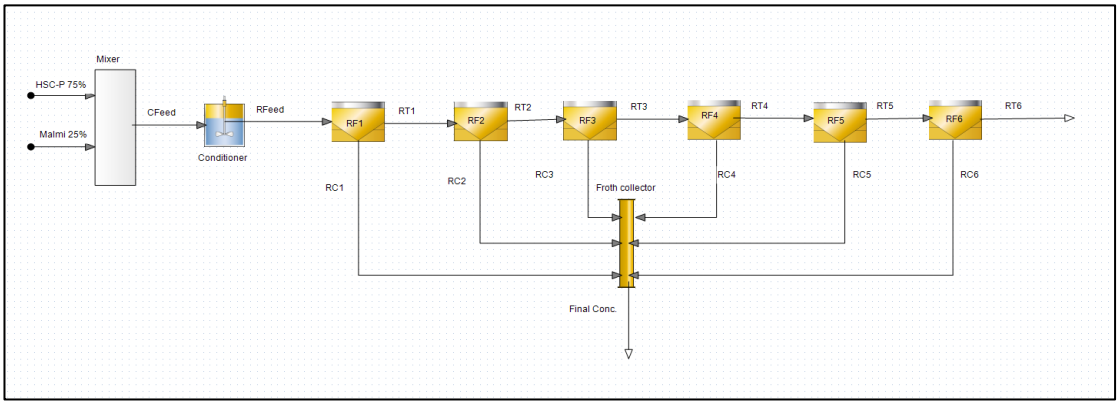

Figure 34 Simulation flowsheet for blend 1

Table 12 Minerals distribution for each feed (Blend I)

Sorter product minerals	Bulk	Unit	Malmi minerals	Bulk	Unit
Sp_P	2,913024	%	Sp_M	0,559621	%
Py_P	3,502692	%	Py_M	4,35987	%
Dys_P	0,014535	%	Dys_M	0,004996	%
Gn_P	0,780108	%	Gn_M	0,135754	%
Ccp_P	0,0804	%	Ccp_M	0,049208	%
Qtz_P	92,70924	%	Qtz_M	94,89055	%

Table 13 Distribution of kinetic parameters according to the mineral distribution of each feed type (blend I)

Rectangular Distribution	Sorter product minerals					
	Sp_P	Py_P	Dys_P	Gn_P	Ccp_P	Qtz_P
R_{inf} (%)	26,5	8,5	87,504	92,851	66,128	6,3
K_{max} (1/min)	0,377	0,331	1,63	4,031	3	0,08
	Malmi minerals					
	Sp_M	Py_M	Dys_M	Gn_M	Ccp_M	Qtz_M
R_{inf} (%)	24	6,9	81	83,6	43	3,69
K_{max} (1/min)	0,65	0,5	2,1	5,926	4,3	0,1

4 RESULTS AND DISCUSSIONS

4.1 Mineralogical studies

The mineralogical study of Sotkamo Silver's samples is conducted by Dr. Jussi Liipo, Director, Geometallurgy & Mineralogy at Metso Outotec Research Center Pori, as a part of an ongoing project and this thesis.

Four samples from Sotkamo (malmi, sorter feed, sorter product, and ore 60, cf. Table 5Table 5 for composition of each) are used for the mineralogical studies. The P80 of malmi, sorter feed, sorter product, and ore 60 are 89 µm, 82 µm, 88 µm, and 89 µm respectively, as shown in Table 14, the particle size distribution is shown in Figure 35.

Table 14 P80 of studied samples

Sample ID	P80 (µm)
Malmi	89
Sorter feed	82
Sorter product	88
Ore 60	89

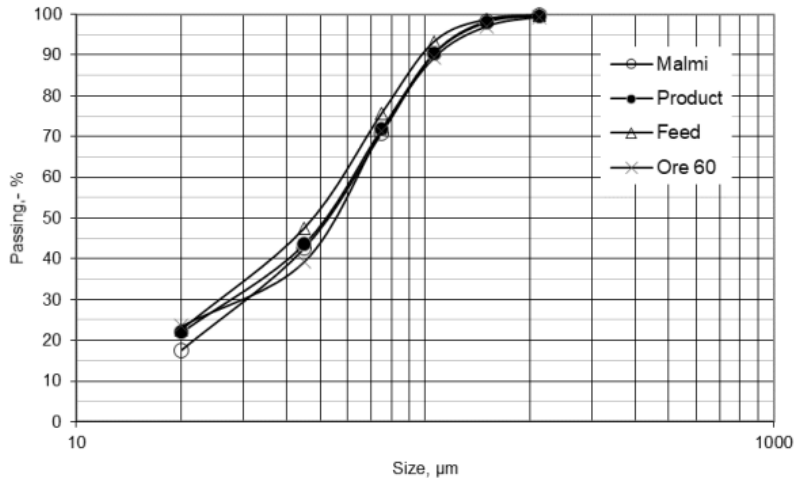

Figure 35 Particle size distribution of studied samples

4.1.1 Mineralogy

The main minerals are quartz, dolomite, muscovite, and pyrite, identified by XRD. The other minerals identified include ankerite and clinochlore. The main silver minerals include dyscrasite, freibergite, diaphorite, argentotetrahedrite. Pygrargyrite and hessite

are the minor silver minerals, while the secondary minerals include achantite, allargentum, and native silver. Galena, pyrite, and pyrrhotite also contain 920ppm, 36ppm, and 39ppm of silver. Silver minerals are primarily associated with galena. The different modes of occurrences of silver are shown in Figure 36.

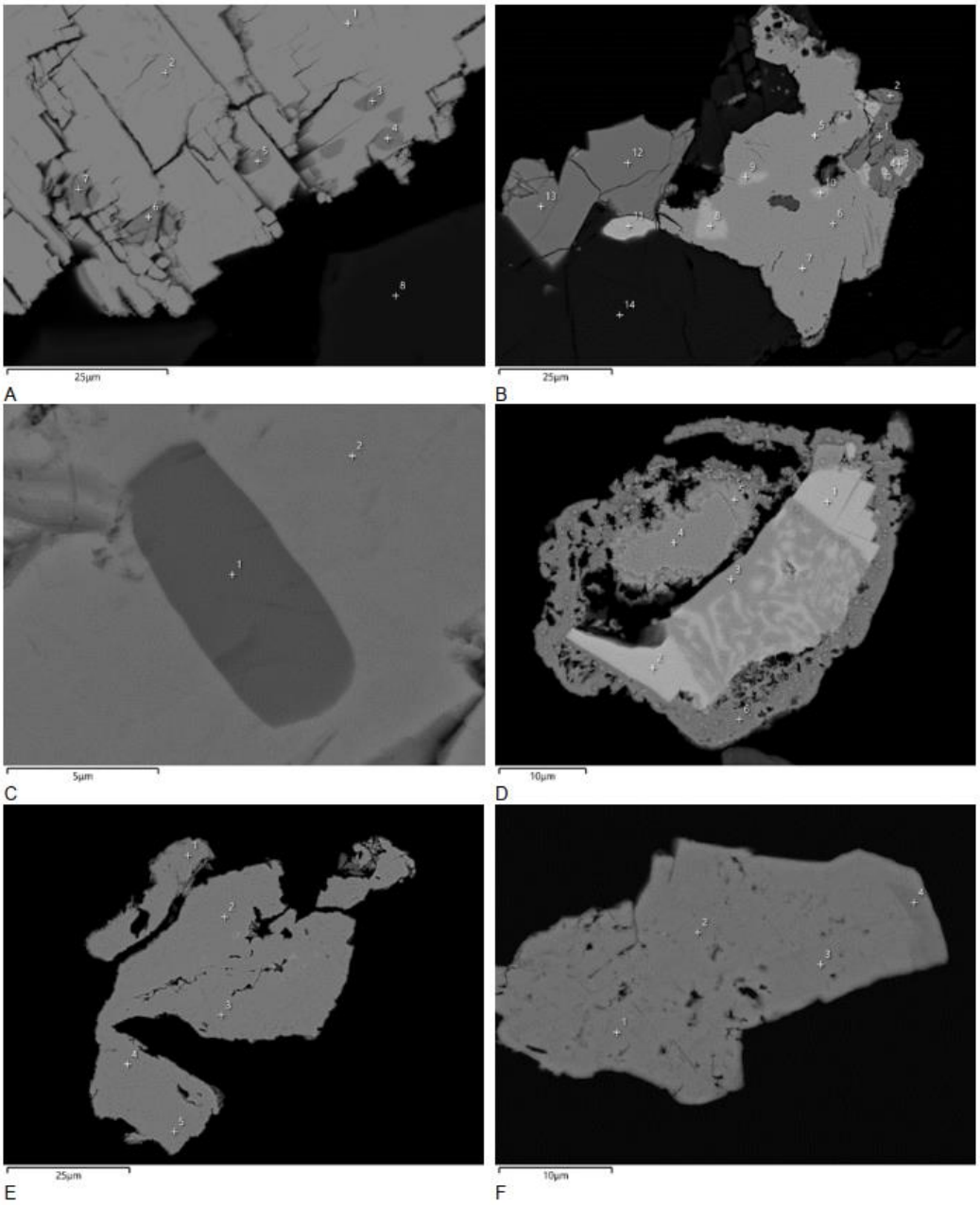

Figure 36 a) malmi, +106µm, diaphorite (3-7) inclusions in galena, b) malmi, 75/106, relatively large freibergite (1-2, 12-13), galena (3-4, 8-11) - dyscrasite (5-7) - dolomite (14) -particle, c) Sorter Product, 45/75, dyscrasite inclusions in galena, d) Sorter Product, 20/45, symplectic intergrowth of galena (1-2) and hessite (3) with dyscrasite (4)- native antimony (5)- rimmed by acanthite (6); e) Ore 60, 45/75,) allargentum (1-2) inclusions in native silver and Ore 60,20/45, liberated pyrargyrite grain

Galena is the main primary lead mineral, occurring as euhedral grains and fine grain inclusions in gangue minerals, shown in Figure 37. The composition of the galena is stoichiometric. The minor lead minerals include diaphorite and bournonite. The secondary lead minerals include hydroxylpyromorphite and mawbyite-type minerals. Alteration of galena to plattnerite is found.

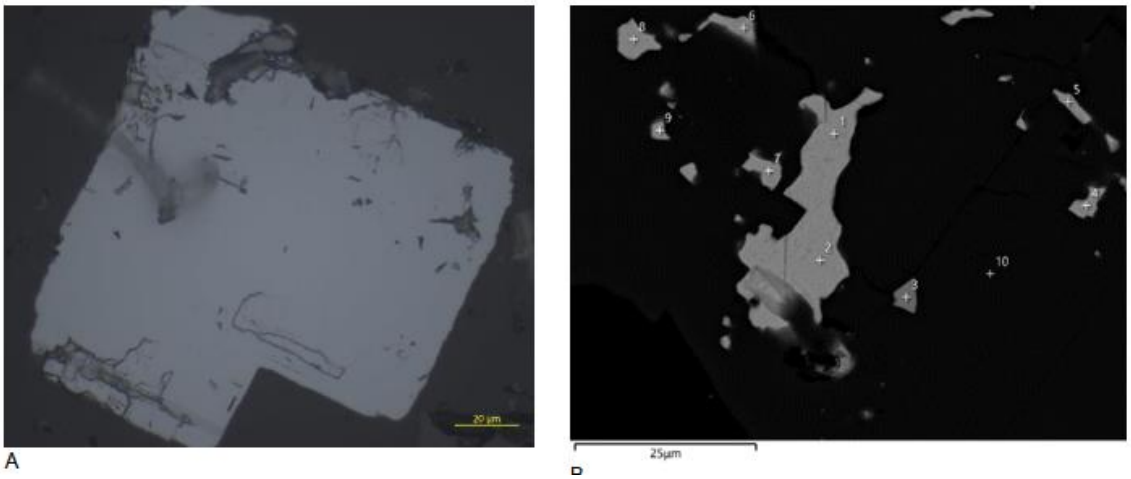

Figure 37 Sorter Product, +106µm, a) liberated euhedral galena grain and b) fine-grained galena and diaphorite inclusions in dolomite

Sphalerite is the main zinc mineral with an average iron content of 6.3%. The other impurities in sphalerite are below the analytical method's detection limit (0.1%). Other encountered minerals include abundant pyrite with accessory chalcopyrite and pyrrhotite. A minor amount of cubanite, arsenopyrite, and covellite is also found. In addition, native grains of antimony, ullmannite, and valentinite were encountered.

4.1.2 Chemical composition

The chemical composition of the studied samples was analyzed using bulk and by-size samples. The bulk malmi sample contains 43ppm silver, 0.1% lead, 0.3% zinc, and 2.3% sulfur. The distribution of main elements by size in the ore sample is shown in Figure 38.

It is observed that the silver and lead minerals are enriched in the finest size fraction while the iron is enriched in the coarsest size fraction.

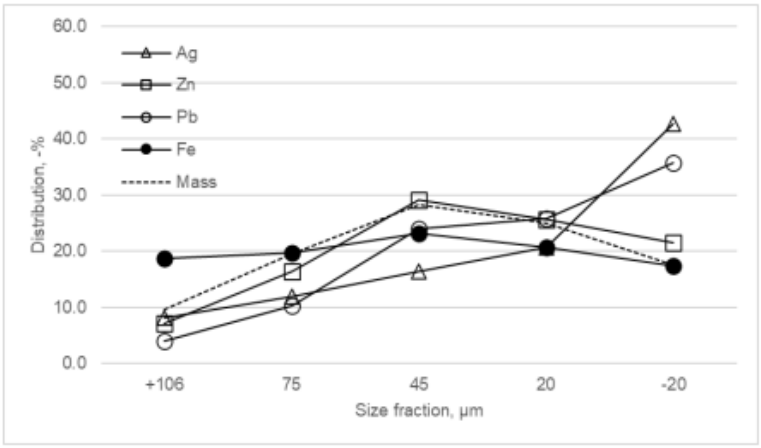

Figure 38 Mass distribution of main elements by size in the malmi sample

Sorter feed bulk sample contains 48ppm silver, 0.2% lead, 0.6% zinc, and 1.9% sulfur. The mass distribution of main elements by size is shown in Figure 39. A similar trend of higher concentration of silver and lead mineral in finest size fraction is found, while the iron is enriched in coarsest size fraction.

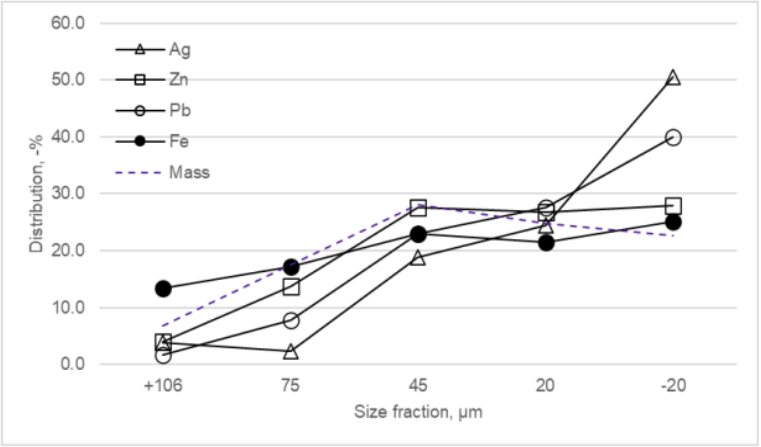

Figure 39 Mass distribution of main elements by size in the sorter feed sample

The bulk sample of the sorter product contains 129ppm silver, 0.6% lead, 1.7% zinc, and 3.1% sulfur. The mass distribution of main elements by size is shown in Figure 40. The silver and lead are enriched in the finest size fraction, while the iron is enriched in the coarsest size fraction.

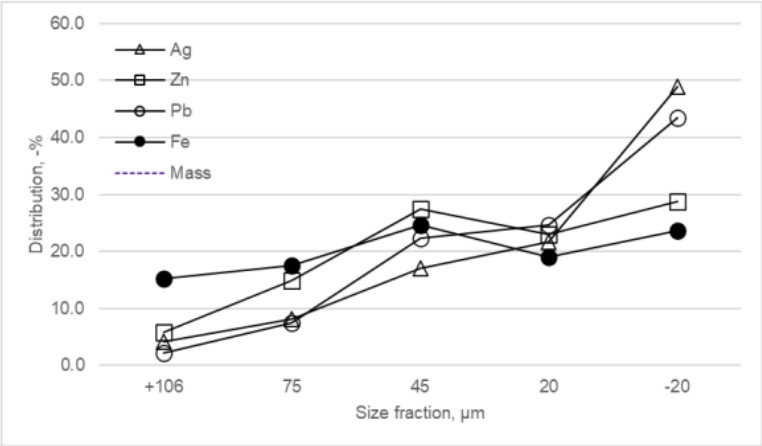

Figure 40 Mass distribution of main elements by size in the sorter product sample

The bulk sample of ore 60 contains 170ppm silver, 0.3% lead, 0.87% zinc, and 1% sulfur. Compared to other samples, ore 60 has higher silver, zinc, and lead content while lower sulfur content. The mass distribution main elements by size are shown in Figure 41. Silver and lead are enriched in the finest size fraction, while iron and zinc are enriched in the coarsest size fraction.

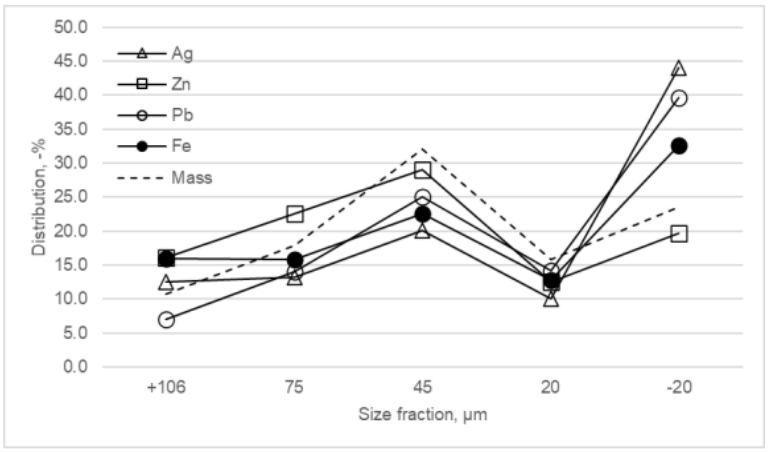

Figure 41 Mass distribution of ore 60 sample by size

4.1.3 Mineral composition

All four sample from Sotkamo Silver contains quartz, muscovite, dolomite, and pyrite as the main sulfide mineral, as shown in Table 15. Dyscrasite is the main silver mineral carrying 93% of the silver. While remaining 7% silver is distributed in galena and pyrite. Galena and sphalerite are the main lead and zinc minerals. The lead and zinc oxide minerals carry 0.6-21.5% lead content and 0.7-15.9% zinc content. Ore 60 has lower pyrite and dolomite content while higher quartz and muscovite content than other

samples. As a comparison between sorter feed and sorter product, the sorter product has higher grades of valuable minerals. Due to pre-sorting sum of valuable minerals improved from 1.25% to 3.52%.

Table 15 Mineral composition of bulk samples, ore represents malmi sample

Sample / Mineral composition		Malmi	Sorter feed	Sorter product	Ore 60
Dyscrasite	ppm	54	60	162	224
Galena	%	0,092	0,234	0,700	0,286
Plattnerite	%	0,025	0,020	0,004	0,043
Sphalerite	%	0,407	0,941	2,748	1,418
Zincite	%	0,058	0,057	0,053	0,008
Pyrite	%	3,62	2,54	3,27	0,93
Pyrrhotite	%	0,47	0,49	0,81	0,05
Chalcopyrite	%	0,02	0,03	0,05	0,04
Arsenopyrite	%	0,15	0,03	0,13	0,00
Muscovite	%	22,59	21,16	18,60	26,38
Dolomite	%	9,21	5,6	9,98	1,84
Quartz	%	63,35	68.9	63,64	68,99

Malmi sample contains 54ppm dyscrasite, 0.09%, 0.4% sphalerite and 3.6% pyrite. Dyscrasite and galena are in higher content in the finest fraction. While the coarsest size fraction has enriched pyrite, shown in Figure 42.

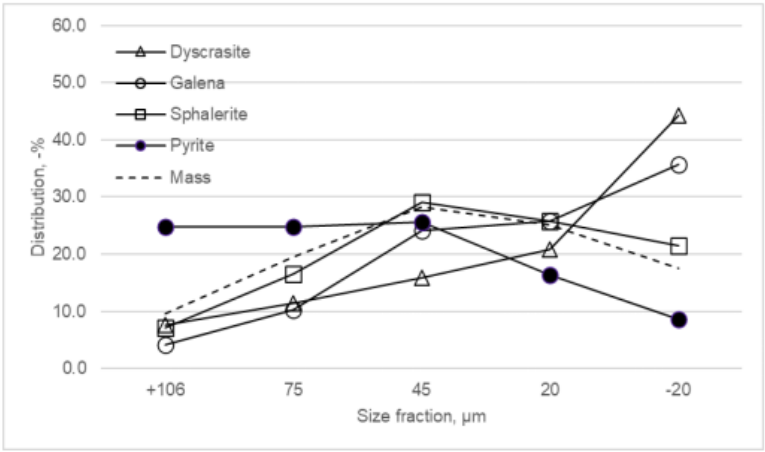

Figure 42 Distribution of the main mineral in malmi sample

Figure 43 demonstrates the distribution of main minerals by size in sorter feed. This sample contains 60ppm dyscrasite, 0.2% galena, 0.9% sphalerite and 2.5% sphalerite. The

main mineral distribution by size is shown in Figure 43. A similar trend of enriched dyscrasite and galena is found in the finest fraction.

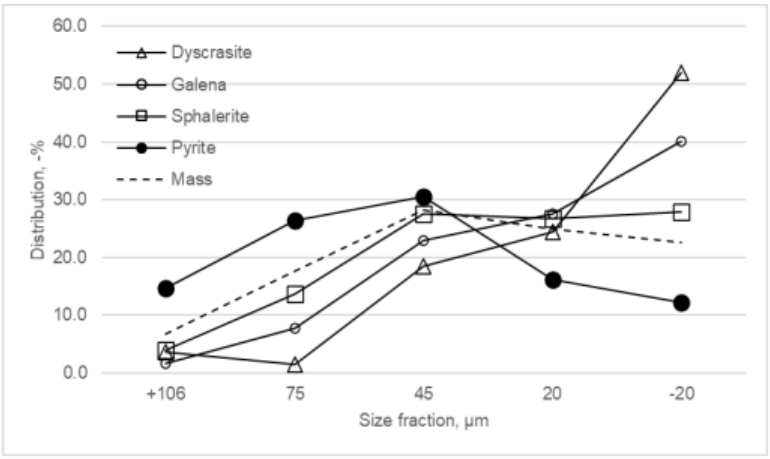

Figure 43 Distribution of main minerals by size in sorter feed

Sorter product contains 162ppm dyscrasite, 0.7% galena, 2.7% sphalerite and 3.3% pyrite. The distribution of main minerals by size is shown in Figure 44. Dyscrasite and galena are enriched in the finest size fraction, while pyrite is enriched in the coarsest size fraction.

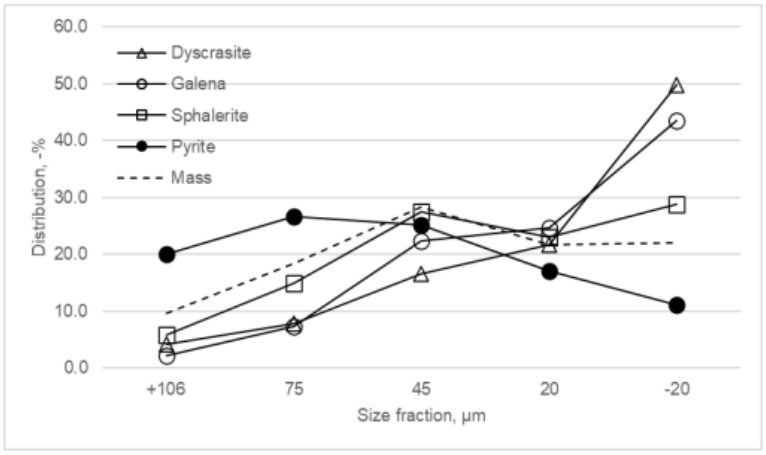

Figure 44 Distribution of main minerals by size in sorter product

Ore 60 bulk sample contains 224ppm dyscrasite, 0.3% galena, 1.4% sphalerite and 0.9% pyrite. The distribution of main minerals by size is shown in Figure 45. Dyscrasite and galena re enriches in the finest size fraction, while pyrite is enriched in the coarsest size fraction. The finest size fraction has a negligible content of pyrite. The coarsest size fraction has lower sphalerite, galena, and dyscrasite content.

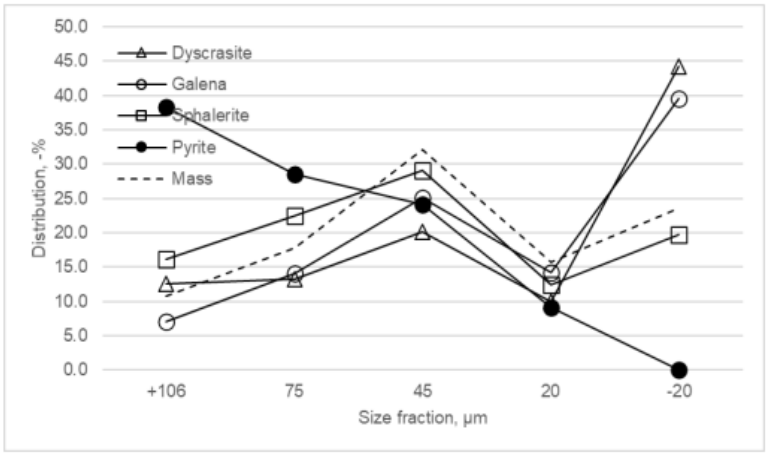

Figure 45 Distribution of main minerals by size in ore 60

Diagnostic EDTA leaching results represent the degree of oxidation in all four bulk samples, shown in Figure 46. It is observed that the galena and sphalerite in malmi sample are relatively more oxidized as compared to ore 60 and other samples. However, Ore 60 has higher oxidation of lead mineral and lowest oxidation of zinc mineral. Sorter product contains the lowest oxidation of lead and zinc minerals.

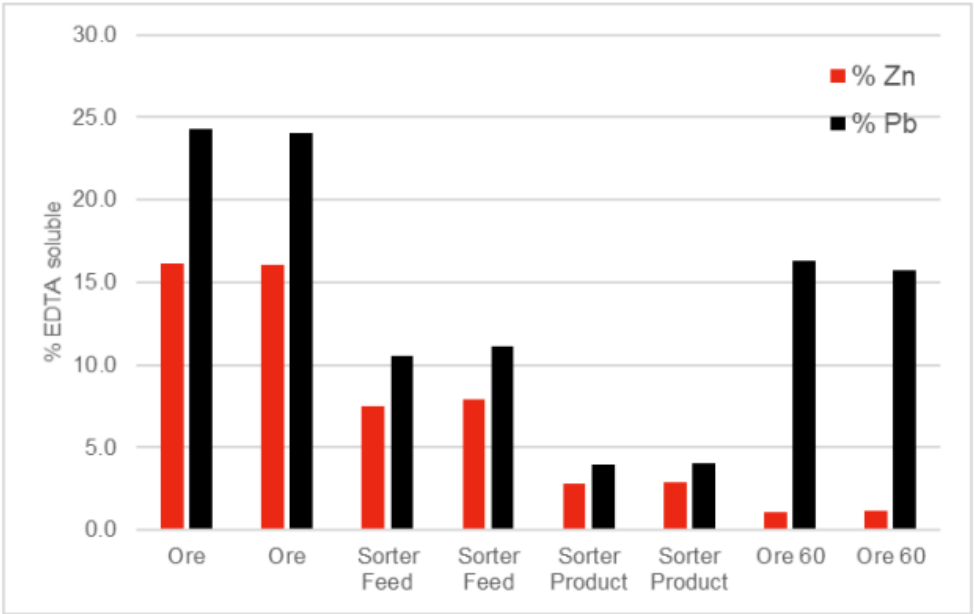

Figure 46 EDTA analysis for zinc and lead, based on duplicate samples, ore represents malmi sample

4.2 Mergan grindability tests

The mergan grindiability tests for four Sotkamo Silver's ore (Malmi, sorter feed, sorter product, and ore 60) samples were conducted by Mr. Hannu Heiskari, Research and

Process Support Engineer at Metso Outotec Research Center Pori. The tests aim to compare the grinadability of different samples, calculating specific grinding energy for required p80, and estimate bond ball mill work index for each sample. The samples were prepared to have a fineness of 100% -3.35mm. The target P80 is 90 µm. The particle size distribution of each sample is calculated using 3350, 2360, 1180, 600, 300, 150, 106, 90, and 75 µm sieves. The P80 is shown in Table 16. The specific grinding energy and P80 after 300, 600, and 900 revolutions are calculated. The plot between specific grinding energy and P80 is shown in Figure 47. This model between specific grinding energy and p80 calculates the required specific grinding energy for p80 of 90µm. The specific grinding energy for required P80, operating work index, and estimated bond work index is shown in Table 16.

It is observed that there is no variability in the grindability of the sorter feed and sorter product sample. However, the malmi sample requires approximately 10% less energy than sorter feed and sorter product. Ore 60 requires less energy to grind and hence the softest sample among others with an approximate bond work index value of 4 kWh/t. The approximate bond work index value for sorter feed and sorter product is 7.5 kWh/t. The bond work index value of the malmi sample is 6.7 kWh/t. Based on the results, all the samples can be considered soft in terms of grinding.

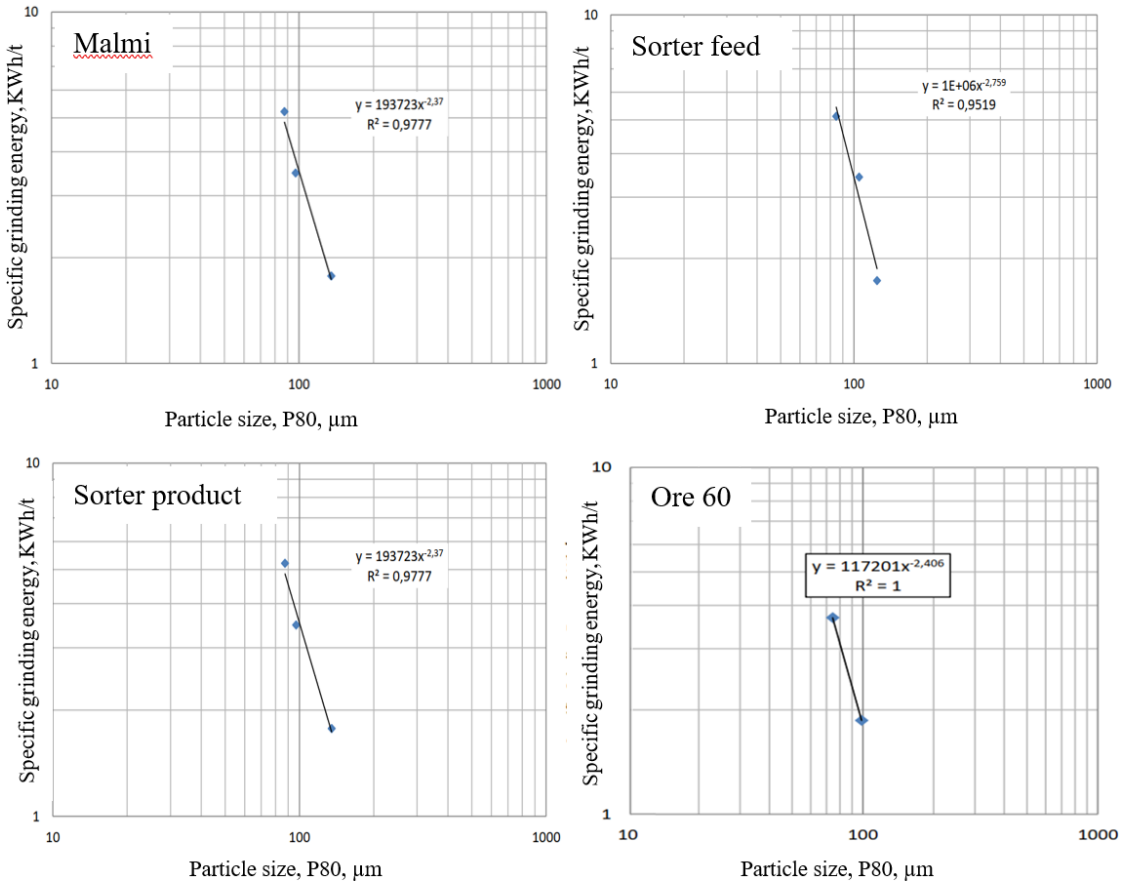

Figure 47 Specific grinding energy vs p80 for all four samples

Table 16 Mergan test results

Sample ID	Malmi	Sorter feed	Sorter product	Ore 60
F80 (µm)	1516	1457	1353	1734
P80 (µm)	90	90	90	9000
Specific grinding energy (SGE, kWh/t)	4.13	4.57	4.53	2.33
Operating work index (kWh/t)	5.18	5.77	5.79	2.87
Bond work index estimation (kWh/t)	6.7	7.5	7.5	3.7

4.3 Grinding calibration tests

Grinding calibration tests were conducted for each ore sample to calculate the required grinding for P80=90µm. Each sample is ground for 5, 10, and 20 minutes and P80 is calculated for each grinding time. Ore 60 sample was ground for 5, 10, and 15 minutes since the required P80 was obtained below 10 minutes of grinding. The P80 for each ore and grinding time is shown in Table 17. A model is generated for each ore type, shown in Figure 48 and Figure 49. This model for each ore type is used to calculate the grinding

time for P80 around 90 µm, shown in Table 18. According to the model, the malmi sample needs 12 minutes of grinding to get P80 of 90,1 µm. Sorter feed, sorter product, and ore 60 require 13, 14, and 9 minutes to get P80 of 90.8, 88.8, and 88.6 µm, respectively. To validate the models, one extra grinding test is conducted for each ore type, shown as triangular points in Figure 48 and Figure 49 where the experimental P80 matches the modeled P80 for that grinding time.

Table 17 Grinding time and P80 for each ore type

	Grind time (min)	P80 (µm)
Malmi	5	109
	10	95
	20	75
	12	91
Ore 60	5	103
	10	87
	15	75
	9	89
Sorter Feed	5	118
	10	99
	20	78
	15,5	82
Sorter Product	5	127
	10	101
	20	78
	14	91

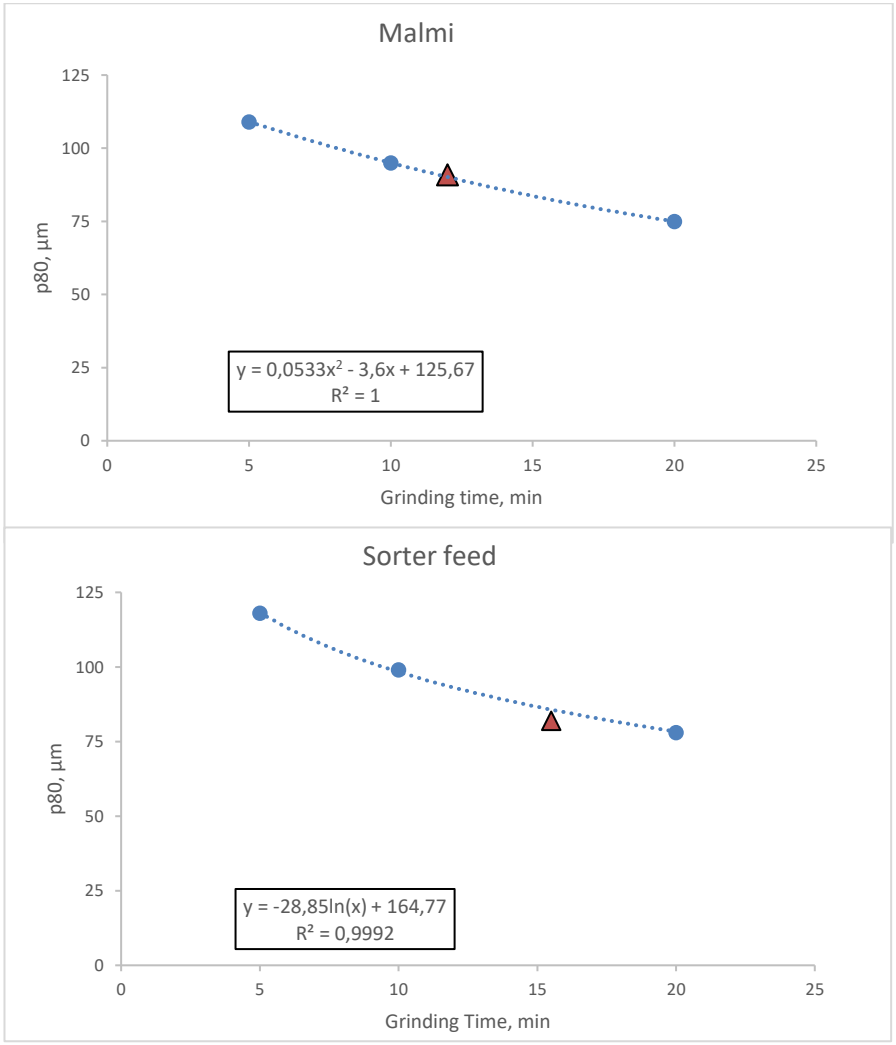

Figure 48 P80 vs grinding time for malmi and sorter feed

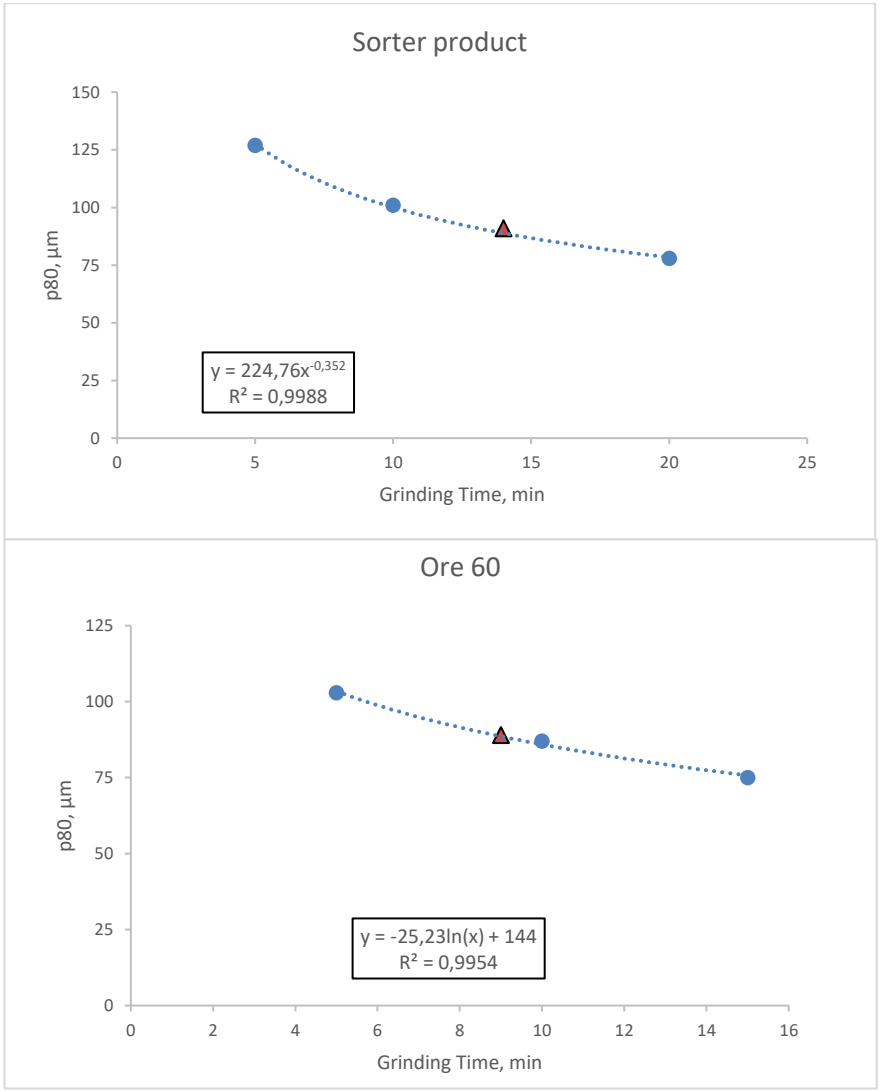

Figure 49 P80 vs grinding time for sorter product and ore 60

Table 18 Grinding time for required p80 of each ore sample

Sample ID	Grinding time (min)	P80 (um)
Malmi	12	90.1
Sorter feed	13	90.8
Sorter product	14	88.8
Ore 60	9	88.6

4.4 Reference flotation tests

Kinetic flotation tests are conducted for each ore type following the reference reagent recipe stated in Table 6, and the flowsheet showed in Figure 32. The flotation kinetic parameters for main minerals in all four samples are shown in Table 19.

Table 19 Flotation kinetic parameters for reference flotation tests

		Sphalerite	Pyrite	Dyscrasite	Galena	Chalcopyrite	NSG
Malmi	R_{Inf}	24	6,9	81	83,6	43	3,69
	k_{Max}	0,65	0,50	2,10	5,93	4,30	0,10
Sorter feed	R_{Inf}	39,0	10,3	84,2	95,2	50,1	5,7
	k_{Max}	0,46	0,36	1,50	4,09	2,40	0,07
Sorter product	R_{Inf}	25,3	7,9	88,7	95,8	66,4	5,0
	k_{Max}	0,17	0,12	1,07	2,59	2,28	0,05
Ore 60	R_{Inf}	34,5	25,8	78,5	60,3	51,2	4,1
	k_{Max}	0,55	0,40	1,00	2,50	2,00	0,12

The graph of mass pull versus flotation time for each sample is shown in Figure 50. It is observed that the mass pull of sorter feed, sorter product, and ore 60 is similar and the final mass pull at 24 minutes of flotation is in the range of 3.76-3.87%. Malmi sample has a lower mass pull than other samples, with a value of 2.83% in the final concentrate. The lower mass pull of the malmi sample is due to the lower content of sulfide ore minerals and higher oxidation.

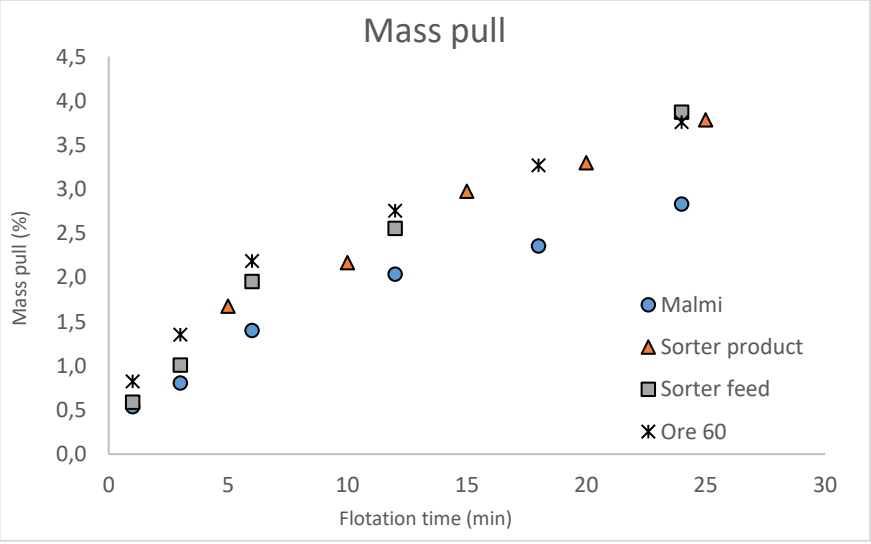

Figure 50 Mass pull for reference flotation tests

The recoveries of dyscrasite in all four flotation tests are shown in Figure 51. The recovery of dyscrasite in the final concentrate of sorter product is 88.0%, the highest as compared to other samples. 80.55 and 83.20% dyscrasite is recovered in the final concentrate of malmi and sorter feed sample, respectively. The recovery of dyscrasite in the final concentrate of ore 60 sample is 77.11%. The highest recovery of dyscrasite reflect the silver minerals are associated with galena particularly sorter product (0.61% Pb). The ore 60 with high silver grade but low lead grade and oxidized galena resulted in lowest recovery of dyscrasite. Also, there is high muscovite content (26.38%, shown in Table 15) on the ore 60 that could be coating particles (as a thin layer), reducing the recovery and competition of adsorption of collector.

The Ag grade in malmi and sorter feed sample is lower, with a value of 43 and 48 ppm respectively, hence the recovery of dyscrasite is 5% less than sorter product. The grade-recovery curves for dyscrasite are also shown in Figure 52. Malmi and sorter feed samples are similar in terms of grade and recovery. The dyscrasite grades in the final concentrates of sorter product and ore 60 are 0.38% and 0.43%, respectively. The higher concentrate grade of dyscrasite in the sorter product is due adequate flotation condition for selective flotation of lead and silver minerals. In case of Ore 60, the higher concentrate grade of dyscrasite could be due to liberated silver minerals, and secondary silver minerals which float selectively and are not associated with oxidized galena.

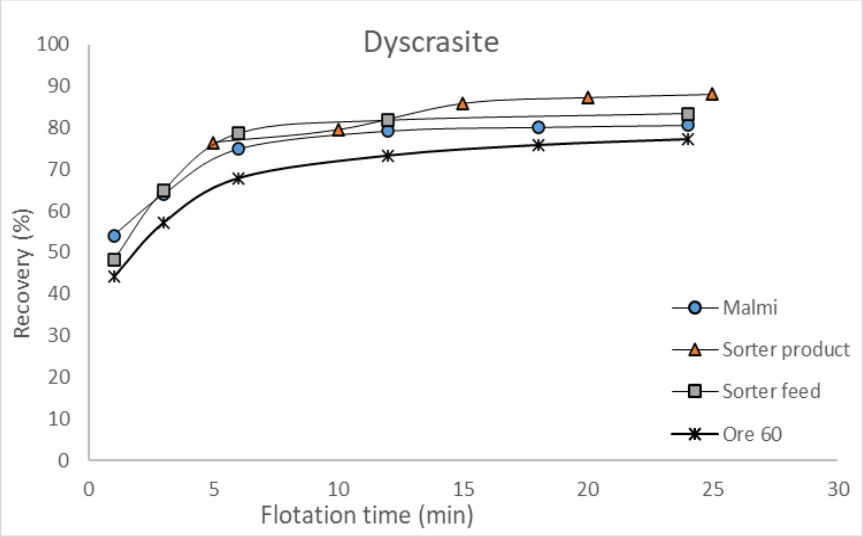

Figure 51 Recoveries of dyscrasite in reference flotation tests

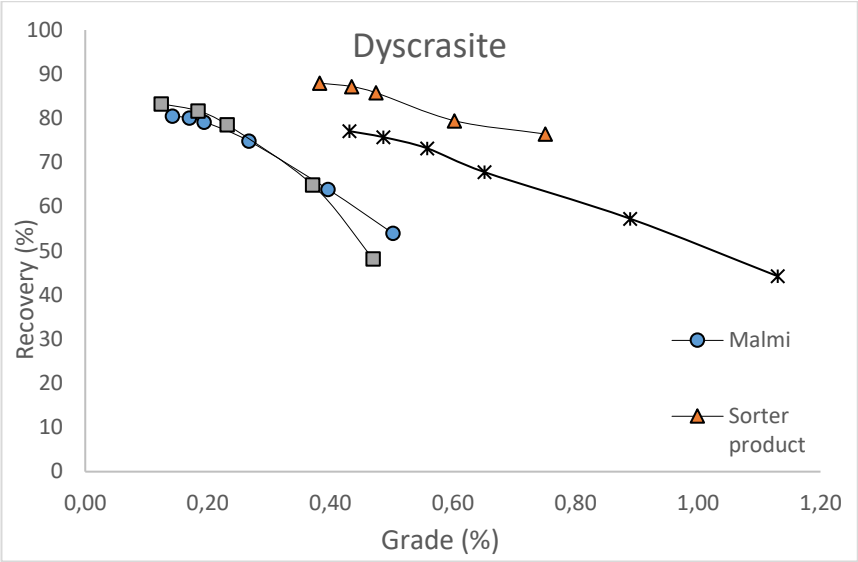

Figure 52 Grade-recovery curves of dyscrasite in reference flotation tests

The recoveries of galena in each reference flotation test are shown in Figure 53. About 95% galena is recovered in the samples of sorter feed and sorter product. The maximum recovery of galena in the final concentrate of malmi sample is 83.5%. The lower recovery of galena in malmi sample is due to the highest oxidation (up to 25%) of galena in the malmi sample, shown in Figure 46. The other reason for the lower recovery of galena is the lead grade of 0.1% in the malmi feed, while the lead grades in the sorter feed and sorter product are 0.22 and 0.61%. The recovery of galena in ore 60 is more complicated, and the maximum recovery in the final concentrate is 60.5%. The ore 60 has about 16% oxidation of lead, causing a lower recovery of galena. The other reason for the most inadequate recovery of galena in ore 60 is the presence of slimes during the flotation. The slimes in ore 60 resulted due to the 26.38% muscovite, oxidation, and lowest bond work index of ore 60 sample. It is also observed that the infinity recovery for galena is reached for all samples due to higher flotation rate constants, shown in Table 19.

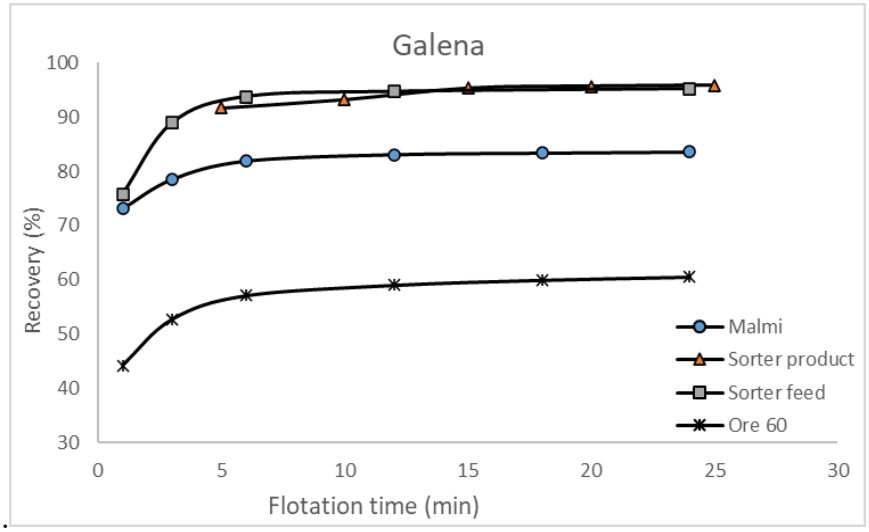

Figure 53 Recoveries of galena in reference flotation tests

The grade recovery curves of galena in reference flotation tests are shown in Figure 54. The grade of galena in the final concentrate of the sorter product is 19.11%. At the same time, the grade of galena in the final concentrate of the sorter feed is about 6%. The reason behind similar recoveries and different grades of galena in sorter feed and sorter product is the grade of lead in the feed samples. Sorter product has about three times higher feed grade of lead (0.61%) than the galena grade in sorter feed (0.22%). The malmi sample has the lowest galena grade of 4% in the final concentrate because of the lowest lead grade of 0.1% in the feed. The grade of galena in the final concentrate of ore 60 is 5.3%.

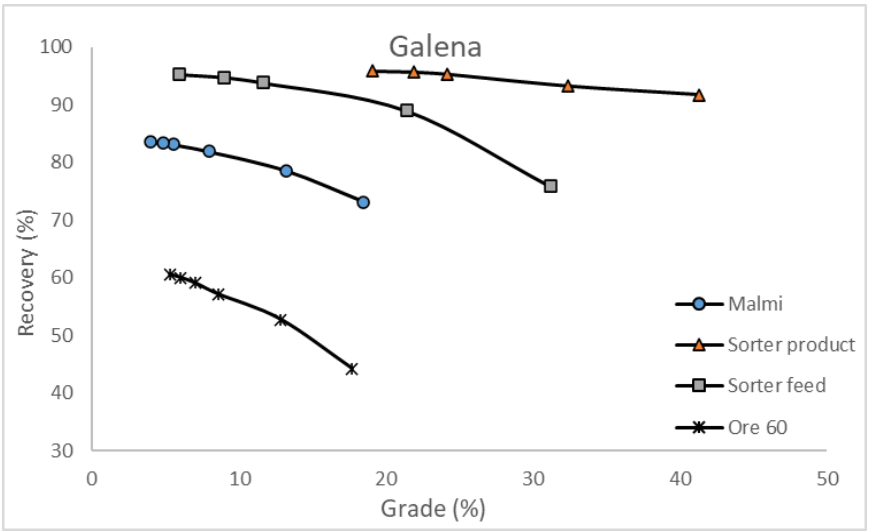

Figure 54 Grade-recovery curves of galena in reference flotation tests

The recoveries of sphalerite in each ore type are shown in Figure 55. The sorter feed sample has the highest recovery of sphalerite (36.5%) in the final concentrate. The recovery of sphalerite in the final concentrate of ore 60 is about 33%. The recoveries of sphalerite in malmi and sorter product are 23.3% and 20.3%, respectively. The higher recovery of sphalerite in ore 60 is due to the higher oxidation and presence of slimes. In this oxidized sample, the sphalerite surface is activated due to the presence of ions and slimes, affecting the efficiency of the collector and depressant. Sorter product sample is least oxidized; hence depression of sphalerite is effective. Despite the higher oxidation of malmi sample, the lower recovery of sphalerite is due to the lowest zinc grade (0.3%) in the malmi sample. These sphalerite recoveries are acceptable at this stage because the cleaner circuit is not included in this studies and sphalerite is further depressed using sodium cyanide.

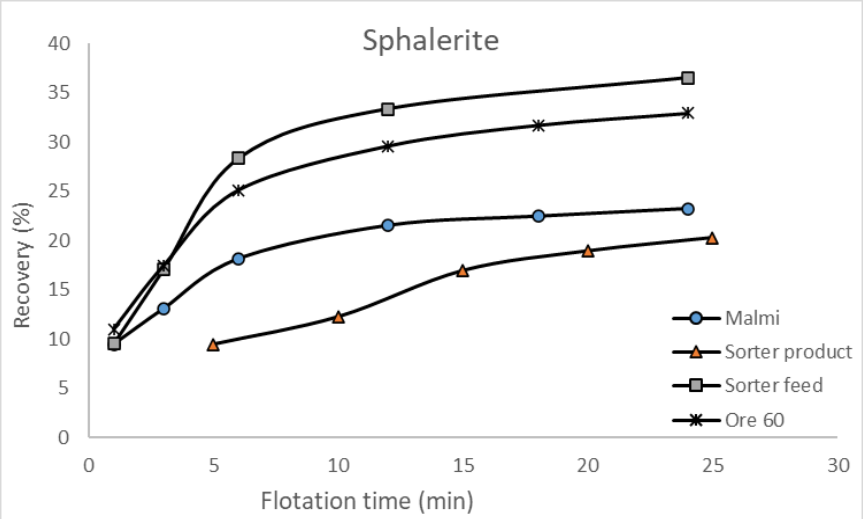

Figure 55 Recoveries of sphalerite in reference flotation tests

The Grade-recovery curves of sphalerite in reference flotation tests are shown in Figure 56. The malmi sample has the lowest grade (4.6%) of sphalerite in the final concentrate. The zinc grade in the malmi feed is the lowest with a value of 0.3%. The sequence of zinc grades in the fee are malmi < sorter feed < ore 60 < sorter product. A similar sequence of zinc grade is found in the final concentrate i.e. malmi < sorter feed < ore 60 < sorter product. The grade of zinc in the feed is determining the grade of zinc in the final concentrate.

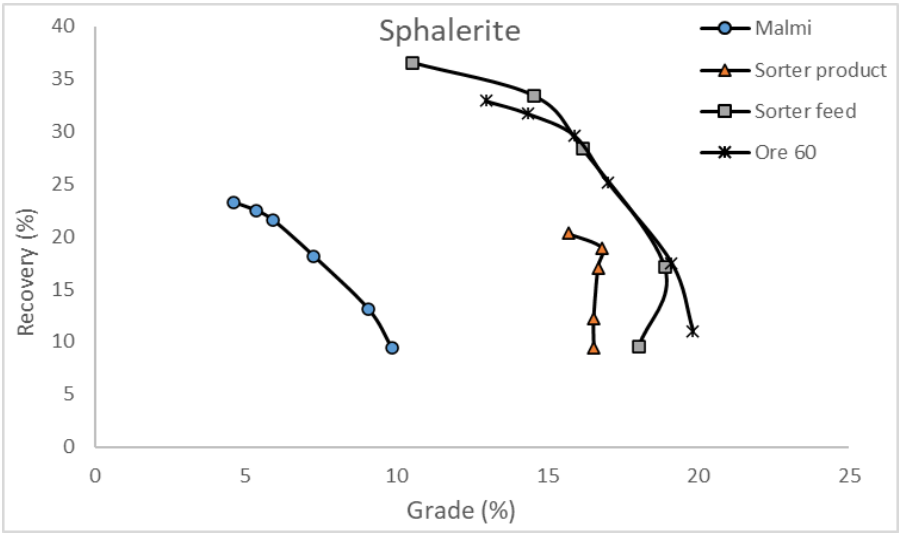

Figure 56 Grade-recovery curves of sphalerite in reference flotation tests

The recoveries of pyrite in each reference flotation test are shown in Figure 57. The recoveries of pyrite in sorter product, sorter feed, and malmi samples are 5.7%, 9.4%, and 6.5%, respectively. The depression of pyrite in these three samples is good at the pH of 11.5-12. The lowest pyrite recovery in the final concentrate of the sorter product resulted from the lowest oxidation.

The recovery of pyrite in the final concentrate of ore 60 is 24.1%. The activation of pyrite in ore 60 resulted due to higher oxidation and the presence of slimes. Due to the presence of slimes, the reagent's efficiency decreased. Due to the higher oxidation of ore 60, the pH during the flotation decreased up to 11 which caused activation of pyrite. Another reason for the highest pyrite recovery in ore 60 is the distribution of pyrite in ore 60. About 60% pyrite is distributed in the +75µm size fraction. The presence of sulfides in this size fraction of oxidized ore has more probability of floating.

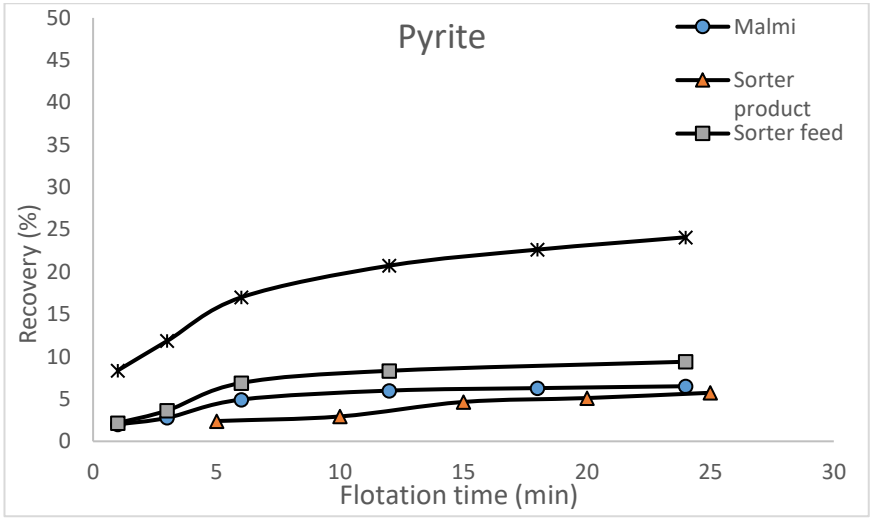

Figure 57 Recoveries of pyrite in reference flotation tests

The grade-recovery curves of NSG are shown in Figure 58. Sorter product and malmi samples have a similar gangue recovery of 2.4% in the final concentrate. The grades of NSG in the final concentrates of sorter product and malmi samples are 58% and 80.5%, respectively. A higher grade of NSG in the final concentrate of malmi sample resulted from higher oxidation of malmi sample and fewer sulfide minerals compared to the sorter product. Sorter feed and ore 60 samples showed a similar grade-recovery curve of NSG. The grades of NSG in the final concentrates of sorter feed and ore 60 are 3.1% and 2.9%, respectively. The recoveries of NSG in the final concentrates of ore 60 are about 76% and 74%, respectively. The similar grade-recovery curves of sorter feed and ore 60 resulted from 5% higher NSG content in ore 60 feed and higher oxidation of ore 60 sample than the sorter feed sample.

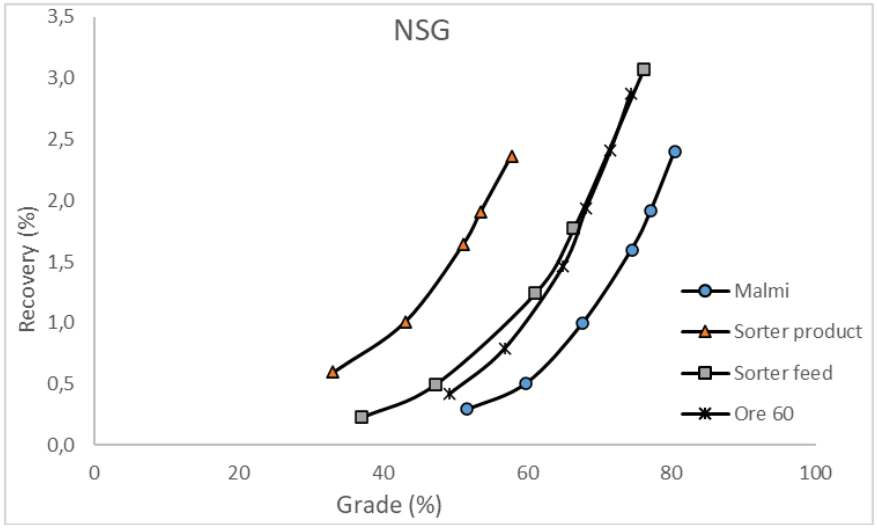

Figure 58 Grade-recovery curves of NSG in reference flotation tests

The galena-sphalerite selectivity curves are shown in Figure 59. These curves are essential since we are floating galena and depressing sphalerite in this rougher-scavenger circuit. The sorter product has an efficient galena-sphalerite selectivity curve with a maximum galena recovery of 95.8% and the lowest sphalerite recovery of 20.3%. Malmi sample has 3% higher sphalerite recovery but about 10% lower recovery of galena than the sorter product sample. Sorter feed and sorter product have higher sphalerite recoveries of 33-37%, but the galena recovery in sorter feed is about 95%, similar to sorter product. Ore 60 has the lowest galena recovery of 60.5% and almost 35% of sphalerite.

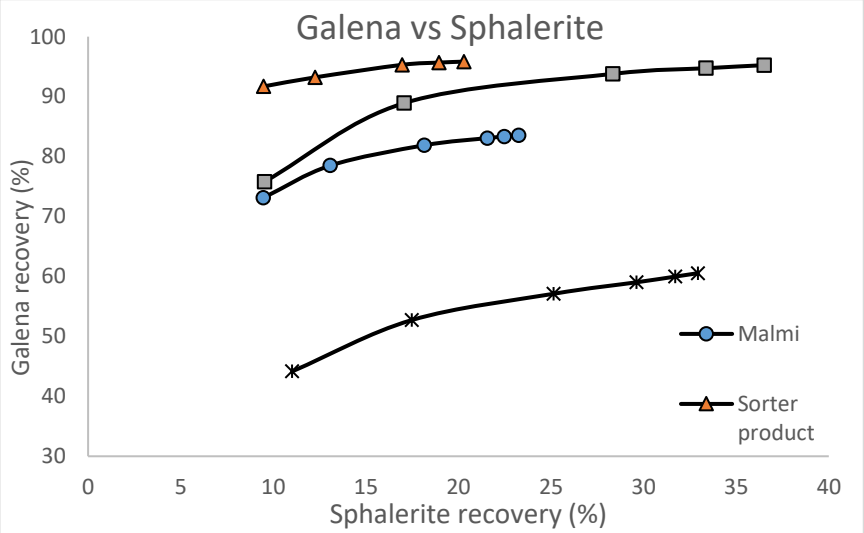

Figure 59 Galena vs sphalerite selectivity curves for each sample

The flotation results are validated by comparing bulk grades with back-calculated grades, shown in Figure 60. The R^2 varies between 0.90 to 1. The R^2 of Pb and Zn are close to 1, showing a good correlation.

The data tables for flotation results are shown in appendix C.

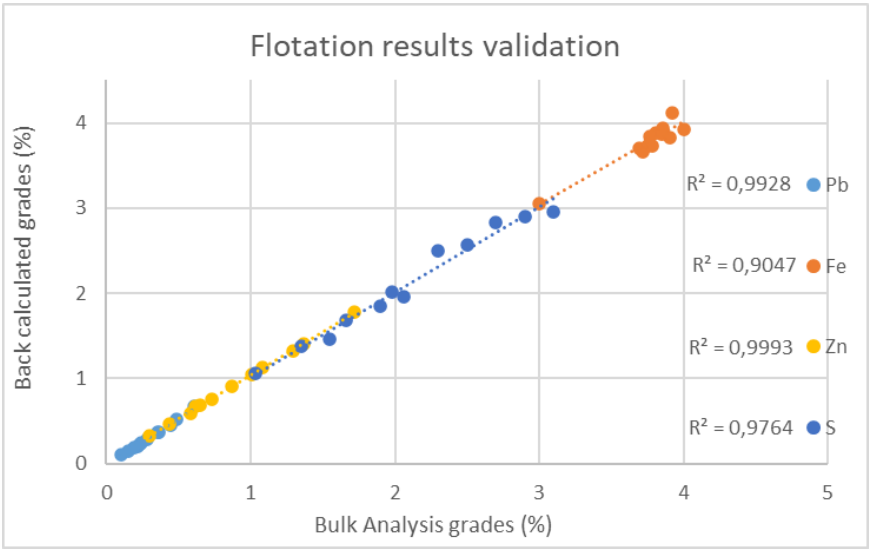

Figure 60 Flotation results validation

4.5 Simulation of reference flotation tests

The simulation results of reference flotation tests are promising and well correlated to the experimental flotation tests. In this part, a comparison between simulated and experimental flotation tests is made. Data tables are shown in appendix E.

A comparison between the simulated and experimental mass pulls of all four samples is shown in Figure 61. The simulated mass pull is represented by a solid line with cross points, while the triangular points represent the experimental mass pull. The overall experimental mass pulls fit well to the simulated mass pulls. The mass pulls in all four samples are in the range of 3-4%.

More specific observations show that the simulated mass pulls of malmi sample correlate to the experimental mass pulls with R^2 values of 0.9922. The experimental mass pull in malmi at 18 minutes of flotation is slightly lower than the simulated mass pull. The simulated mass pulls of the sorter product sample also show a good fit to the experimental mass pulls with a R^2 value of 0.9898, a slight deviation of mass pull at 10 minutes of flotation caused a slightly lower R^2 value. The same trend can be observed for ore 60 and sorter feed with R^2 values of 0.9925 and 0.9898, respectively. Overall, the simulated mass pulls fit the experimental mass pulls with R^2 ranging from 0.9844 to 0.9925.

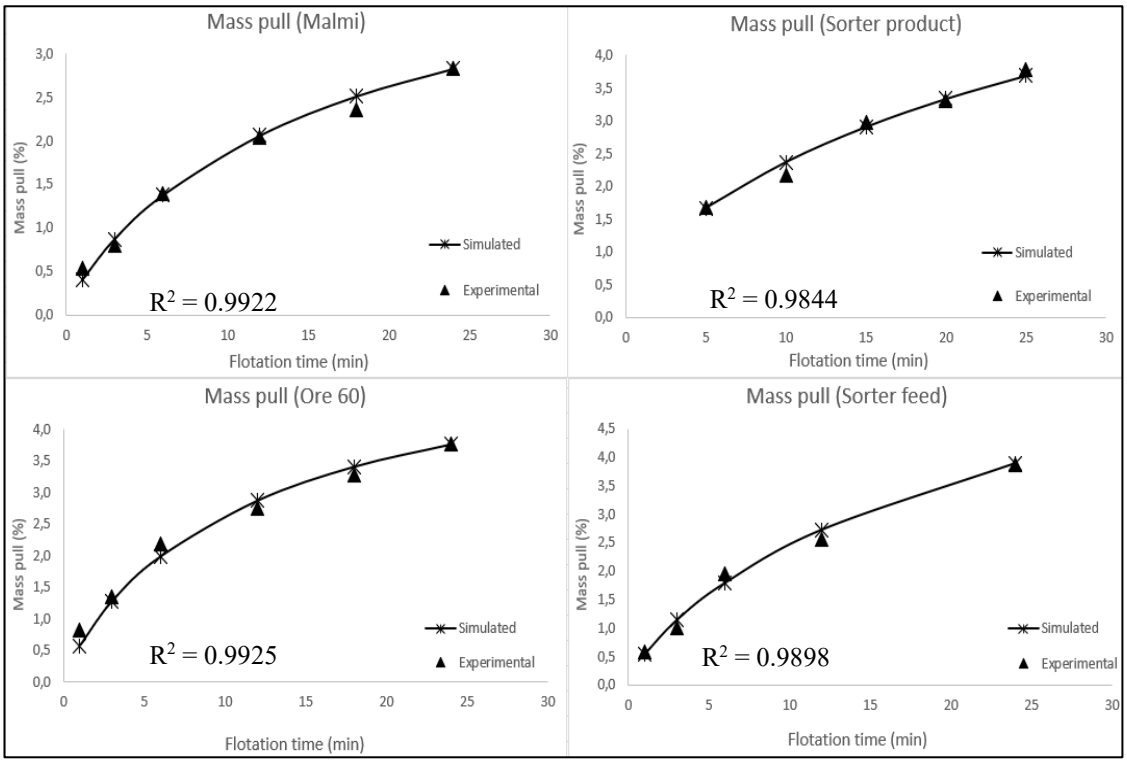

Figure 61 Comparison between the simulated and experimental mass pull of four Sotkamo Silver's samples

4.5.1 Malmi samples

The comparisons between experimental and simulated grades and recoveries of dyscrasite and galena are shown in Figure 62. The kinetic rate of simulated recoveries of dyscrasite is slightly faster than the experimental recoveries. Still, after 10 minutes of flotation, the simulated and experimental recoveries show a good fit with an overall R^2 value of 0.9125. The experimental and simulated grades of dyscrasite offer a good fit with R^2 value of 9812, except for the first point where the simulated grade is about 0.1% higher than the experimental grade. A similar trend can be observed for the galena grade and recovery with R^2 values of 0.9595 and 9311, respectively.

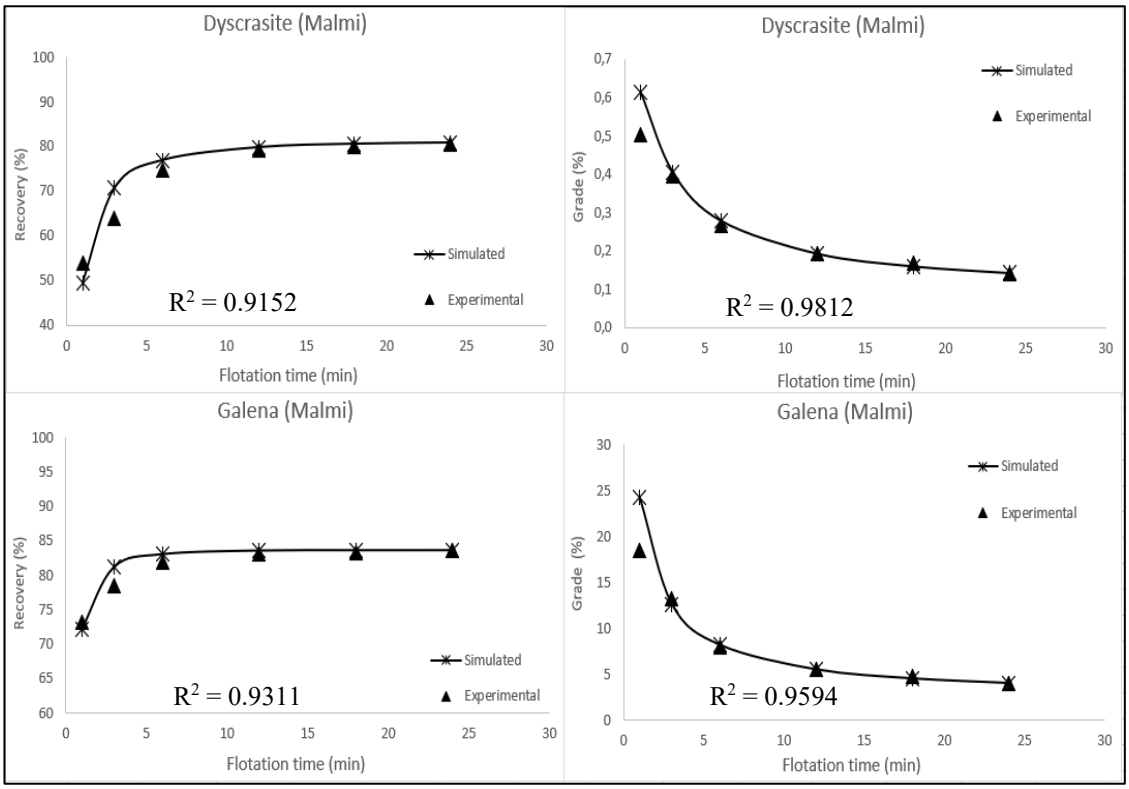

Figure 62 Comparison between experimental and simulated grade and recovery of dyscrasite and galena in ore samples

The comparisons between simulated and experimental grades and recoveries of sphalerite and NSG are shown in Figure 63. The comparison between experimental and simulated recoveries of sphalerite shows a good fit with R^2 value of 0.9682. This R^2 value resulted from the deviation of the first point where the simulated recovery is slightly lower than the experimental recovery. A similar trend can be observed in the sphalerite grade, with an R^2 value of 0.9814. The first point has a slightly lower simulated grade than the experimental grade of sphalerite. The simulated grades and recoveries of NSG show a better fit to the experimental observations with R^2 values of 0.9913 and 0.9931, respectively.

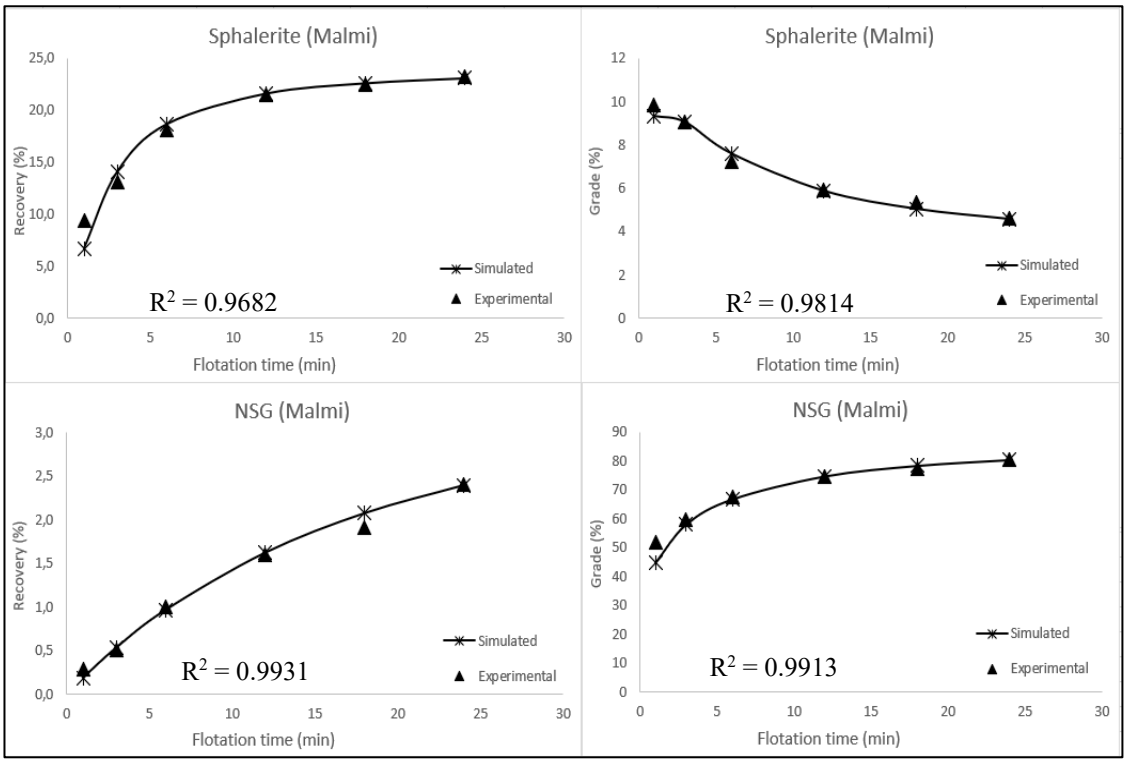

Figure 63 Comparison between experimental and simulated grade and recovery of sphalerite and NSG in malmi sample

4.5.2 Sorter feed

The comparison between experimental and simulated grades and recoveries of dyscrasite and galena are shown in Figure 64. The fit between experimental and simulated recoveries of dyscrasite shows an R^2 value of 0.9741. The lower R^2 resulted from underestimating dyscrasite simulated recovery. While the comparison between dyscrasite grades in simulated and experimental results show a better for with an R^2 value of 0.9897, a slight deviation of the third point at 6 minutes of flotation can be observed. There is a perfect fit between simulated and experimental recoveries of galena in sorter feed with an R^2 value of 0.9941. the fit between simulated and experimental grades of galena is reasonably acceptable with an R^2 value of 0.9774, resulting in slight deviations at the first and second points.

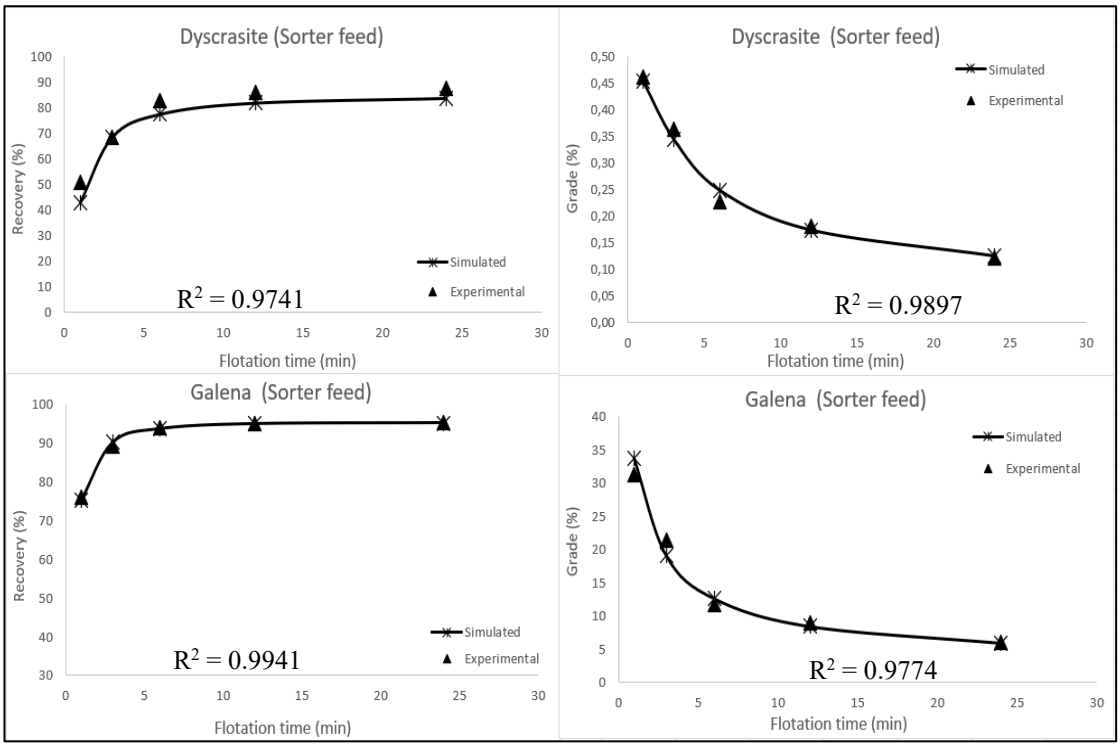

Figure 64 Comparison between experimental and simulated grade and recovery of dyscrasite and galena in sorter feed samples

The comparisons between simulated and experimental grades-recoveries of NSG are demonstrated in Figure 65. In the case of NSG recoveries, the fit between experimental and simulated observations is better with R^2 value of 0.9893. A good fit with slight deviations can be observed for the experimental and simulated grades of NSG with an R^2 value of 0.9855.

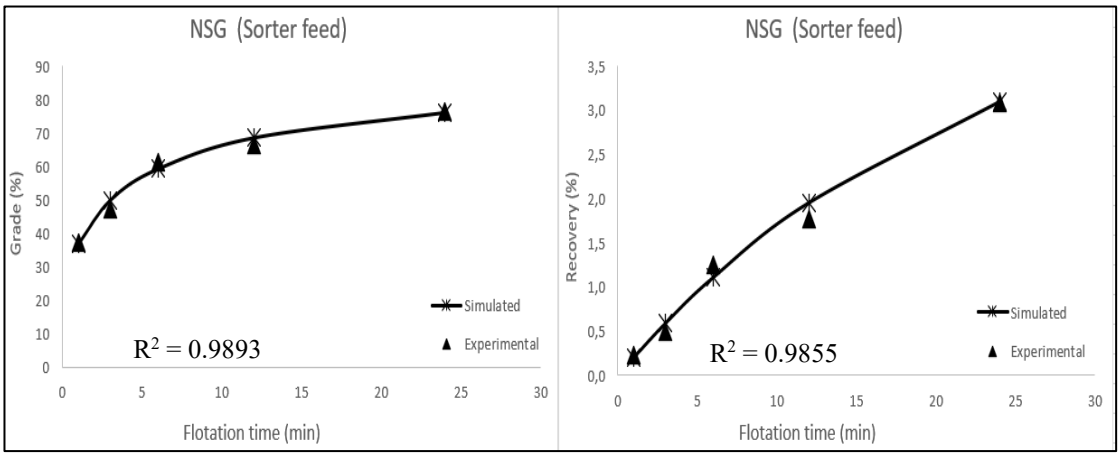

Figure 65 Comparison between experimental and simulated grade and recovery of NSG in sorter feed samples

4.5.3 Sorter product

The comparisons between experimental and simulated grades and recoveries of dyscrasite and galena are shown in Figure 66. Dyscrasite and galena recoveries show a similar trend with R^2 values of 0.8621 and 0.8808, respectively, where the first and last three observations show a good fit while the second observations show the underestimation of experimental recoveries of dyscrasite and galena. There is a perfect fit between the simulated and experimental grades of dyscrasite with an R^2 value of 0.9929. The fit between experimental and simulated grades of galena has an R^2 value of 0.9839.

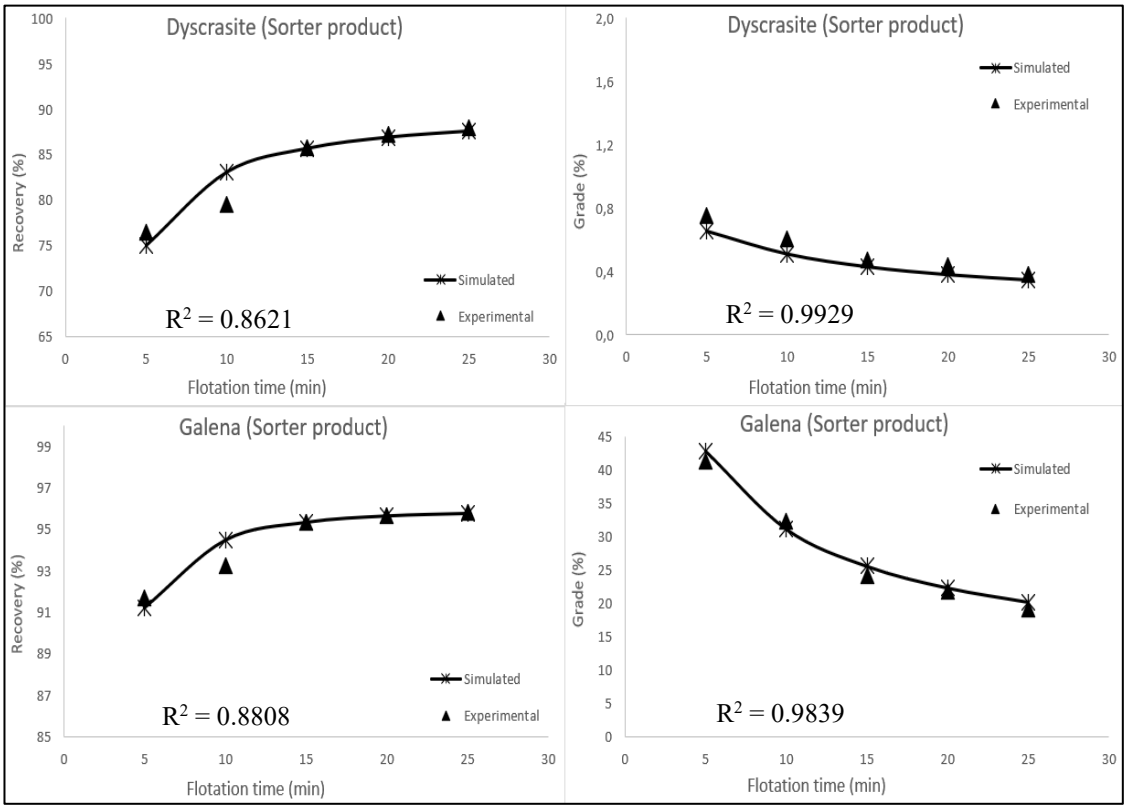

Figure 66 comparison between experimental and simulated grade and recovery of dyscrasite and galena in sorter product samples

The experimental and simulated grades and recoveries of NSG are shown in Figure 67. Overall, there is a decent fit for the grades and recoveries of NSG with R^2 values of 0.9935 and 0.9885, respectively. Some deviations can be observed in the case of NSG recoveries, while the simulated grades of NSG perfectly fit the experimental grades of NSG.

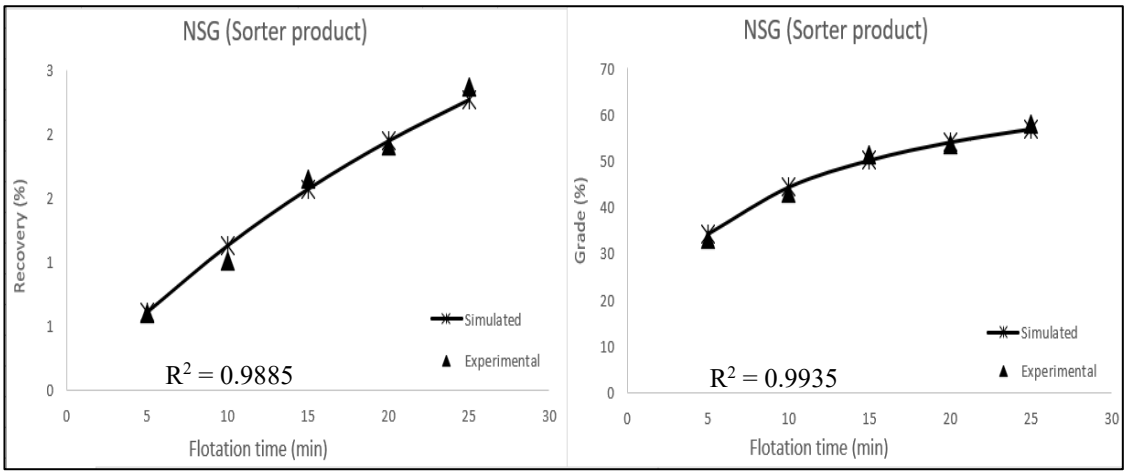

Figure 67 Comparison between experimental and simulated grade and recovery of NSG in sorter product samples

4.5.4 Ore 60

The comparisons between the experimental and simulated grades and recoveries of dyscrasite and galena are shown in Figure 68. The recoveries of dyscrasite and galena show a similar and decent fit with R2 values of 0.9775 and 0.9693, respectively. The experimental recoveries of dyscrasite and galena at the first point are slightly higher than the simulated recoveries.

The grades of dyscrasite show a good fit (R^2 = 0.9855) between experimental and simulated values except for the second point, where the experimental value is slightly lower than the simulated value. There is also a satisfactory fit (R^2 = 0.9865) between experimental and simulated grades of galena, where the experimental grades of the first three observations are slightly lower.

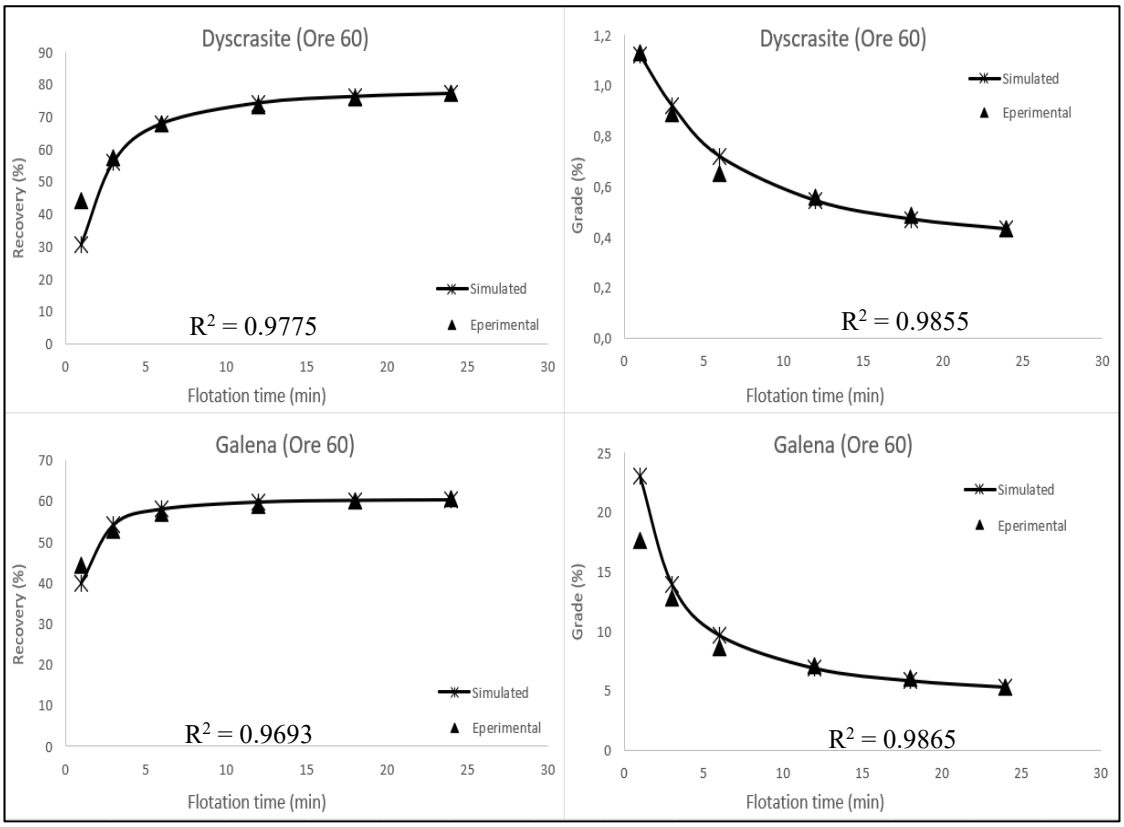

Figure 68 Comparison between experimental and simulated grade and recovery of dyscrasite and galena in ore 60 samples

The grade and recovery curves of NSG show a similar trend between experimental and simulated observations, where the first three experimental observations have slightly higher values and the last three observations have somewhat lower values. The R^2 values for recovery and grade fit are 0.9904 and 0.9896, respectively.

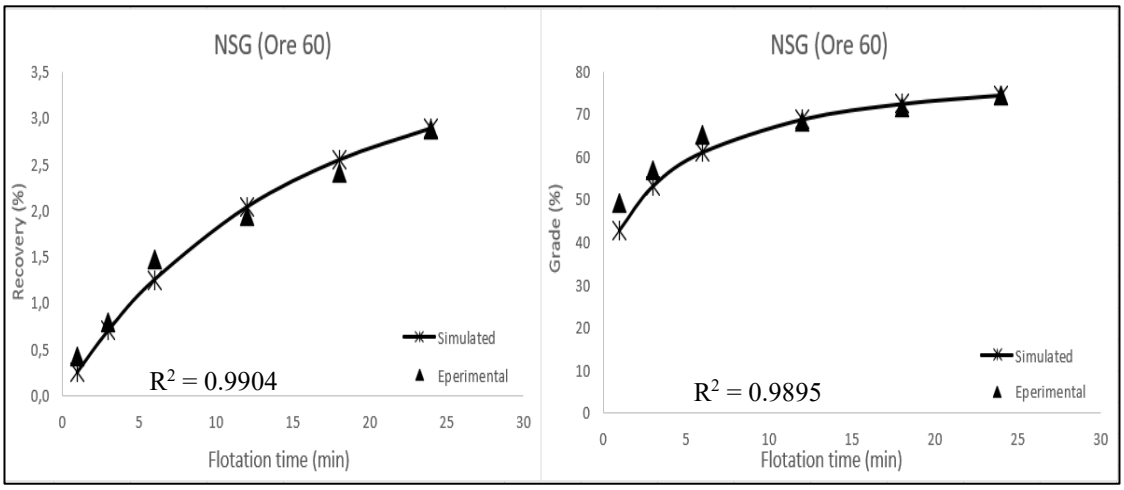

Figure 69 Comparison between experimental and simulated grade and recovery of NSG in ore 60 samples

4.6 Blends flotation test results

The flotation results of blends are presented according to the blend series explained in Table 9. The results are divided into three series. All flotation tests of blends are conducted at similar conditions and reagent dosages. The flotation kinetic for blends are presented in this section.

4.6.1 Blends of sorter product and malmi

Blend I, Blend II, and Blend III contain sorter product and malmi samples at different proportions, as shown in Table 7. The flotation kinetic parameters for Blend I, Blend II, and Blend III are shown in Table 20. Data tables are shown in appendix C.

Table 20 Flotation kinetic parameters of Blend I, Blend II, and Blend III

		Sphalerite	Pyrite	Dyscrasite	Galena	Chalcopyrite	NSG
Blend I	R_{Inf}	23,0	6,3	86,1	96,2	60,8	2,3
	k_{Max}	0,40	0,35	1,80	4,90	4,16	0,13
Blend II	R_{Inf}	24,0	5,4	82,9	94,8	55,8	2,3
	k_{Max}	0,43	0,39	1,50	4,00	3,50	0,09
Blend III	R_{Inf}	22,5	4,9	76,0	92,2	49,0	2,2
	k_{Max}	0,59	0,60	2,40	5,61	4,23	0,12

The dyscrasite recovery curves for blend I, blend II, and blend III are illustrated in Figure 70. The recoveries of dyscrasite in the final concentrate of blend I, blend II, and blend III are 85.9%, 82.3%, and 76.3%, respectively. These dyscrasite recoveries are closer to the infinity recoveries, as shown in Table 20. The highest dyscrasite recovery of blend I resulted from the higher proportion of sorter product in this blend. In blend II, the dyscrasite recovery is lowest due to the higher proportion of malmi. A higher proportion of sorter product in a blend results in a higher dyscrasite recovery. Since the recovery of dyscrasite in the sorter product sample is about 8% higher than the malmi sample in reference flotation tests.

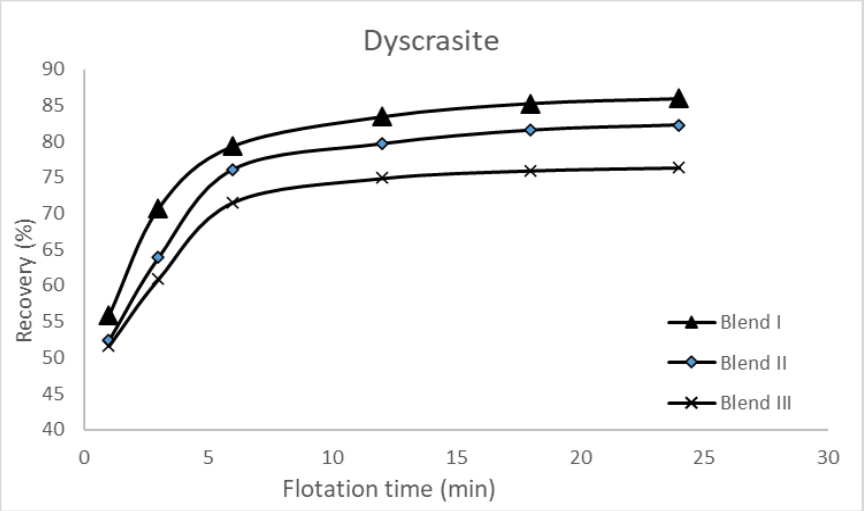

Figure 70 Dyscrasite recovery in the blend I, blend II, and blend III

The dyscrasite grade plots of blend I, blend II, and blend III are illustrated in Figure 71. The dyscrasite grade in the final concentrate of blend I is 0.423%, the highest compared to other blends. Blend III has the lowest grade of dyscrasite with a value of 0.284%. A higher proportion of sorter product in a blend resulted in a higher dyscrasite grade in the final concentrate. The reason is the 0.24% higher dyscrasite grade in sorter product compared to malmi sample in reference flotation tests.

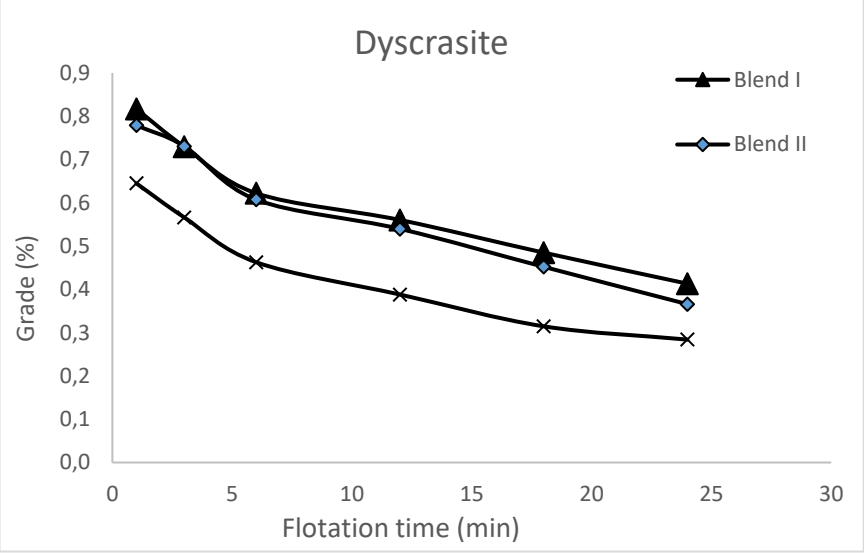

Figure 71 Dyscrasite grade in the blend I, blend II, and blend III

The galena recovery plots for blend I, blend II, and blend III are illustrated in Figure 72. The recoveries of galena in the final concentrate of blend I, blend II, and blend III are 96.3%, 94.8%, and 92.5%, respectively. These galena recoveries at 24 minutes of

flotation are very close to the infinity recoveries as shown in Table 20, like dyscrasite recoveries. The highest galena recovery of blend I resulted due to the higher proportion of sorter product in this blend. In blend II, the galena recovery is lowest due to the higher proportion of malmi. A higher proportion of sorter product in a blend results in a higher galena recovery. The recovery of dyscrasite in the sorter product sample is about 12.5% higher than the malmi sample in reference flotation tests.

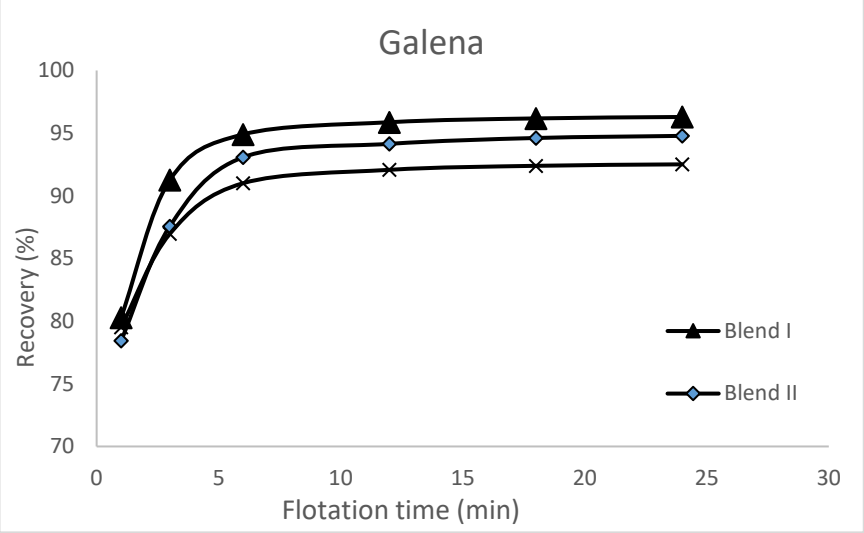

Figure 72 Galena recovery in the blend I, blend II, and blend III

The galena grade plots of blend I, blend II, and blend III are illustrated in Figure 73. The galena grade in the final concentrate of blend I is 20.2%, the highest compared to other blends. Blend III has the lowest grade of galena with a value of 11.4%. A higher proportion of sorter product in the blend resulted in a higher galena grade in the final concentrate. The reason is the 15% higher galena grade in the sorter product as compared to malmi in reference flotation tests.

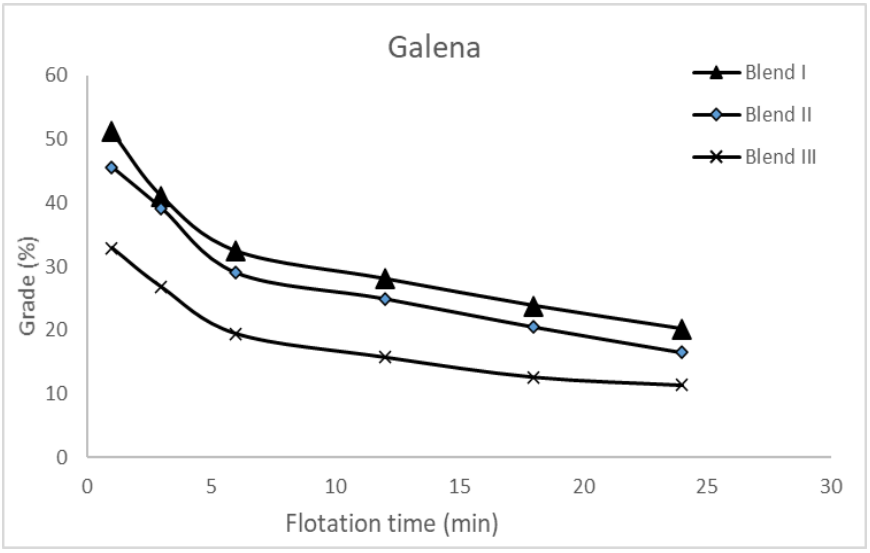

Figure 73 Galena grade in the blend I, blend II, and blend III

The recoveries of NSG in blend I, blend II, and blend III are almost similar at 1 and 24 minutes of flotation with 0.1% difference, as illustrated in Figure 74. The blend I has a maximum gangue recovery of 1.64%. The recovery in the final concentrate of blend II is about 1.6%. Blend III has a gangue recovery of 1.53% at 24 minutes of flotation.

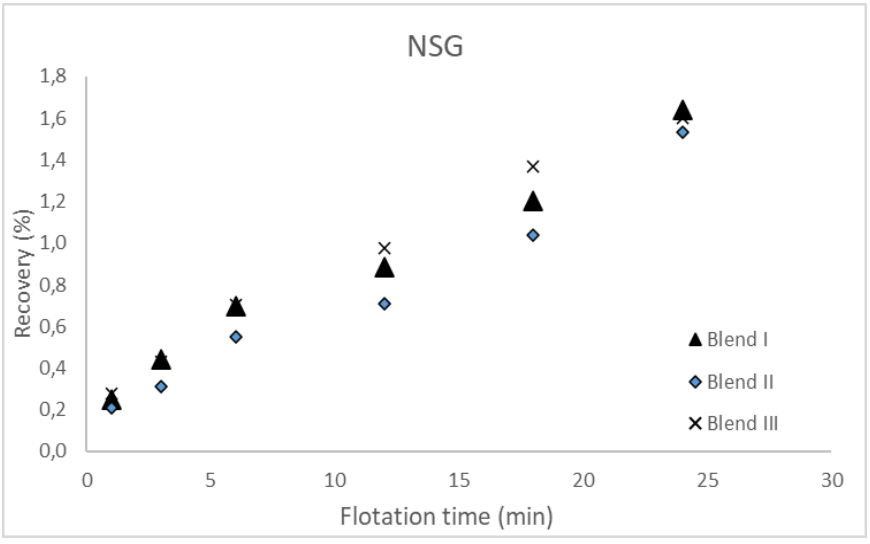

Figure 74 NSG recovery in the blend I, blend II, and blend III

The grade of NSG in blend III is 67.8% in the final concentrate, as illustrated in Figure 75, which is the highest compared to other blends. Blend I has the lowest NSG grade of 53.2%. The blend I and blend II show similar NSG grades with a highest-grade difference

of 5% at 24 minutes of flotation. The highest proportion of malmi in a blend results in a higher grade of NSG in the concentrate.

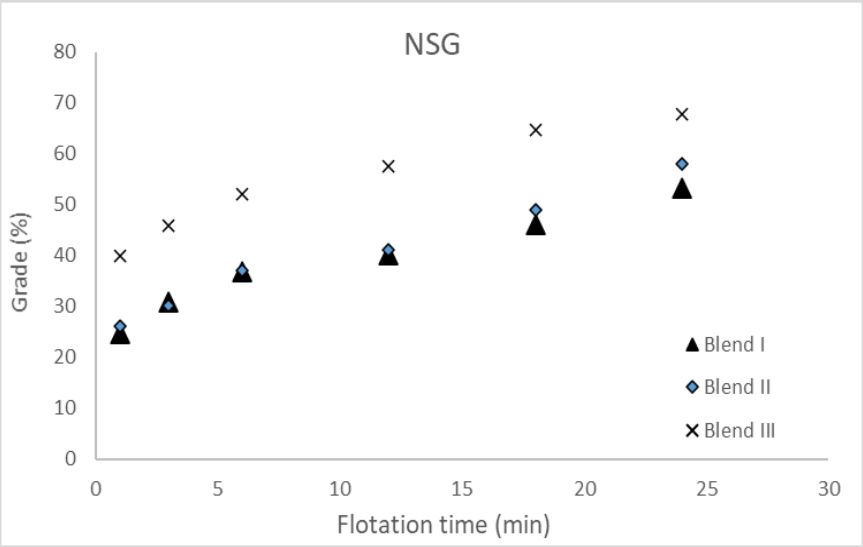

Figure 75 NSG grade in the blend I, blend II, and blend III

4.6.2 Blends of malmi and ore 60

The blend IV, blend V, and blend VI contain malmi and ore 60 samples at different proportions, as shown in Table 7. The flotation kinetic parameters for blend IV, blend V, and blend VI are shown in Table 21.

Table 21 Flotation kinetic parameters of Blend IV, Blend V, and Blend VI

		Sphalerite	Pyrite	Dyscrasite	Galena	Chalcopyrite	NSG
Blend IV	R_{Inf}	27,0	6,0	78,0	65,5	42,5	4,3
	k_{Max}	0,41	0,24	1,05	1,80	2,28	0,10
Blend V	R_{Inf}	34,0	9,3	80,0	70,0	47,0	5,3
	k_{Max}	0,68	0,52	1,61	4,19	3,00	0,10
Blend VI	R_{Inf}	32,0	9,0	78,0	66,0	50,0	6,7
	k_{Max}	0,70	0,58	1,81	4,25	3,31	0,08

The dyscrasite recoveries for blend V and blend VI are similar (about 49%) at the first point of 1-minute flotation. At this point, the dyscrasite recovery in blend IV is 38.3%. The differences in the dyscrasite recovery between all blends decrease after 6-minutes of flotation. In the final concentrate at 24 minutes of flotation, the dyscrasite recovery in blend IV and blend VI is almost 77%. At this point, the recovery of dyscrasite in blend V is about 2% higher than the other two blends.

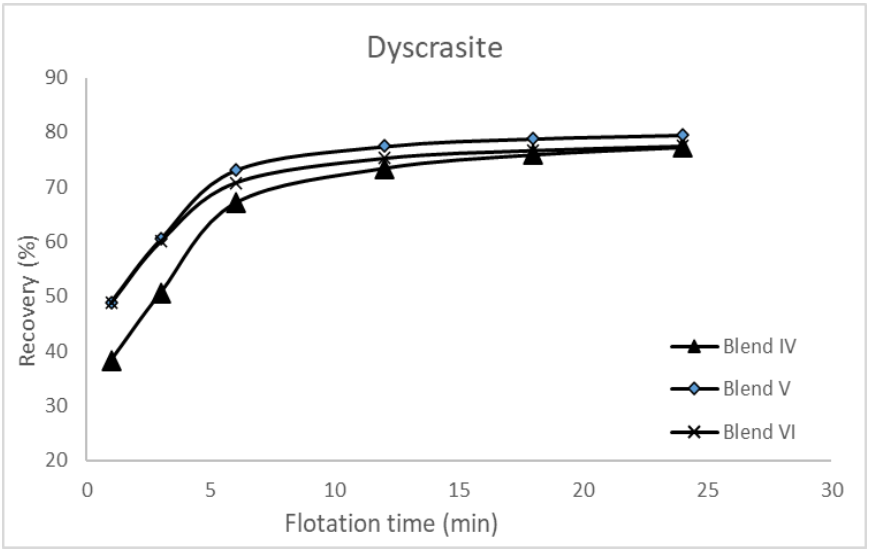

Figure 76 Dyscrasite recovery in blend IV, blend V and blend VI

The dyscrasite grades of blend IV, blend V and, blend VI at one minute of flotation are 0.74%, 0.96%, and 1.18%, respectively, illustrated in Figure 77. This difference in grade decreases with an increase in the flotation time. At 24-minutes flotation, the grade difference between the three blends is about 0.08%, with the range of 0.21 to 0.28%. The grades and recoveries of dyscrasite in the final concentrate for all three blends are close.

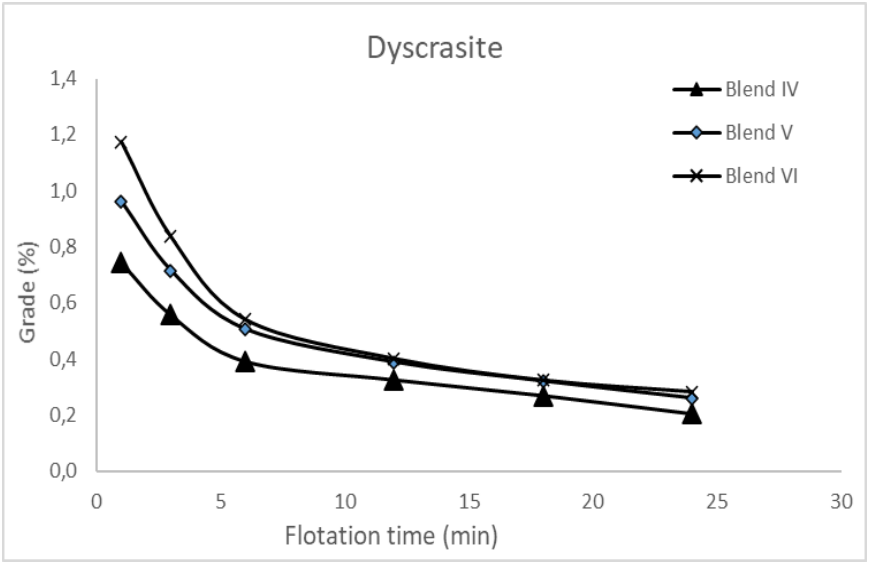

Figure 77 Dyscrasite grade in blend IV, blend V, and blend VI

The recoveries of galena in blend IV, blend V and blend VI are demonstrated in Figure 78. The final recoveries of blend IV and blend VI are almost alike, about 66%. At this point, the recovery of blend V is 70.1%. The dyscrasite recovery in blend VI at one minute

of flotation is 39%, while at this point, the recoveries dyscrasite in blend V and blend VI are more than 54%. There is a sharp increase in the dyscrasite recovery till 6-minutes flotation, slightly increased in further flotation. The difference in the dyscrasite recovery between the three blends is about 4% in the final concentrate.

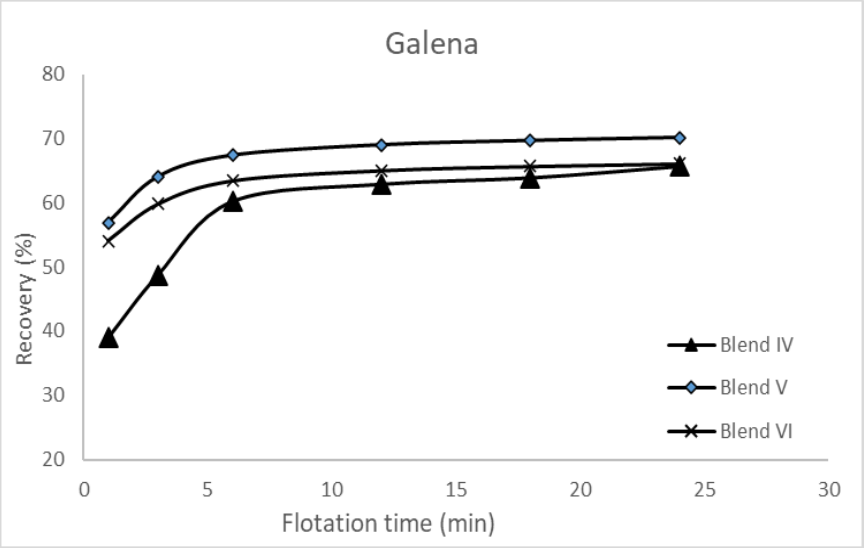

Figure 78 Galena recovery in blend IV, blend V and blend VI

There is about a 7% grade difference of galena between three blends at one minute of flotation, shown in Figure 79. With further flotation, the grade difference is decreased, and in the final concentrate, the grade difference is about 0.5%. The galena grade in the final concentrate of three blends is 3.6 to 4.14%. After 12 minutes of flotation, the galena grades in all three blends are close to each other.

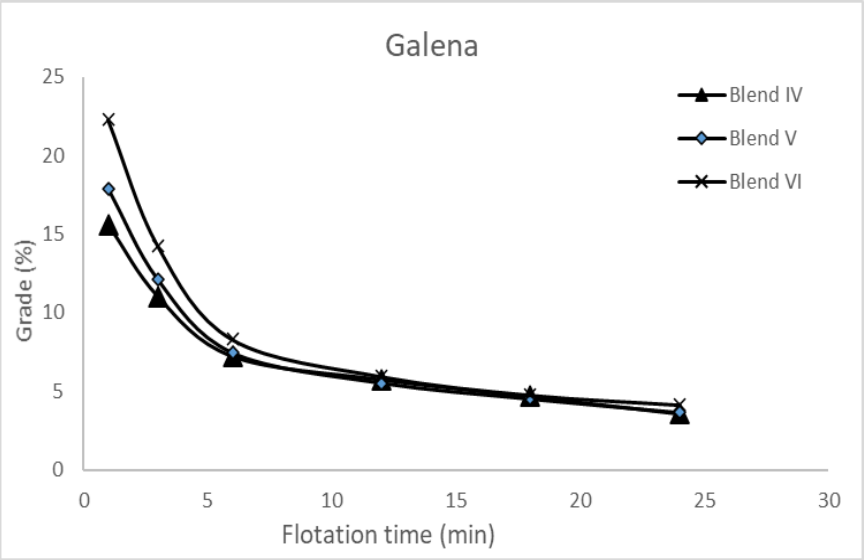

Figure 79 Galena grade in blend IV, blend V and blend VI

The recoveries of the NSG in the final concentrate of blend IV, blend V, and blend VI are in the range of 2.8% to 4%, as demonstrated in Figure 80. At the beginning of the flotation, the NSG-recovery difference is slight and increases gradually with further flotation. The recovery of NSG in the blend IV is about 2.8%. The NSG recovery in blend V and blend VI are about 3.7% and 4%, respectively. The increase of ore 60 proportion in a blend caused higher NSG recovery directly. The presence of more oxidized ore in the blend caused a higher recovery of gangue in the final concentrate.

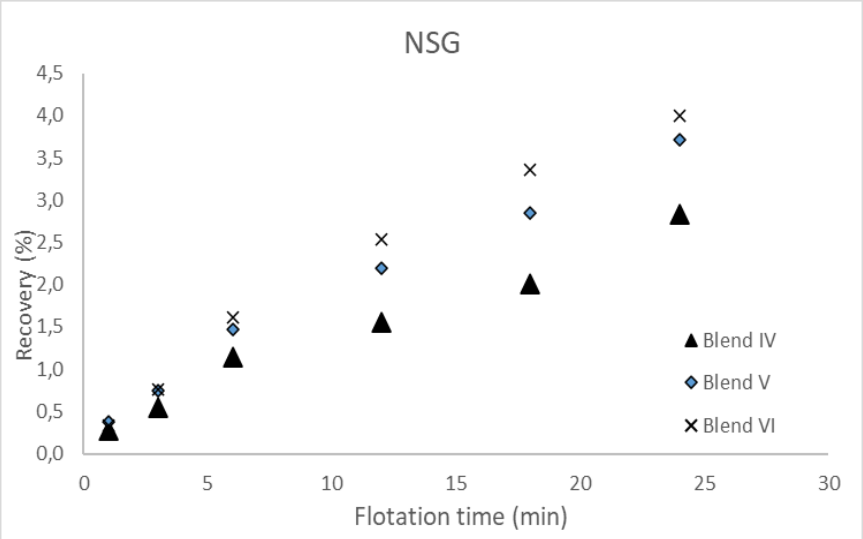

Figure 80 NSG recovery in blend IV, blend V and blend VI

The grades of NSG in blend IV, blend V, and blend VI are shown in Figure 81. The grade difference of NSG between the three blends is about 14% at the start of the flotation, and this difference decreased gradually with further flotation. At the last three points, the grades of NSG are roughly similar in all blends. In the final concentrate, the NSG grades are in the range of 83% to 84.3%.

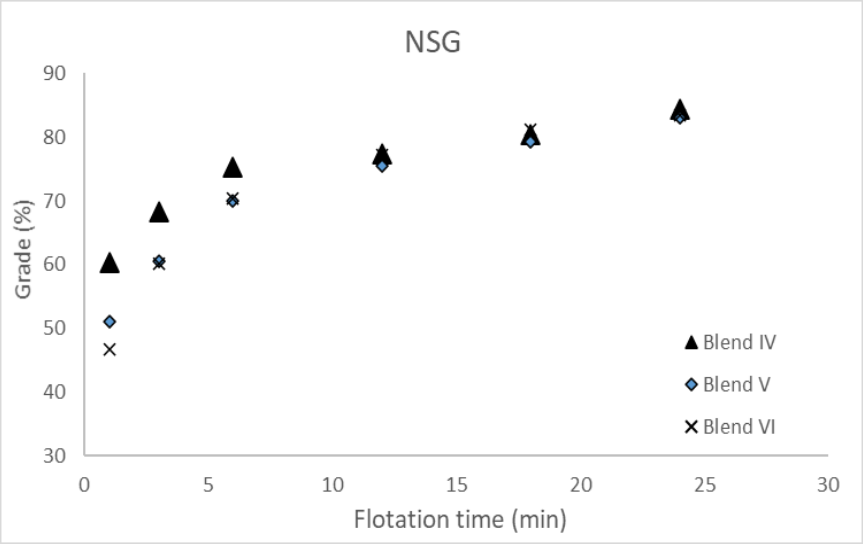

Figure 81 NSG grade in blend IV, blend V and blend VI

4.6.3 Blends of sorter product and ore 60

The blend VII, blend VIII, and blend IX contain sorter product and ore 60 samples at different proportions, as shown in Table 7. The flotation kinetic parameters for blend IV, blend V, and blend VI are shown in Table 22.

Table 22 Flotation kinetic parameters of Blend VII, Blend VIII, and Blend IX

		Sphalerite	Pyrite	Dyscrasite	Galena	Chalcopyrite	NSG
Blend VII	R_{Inf}	25,7	7,4	88,9	92,3	63,8	5,5
	k_{Max}	0,45	0,45	1,90	4,00	3,00	0,10
Blend VIII	R_{Inf}	25,7	9,5	84,6	85,3	59,5	5,1
	k_{Max}	0,57	0,65	1,80	4,00	3,00	0,12
Blend IX	R_{Inf}	27,2	14,2	81,2	76,7	56,0	5,4
	k_{Max}	0,58	0,54	1,60	5,23	2,50	0,10

The dyscrasite recoveries in blend VII, blend VIII, and blend IX are illustrated in Figure 82. The final recovery of dyscrasite in blend VII is 88.5%, the highest among the other two blends. The dyscrasite final recovery in blend VII is 84.1%, while the dyscrasite recovery in blend IX is 80.9%. The increase in the proportion of ore 60 in a blend caused a lower recovery of dyscrasite in the final concentrate. The reason is the 11% lower dyscrasite recovery in ore 60 compared to sorter product in reference flotation tests.

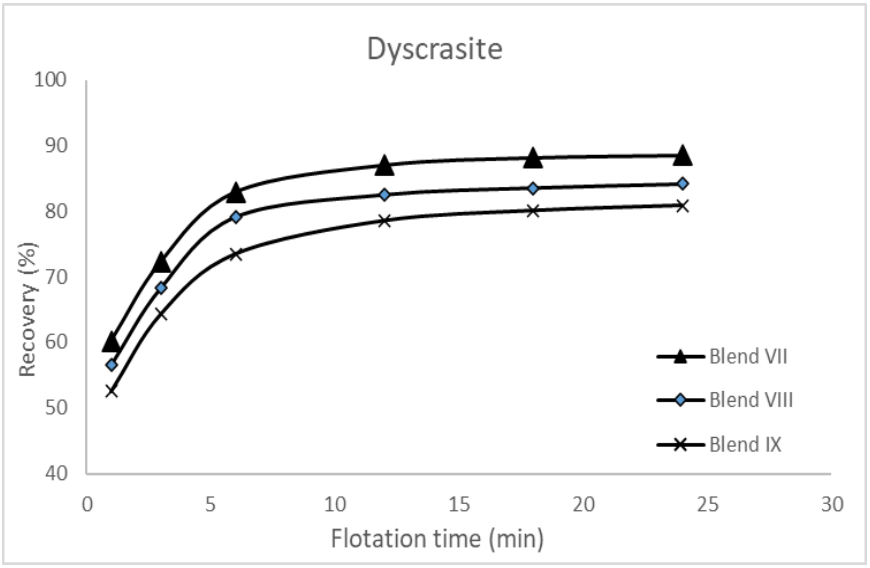

Figure 82 Dyscrasite recovery in Blend VII, Blend VIII, and Blend IX

There is about a 0.33% grade difference of dyscrasite between blend VII, blend VIII, and blend IX at one minute of flotation, illustrated in Figure 83. With further flotation, the grade difference is decreased, and in the final concentrate, the grade difference is about 0.06%. The dyscrasite grade in the final concentrate of three blends is in the range of 0.3% to 0.36%%. After 6 minutes of flotation, the dyscrasite grades in blend VII and blend VIII are close to each other with a difference of 0.02%.

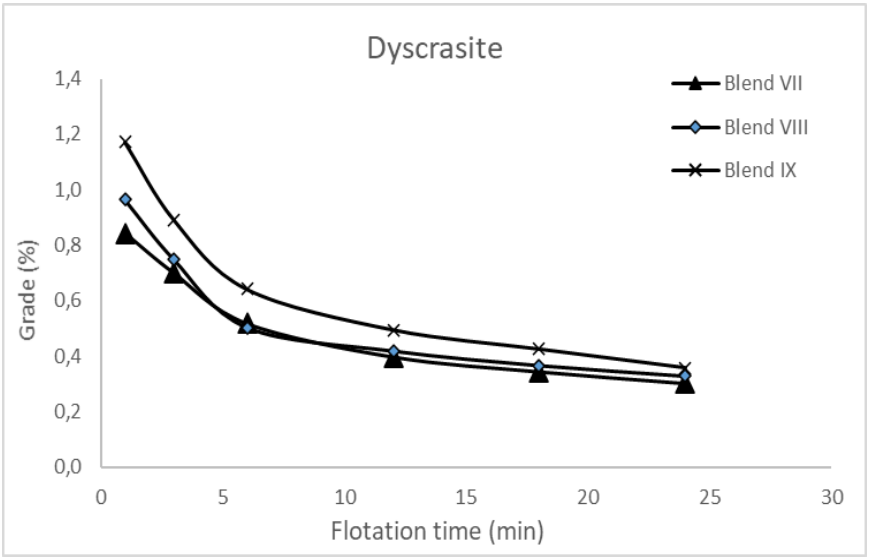

Figure 83 Dyscrasite grade in Blend VII, Blend VIII, and Blend IX

The galena recovery curves for blend VII, blend VIII, and blend IX are illustrated in Figure 84. The recoveries of galena in the final concentrate of blend VII, blend VIII, and

blend IX are 91.8%, 85.1%, and 77.6%, respectively. These galena recoveries are closer to the infinity recoveries, as shown in Table 22. The highest galena recovery of blend VII resulted from the higher proportion of the sorter product. In blend VIII, the galena recovery is lowest due to the higher proportion of ore 60. The higher proportion of sorter product in this blend results in a higher galena recovery. Since the recovery of galena in sorter product is about 35% higher than the ore 60 sample.

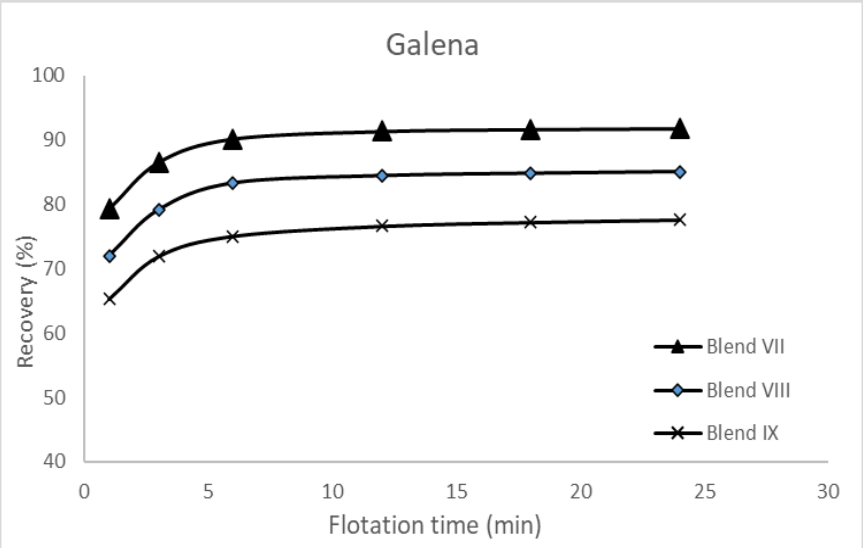

Figure 84 Galena recovery in Blend VII, Blend VIII, and Blend IX

The galena grades in blend VII, blend VIII, and blend IX are 11.9%, 9.5%, and 7.32%, respectively, as shown in Figure 85. The higher content of ore 60 in the blend resulted in a lower grade of galena in the final concentrate. The reason is the 13.8% higher galena grade as compared to ore 60 in reference flotation tests.

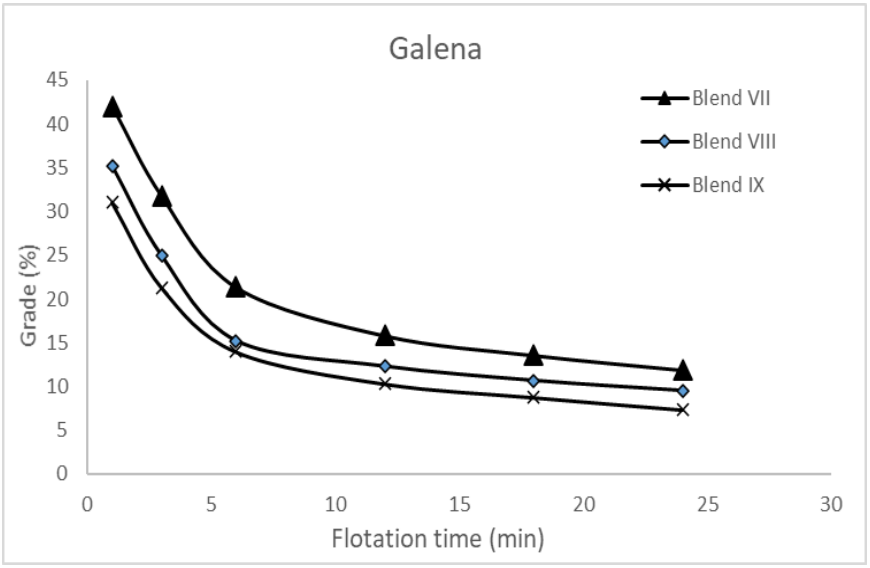

Figure 85 Galena grade in Blend VII, Blend VIII, and Blend IX

All three blends show similar NSG recovery over the flotation time, as shown in Figure 86. The maximum NSG recovery in the final concentrates of all blends is about 3.6%. Hence different proportions of sorter product and ore 60 show no effect on the NSG recovery.

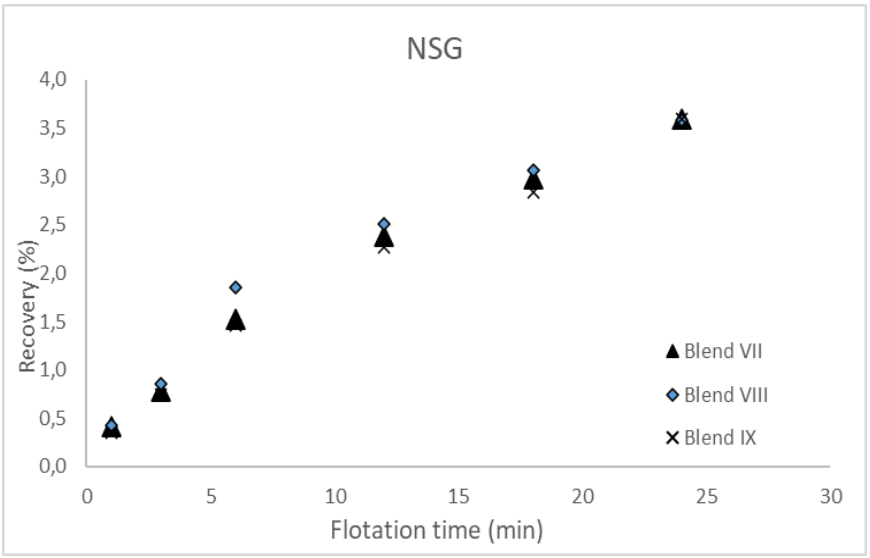

Figure 86 NSG recovery in Blend VII, Blend VIII, and Blend IX

The grades distribution of NSG in blend VII, blend VIII and blend IX are demonstrated in Figure 87. In the final concentrate, the grades of blend VII, blend VIII, and blend IX are 69.3%, 73.4, and 76.4%, respectively. A higher proportion of ore 60 in the blend resulted in a higher grade of NSG in the concentrate.

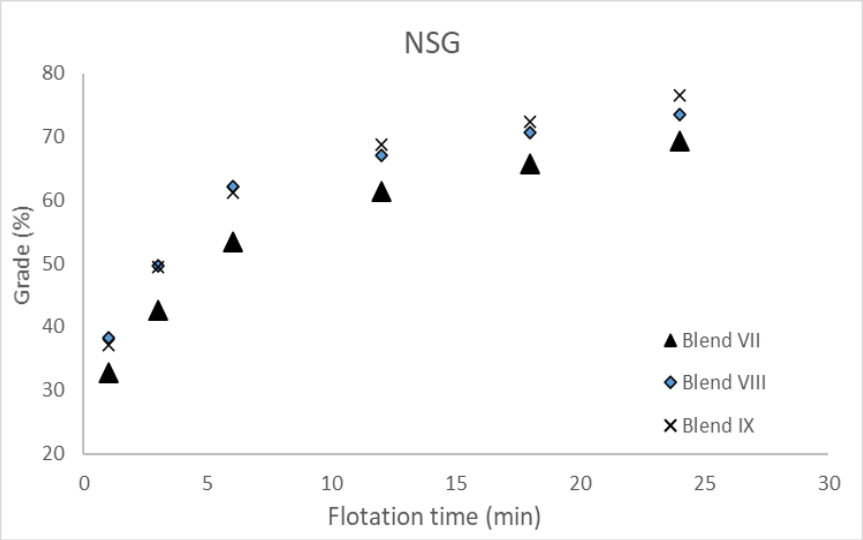

Figure 87 NSG grade in Blend VII, Blend VIII, and Blend IX

4.7 Comparison between simulated and experimental blends-flotation tests

The flotation and simulation results of the blend series explained in Table 9 are presented. The results are divided into three series. All flotation tests of blends are conducted at similar conditions and reagent dosages. Here, the grades and recoveries after 24 minutes of flotation are compared. The comparison between simulated and experimental results over flotation times are shown in appendix A. The horizontal axis of the graphs shows blend series while the primary y-axis and secondary y-axis show recoveries and grades, respectively. The simulated recoveries are presented solid bars, while experimental recoveries are presented as pattern pars. Solid lines represent the experimental grades with triangular points, and solid lines show simulated grades with cross points.

The data tables are shown in appendix E. The graphs for sphalerite and pyrite are shown in appendix B.

4.7.1 Blend series 1

The blend series 1 include sorter product, blend I, blend II, blend III, and malmi sample, simulated and experimental results of dyscrasite are demonstrated in Figure 88. The simulated and experimental grades/ recoveries of malmi and sorter product are almost similar. The recovery difference is about 0.44%, while the grade difference is below 0.04%. The recovery difference between simulated and experiment results of blend I is

about 0.8%, raised to 8% till blend III. The more content of malmi in a blend resulted in the lower experimental recovery of dyscrasite. The simulated recoveries between sorter product and malmi are uniformly distributed in 80.5% to 88%. The grade difference varies between 0.08 to 0.11% for blend I, blend II, and blend III. Compared to the simulated grades, the blends of sorter product and malmi result in higher experimental dyscraside grades. In comparison, the experimental recoveries in these blends are lower than the simulated recoveries.

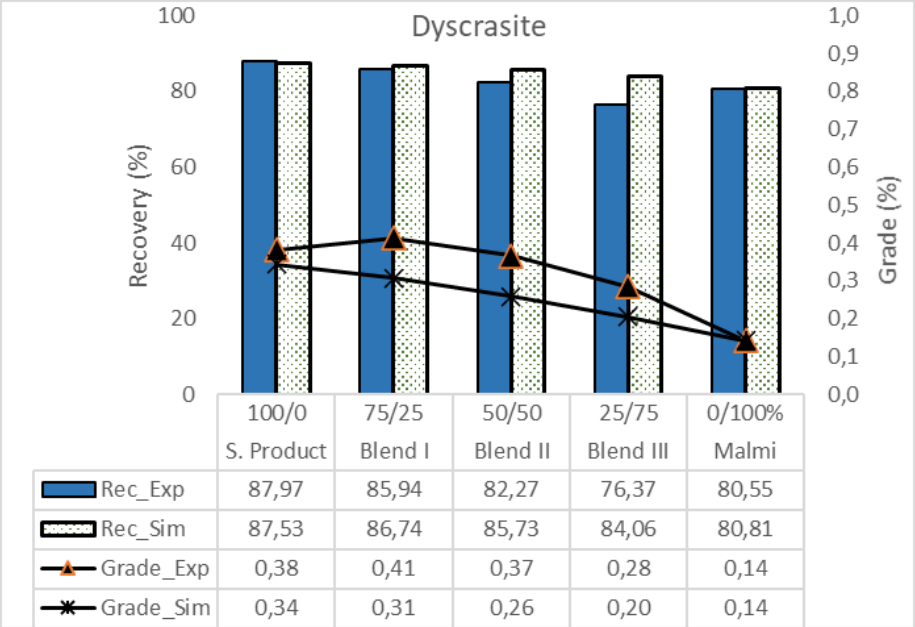

	100/0 S. Product	75/25 Blend I	50/50 Blend II	25/75 Blend III	0/100% Malmi
Rec_Exp	87,97	85,94	82,27	76,37	80,55
Rec_Sim	87,53	86,74	85,73	84,06	80,81
Grade_Exp	0,38	0,41	0,37	0,28	0,14
Grade_Sim	0,34	0,31	0,26	0,20	0,14

Figure 88 Comparison between simulated and experimental grades-recoveries of dyscrasite in blend series 1

The simulated and experimental flotation results of galena are demonstrated in Figure 89. The simulated and experimental grades and recoveries of both malmi and sorter product are almost similar. The recovery difference is about 0.08%, while the grade difference is below 1.12%. The recovery difference between simulated and experiment blend I result is about 1.2%, about 1% in blend II and blend III. The blends of sorter product and malmi have similar simulated and experimental galena recoveries, with about 1% difference. The simulated recoveries between sorter product and malmi are uniformly distributed in 95.75% to 83.6%. The simulated and experimental recoveries/grades of galena are decreased with an increase in the malmi content of the blend. The simulated grades between sorter product and malmi are uniformly distributed in the range of 20.23% to 4.01%. The galena grade difference between blend I, blend II and blend III varies between 2.4% to 3.1%. The blends of sorter product and malmi result in higher experimental

galena grades compared to the simulated. While the experimental recoveries in these blends slightly higher than the simulated recoveries.

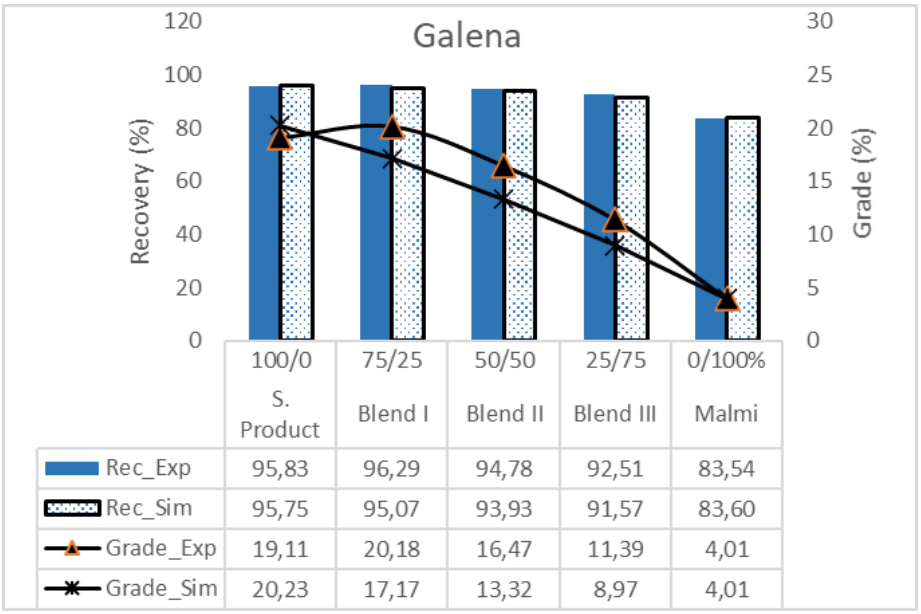

	100/0 S. Product	75/25 Blend I	50/50 Blend II	25/75 Blend III	0/100% Malmi
Rec_Exp	95,83	96,29	94,78	92,51	83,54
Rec_Sim	95,75	95,07	93,93	91,57	83,60
Grade_Exp	19,11	20,18	16,47	11,39	4,01
Grade_Sim	20,23	17,17	13,32	8,97	4,01

Figure 89 Comparison between simulated and experimental grades-recoveries of galena in blend series 1

The simulated and experimental flotation results of NSG are demonstrated in Figure 90. The simulated and experimental grades and recoveries of malmi and sorter product are almost similar. The recovery difference is about 0.1%, while the grade difference is below 1%. The recovery difference between simulated and experimental blend I result is 0.61%, about 0.8% in blend II and blend III.The blends of sorter product and malmi have similar simulated and experimental NSG recoveries, with about 0.8% difference. The simulated recoveries between sorter product and malmi are uniformly distributed in the range of 2.26% to 2.4%. The simulated and experimental recoveries/grades of NSG are increased with an increase in the malmi content of the blend. The simulated grades between sorter product and malmi are uniformly distributed in the range of 56.8% to 80.5%. The NSG grade difference between blend I, blend II, and blend III varies between 6.5 to 11%. The blends of sorter product and malmi result in lower experimental NSG grades compared to the simulated. While the simulated recoveries in these blends slightly higher than the experimental recoveries. The lower experimental NSG grade of blends resulted in a higher experimental grade of sulfide minerals than simulation results, shown in Figure 88, Figure 89, and Figure 90.

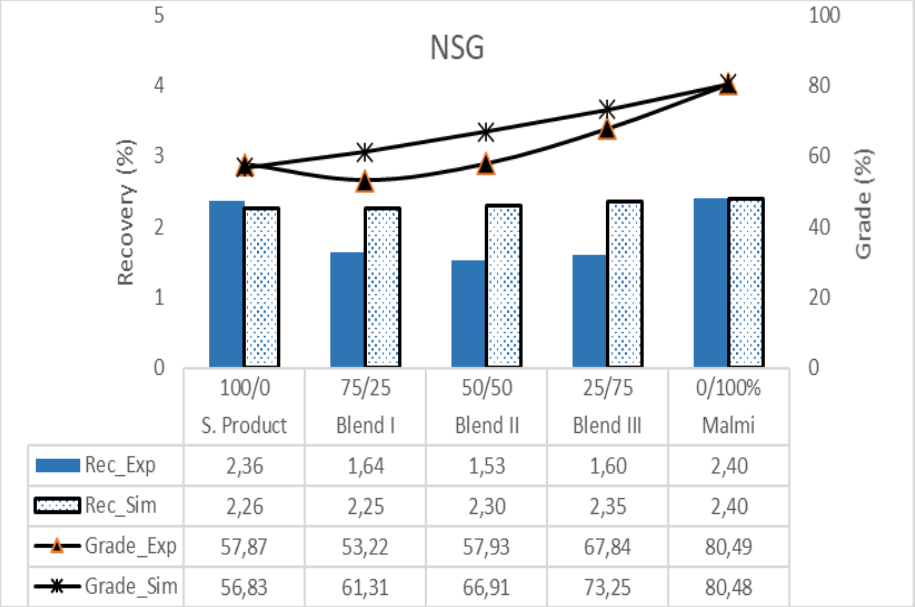

	100/0 S. Product	75/25 Blend I	50/50 Blend II	25/75 Blend III	0/100% Malmi
Rec_Exp	2,36	1,64	1,53	1,60	2,40
Rec_Sim	2,26	2,25	2,30	2,35	2,40
Grade_Exp	57,87	53,22	57,93	67,84	80,49
Grade_Sim	56,83	61,31	66,91	73,25	80,48

Figure 90 Comparison between simulated and experimental grades-recoveries of NSG in blend series 1

4.7.2 Blend series 2

The blend series 2 include malmi, blend IV, blend V, blend VI, and ore 60 sample. Simulated and experimental results of dyscrasite are demonstrated in Figure 91. The simulated and experimental grades/ recoveries of malmi and ore 60 are almost similar. The recovery difference is about 0.34%, while the grade difference is negligible. The recovery difference between simulated and experiment results of blend IV is about 0.57%, raised to 1.5% in blend V. The simulated recoveries between ore 60 and malmi are uniformly distributed in the range of 77.18% to 80.81%. The grade difference varies between 0.03 to 0.09% for blend IV, blend V and blend VI. The blends of ore 60 and malmi result in the lower experimental dyscrasite grades as compared to the simulated grades. In comparison, the experimental recoveries in these blends are close to the simulated recoveries.

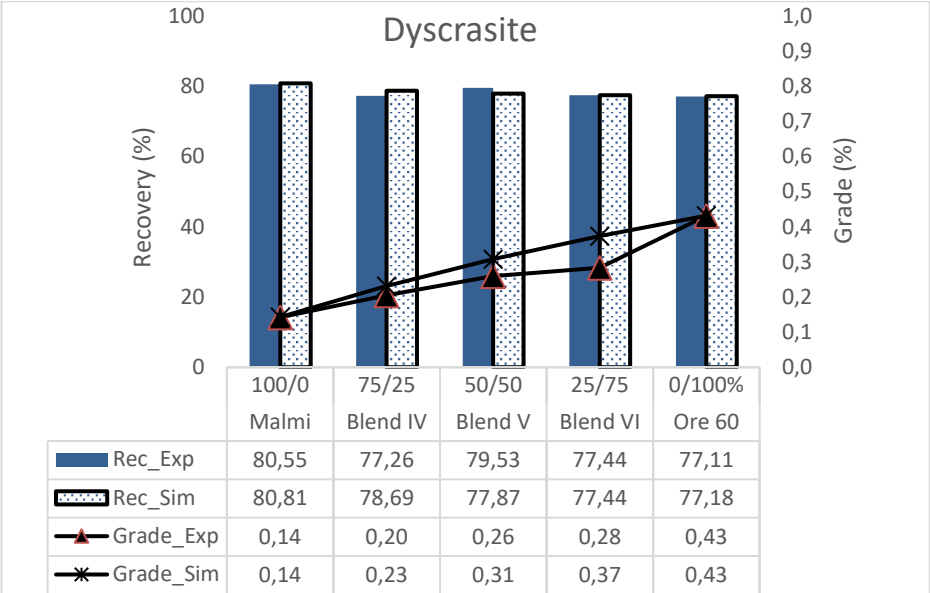

	100/0 Malmi	75/25 Blend IV	50/50 Blend V	25/75 Blend VI	0/100% Ore 60
Rec_Exp	80,55	77,26	79,53	77,44	77,11
Rec_Sim	80,81	78,69	77,87	77,44	77,18
Grade_Exp	0,14	0,20	0,26	0,28	0,43
Grade_Sim	0,14	0,23	0,31	0,37	0,43

Figure 91 Comparison between simulated and experimental grades-recoveries of dyscrasite in blend series 2

The simulated and experimental flotation results of galena blend series 2 are demonstrated in Figure 92. The simulated and experimental grades and recoveries of malmi and ore 60 are almost similar. The recovery difference is about 0.1%, while the grade difference is below 1%. The recovery difference between simulated and experimental results of blend IV is 7.5%, about 3% in blend V and blend VI. The simulated recoveries between ore 60 and malmi are uniformly distributed in the range of 60.26% to 83.6%. The simulated and experimental recoveries of galena are decreased with an increase in the ore 60 content of the blend. The simulated grades between ore 60 and malmi are uniformly distributed in the range of 5.28 % to 4%. The galena grade difference between blend IV, blend V, and blend VI varies between 0.8% to 1%. The blends of ore 60 and malmi result in the lower experimental galena grades compared to the simulated. While the simulated recoveries in these blends slightly lower than the experimental recoveries in blend V and blend VI.

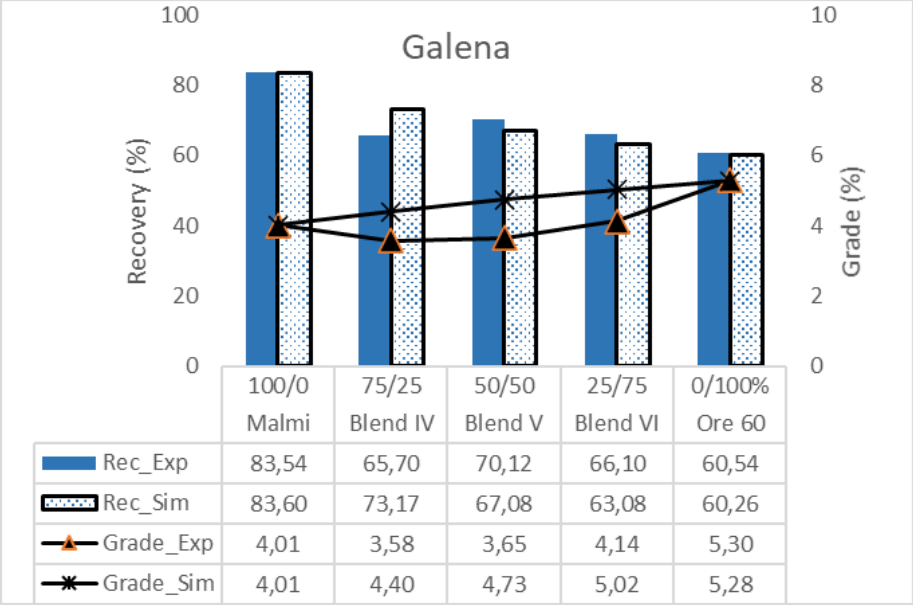

	100/0 Malmi	75/25 Blend IV	50/50 Blend V	25/75 Blend VI	0/100% Ore 60
Rec_Exp	83,54	65,70	70,12	66,10	60,54
Rec_Sim	83,60	73,17	67,08	63,08	60,26
Grade_Exp	4,01	3,58	3,65	4,14	5,30
Grade_Sim	4,01	4,40	4,73	5,02	5,28

Figure 92 Comparison between simulated and experimental grades-recoveries of galena in blend series 2

The simulated and experimental flotation results of NSG in blend series 2 are demonstrated in Figure 93. The simulated and experimental grades and recoveries of malmi and ore 60 are almost similar. The recovery difference is negligible, while the grade difference is below 0.01%. The recovery difference between simulated and experimental blend IV results is 0.31%, about 1% in blend V and blend VI. The simulated recoveries between ore 60 and malmi are uniformly distributed in the range of 2.99% to 2.4%. The simulated and experimental recoveries of NSG are increased with an increase in the ore 60 content of the blend. The simulated grades between ore 60 and malmi are uniformly distributed in the range of 74.46% to 80.48%. The NSG grade difference between blend IV, blend V and blend VI varies between 5.7% to 7.8%. The blends of ore 60 and malmi result in higher experimental NSG grades and recoveries as compared to the simulated. The higher experimental NSG grade of blends resulted in a lower experimental grade of sulfide minerals as compared to simulation results, shown in Figure 91, Figure 92, and Figure 93.

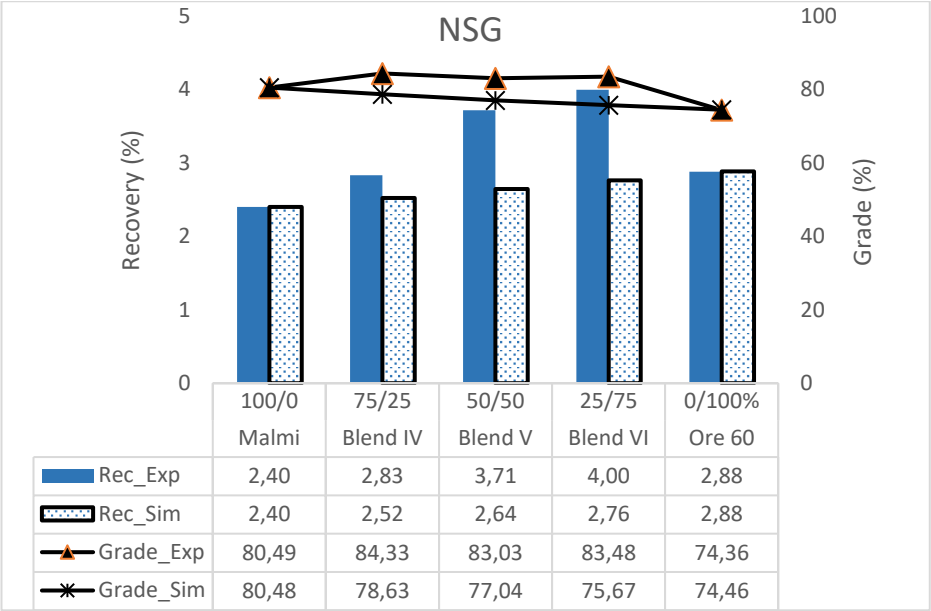

	100/0 Malmi	75/25 Blend IV	50/50 Blend V	25/75 Blend VI	0/100% Ore 60
Rec_Exp	2,40	2,83	3,71	4,00	2,88
Rec_Sim	2,40	2,52	2,64	2,76	2,88
Grade_Exp	80,49	84,33	83,03	83,48	74,36
Grade_Sim	80,48	78,63	77,04	75,67	74,46

Figure 93 Comparison between simulated and experimental grades-recoveries of NSG in blend series 2

4.7.3 Blend series 3

The blend series 3 include sorter product, blend VII, blend VIII, blend IX, and ore 60 sample. Simulated and experimental results of dyscrasite are demonstrated in Figure 94. The simulated and experimental grades/ recoveries of sorter product and ore 60 are almost similar. The recovery difference is about 0.44%, while the grade difference is 0.04%. The recovery difference between simulated and experiment results of blend VII is about 4.4%, raised to 1.8% in IX. The simulated recoveries between ore 60 and sorter product are uniformly distributed in the range of 77.18% to 87.53%. The grade difference varies between 0.04 to 0.07% for blend VII, blend VIII, and blend IX. The blends of ore 60 and sorter product result in the lower experimental dyscrasite grades as compared to the simulated grades. In comparison, the experimental recoveries in these blends are slightly higher than the simulated recoveries.

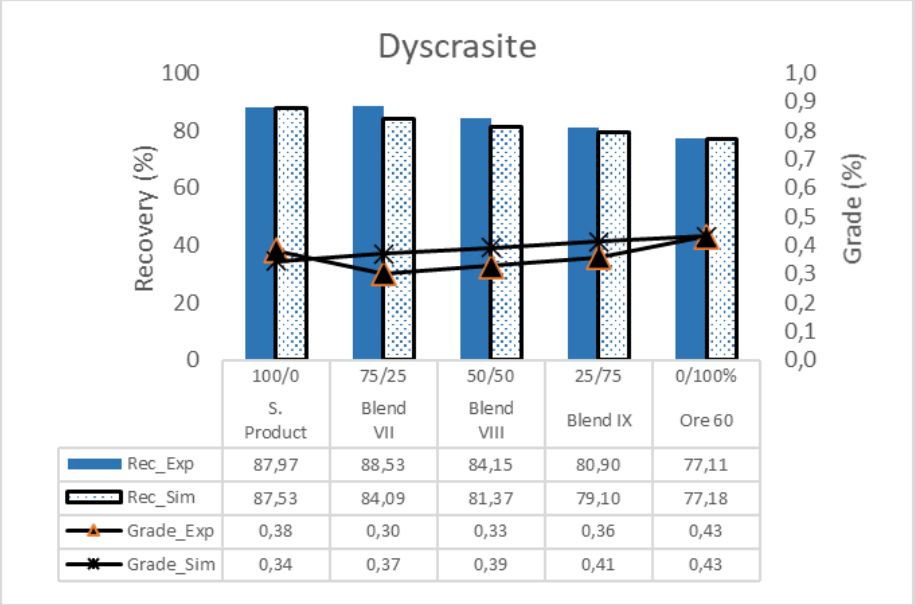

	100/0 S. Product	75/25 Blend VII	50/50 Blend VIII	25/75 Blend IX	0/100% Ore 60
Rec_Exp	87,97	88,53	84,15	80,90	77,11
Rec_Sim	87,53	84,09	81,37	79,10	77,18
Grade_Exp	0,38	0,30	0,33	0,36	0,43
Grade_Sim	0,34	0,37	0,39	0,41	0,43

Figure 94 Comparison between simulated and experimental grades-recoveries of dyscrasite in blend series 3

The simulated and experimental flotation results of galena in blend series 3 are demonstrated in Figure 95. The simulated and experimental grades and recoveries of sorter product and ore 60 are almost similar. The recovery difference is about 0.28%, while the grade difference is below 1.2%. The recovery difference between simulated and experimental results of blend VII is 0.5%, about 0.2% in blend VIII, and 1.7% in blend IX. The simulated recoveries between ore 60 and sorter products are uniformly distributed in the range of 60.26% to 95.75%. The simulated and experimental recoveries/grades of galena are decreased with an increase in the ore 60 content of the blend. The simulated grades between ore 60 and sorter product are uniformly distributed in the range of 5.28 % to 20.23%. The galena grade difference between blend VII, blend VIII and blend IX varies between 4.7% to 1.7%. The blends of ore 60 and sorter product result in the lower experimental galena grades/recoveries as compared to the simulated.

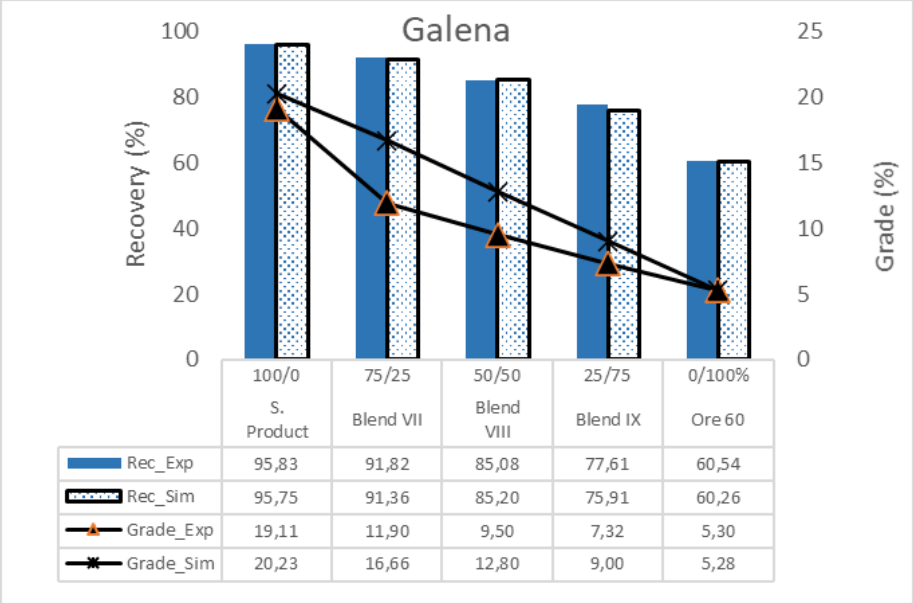

	100/0 S. Product	75/25 Blend VII	50/50 Blend VIII	25/75 Blend IX	0/100% Ore 60
Rec_Exp	95,83	91,82	85,08	77,61	60,54
Rec_Sim	95,75	91,36	85,20	75,91	60,26
Grade_Exp	19,11	11,90	9,50	7,32	5,30
Grade_Sim	20,23	16,66	12,80	9,00	5,28

Figure 95 Comparison between simulated and experimental grades-recoveries of galena in blend series 3

The simulated and experimental flotation results of NSG in blend series 3 are demonstrated in Figure 96. The simulated and experimental grades and recoveries of sorter product and ore 60 are almost similar. The recovery difference is about 0.1%, while the grade difference is below 1.1%. The recovery difference between simulated and experimental blend VII results is 1.2%, about 1% in blend VIII and blend IX. The simulated recoveries between ore 60 and sorter product are uniformly distributed in the range of 2.88% to 2.26%. The simulated and experimental recoveries of NSG are increased with an increase in the ore 60 content of the blend. The simulated grades between ore 60 and sorter product are uniformly distributed in the range of 74.46% to 56.83%. The NSG grade difference between blend VII, blend VIII and blend IX varies between 8.3% to 6.38%. The blends of ore 60 and sorter product result in higher experimental NSG grades and recoveries as compared to the simulated. The higher experimental NSG grade of blends resulted in a lower experimental grade of sulfide minerals as compared to simulation results, shown in Figure 94, Figure 95, and Figure 96.

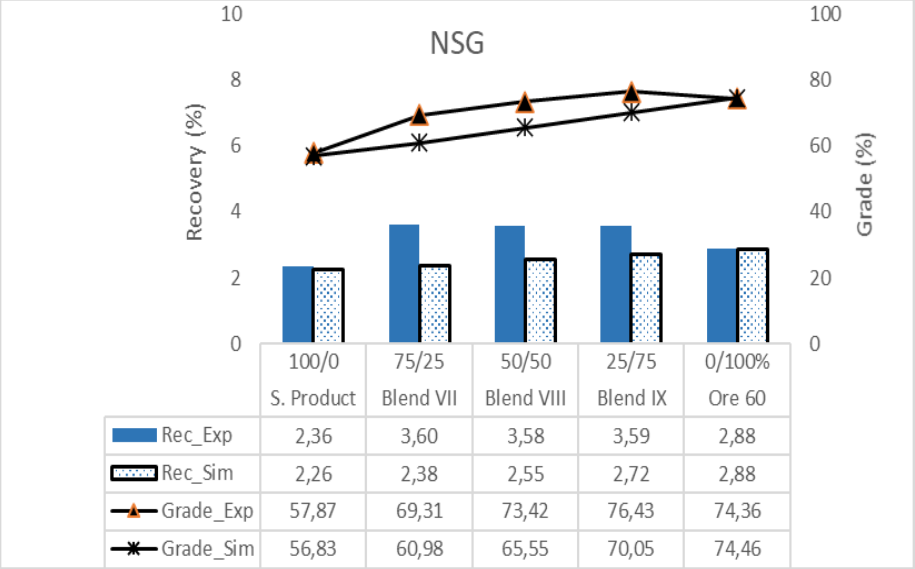

	100/0 S. Product	75/25 Blend VII	50/50 Blend VIII	25/75 Blend IX	0/100% Ore 60
Rec_Exp	2,36	3,60	3,58	3,59	2,88
Rec_Sim	2,26	2,38	2,55	2,72	2,88
Grade_Exp	57,87	69,31	73,42	76,43	74,36
Grade_Sim	56,83	60,98	65,55	70,05	74,46

Figure 96 Comparison between simulated and experimental grades-recoveries of NSG in blend series 3

5 CONCLUSIONS AND RECOMMENDATIONS

The variability of four types of ore from Sotkamo and the blend of those in different ratios were studied and validation of simulation models (rectangular distribution model) for ore blends was carried out. The response of different ore and blends were carried out under similar conditions of flotation. Finding first their grindability (classic and Mergan methods). Results were evaluated by modelling, and simulations.

The grinding calibration test for each ore sample determined the relation between particle size and grinding time. A comparison of the grindability of different samples, specific grinding energy for required p80 calculation, and bond ball mill work index were obtained with the Mergan grindability tests. Flotation tests demonstrated the kinetic response of each sample and their blends. Depending on flotation kinetic parameters of each ore type, the flotation response for each blend is predicted using simulation.

The four samples tested contain different grades of silver, lead, and zinc as valuable elements in the form of sulphide minerals and various degrees of oxidation. Iron and NSG are the non-valuable. Silver and lead minerals are enriched in the finest size fraction, while iron minerals are enriched in the coarsest size fraction. Malmi and sorter feed are low-grade ores while sorter product and ore 60 higher-grade ores. Malmi is the highest oxidized ore with 25% lead and 16% zinc oxidation. Ore 60 has up to 16% lead oxidation and 1% zinc oxidation. Sorter product has less than 5% oxidation of lead and zinc. Sorter feed has up to 11% Pb oxidation and 7.5% Zn oxidation.

Mergan tests concluded that the sorter feed and sorter product have a similar estimated bond work index of 7.5 kWh/t. The estimated bond work index of malmi is 6.7 kWh/t, 10% lower than the sorter feed and sorter product. The ore 60 is the softest with an estimated bond work index of 3.7 kWh/t. A similar grindability trend is found in grinding calibration tests.

In reference to flotation tests, the sorter product has 88% dyscrasite recovery. The high grade and recovery when using this type of ore were obtained as it has better quality and it is less oxidized which is resulted by pre-sorting stage that has a positive effect. Malmi and sorter feed have recoveries around 83%. Ore 60 has the lowest recovery of 77%. The recovery of galena in sorter feed and sorter product is about 95%. Malmi has the recovery

of 80%, while Ore 60 has the lowest galena recovery of 60.5%. The lowest recoveries of dyscrasite and galena in Ore 60 reflect the high oxidation and presence of slimes in this sample. The higher muscovite content of Ore 60 affected the reagent's effectiveness by making a thin layer at the particle surface. The flotation of Ore is considered challenging to achieve comparative recoveries and grades.

In terms of mineralogy, the pre-sorting of sorter feed resulted in higher grades of ore minerals. The sum of valuable minerals improved from 1.25% to 3.27%. Pre-sorting also resulted in higher pyrite and dolomite content, while the content of quartz and muscovite decreased. There are no effects of pre-sorting on grindability. Hence the specific grinding energy and estimated bond work index are similar for sorter feed and sorter product. The behind is the higher content of gangue i.e. 98.75% in sorter feed and 96.73%. A slight difference in gangue content resulted in no effect on grindability. In terms of flotation kinetics, pre-sorting resulted in similar galena recovery and 5% higher dyscrasite recovery, minor impact on flotation kinetics.

There is a good comparison between experimental and simulated flotation results. The flotation kinetics for each blend are different, and the sample's content in a blend impacted the flotation kinetics. The higher content of malmi in sorter product causes lower recoveries and grades. The higher content of Ore 60 in malmi and sorter product cause lower recoveries in the final concentrate.

The simulation of blends shows similar recoveries as compared to experimental recoveries. While the experimental grades of ore minerals in blend series 1 are higher than the simulated grades. The grade of gangue in experimental tests is lower than the simulated grades of blend series 1. Thus, the lower gangue grade resulted in a higher grade of ore minerals in the final concentrate of blend series 1. The experimental grades of ore minerals in blend series 2 and 3 are lower than the simulated grade. In these series, the experimental gangue grade is higher than the simulated grade. The higher grade of gangue causes a lower grade of ore minerals in experimental tests. The presence of ore 60 in a blend cause higher gangue grade and lower grades of ore minerals due to the presence of slimes and oxidation.

In general, the HSC's simulation module is predictive for the blend's flotation simulations. In this study, the comparison between simulated and experimental floatation results is good. For blends simulation, the higher grade of gauge in experimental tests

affected the estimation of grade, due to low mass pull of concentrate (3-4%). At the same time, the simulated and experimental recovers are close to each other.

The recommendation for further study is to blend more than two ore and test the flotation kinetics and simulations. The ore 60 is oxidized and flotation recoveries of ore minerals are lower, hence this ore should be studied for different dosages of and removal of slimes to achieve maximum recovery. Once the new recipe is developed for ore 60, blends of ore 60 should be studied using the new flotation recipe. Another recommendation is to conduct the grindability tests for the blends. The mixing of soft and hard ores might cause under/over-grinding; hence, the impact of grindability of blends on flotation kinetics should be studied. Despite using standard procedures and equipment, the reproducibility should be examined by conducting multiple similar tests. Multiple blend tests can provide the variance for the flotation results, which can help in simulation and modeling f the results. In this study, rougher and scavenger is studied. Hence cleaner tests should be conducted with recirculation to overprint the actual plant process.

6 SUMMARY

Geometallurgical models are more often used in concentrator plants. Geometallurgy is essential for efficient resource utilization and risk management. Geometallurgy provides comprehensive knowledge of ore bodies, including metallurgical response before the deposits are mined. High-grade ore deposits are already extracted, and new low-grade complex deposits offer no room for errors. Hence efficient resource utilization is essential.

Heterogeneity of ore deposits usually causes the variable feed to a process plant. The performance of the processing plant is affected by the variation in the feed. Optimum and controlled processing requires a uniform feed to a plant. The ore from different parts of a deposit is different, and optimum blending is often to provide a controlled feed. Blends are commonly used, and investigation of metallurgical performance of blends helps predict the metallurgical response of processing plant and enables effective mineral processing and resource utilization.

The main objective of the thesis is to investigate the productivity of simulation for the prediction of flotation response of different types of ore and their blends. In addition, the effect of ore pre-sorting on grindability and flotation response is studied. The main research questions are:

- Effect of ore variations and blends on flotation performance, can be simulated?
- May the product of sorting before flotation bank affect flotation kinetics?

The literature review includes the previous comprehensive study of the Taivaljärvi ore deposit. The traditional lead-zinc flotation practices are also reviewed. Earlier studies about blends conclude that the ore blends present linear grindability response while recovery response is non-linear. A chapter about available flotation models is also presented.

This thesis work is conducted using four samples from Sotkamo Silver Oy: malmi, sorter feed, sorter product, and ore 60. Grinding calibration tests were conducted to study the relationship between grinding times and particle size for each sample. Mergan grindability tests were conducted for each ore type for sample classification based on grindability. Mineralogical studies for each sample are conducted to study elemental and

mineral distribution in each sample. EDTA analysis is used to study the oxidation of lead and zinc. Reference flotation tests were conducted to study the flotation kinetics of each sample. The reference flotation tests were simulated using HSC Chemistry ® software. Nine blends are prepared using three different ore types. The kinetic flotation tests were conducted to study the kinetics of each blend. The blend's flotation tests are simulated and compared to the experimental tests, to investigate the productivity of the simulations.

Sorter product and sorter feed samples are similar in terms of grindability and recoveries, hence presorting of ore is not affecting upstream processes. Malmi sample has 10% less specific grinding energy than sorter feed and sorter product. Ore 60 is the softest in terms of grindability as compared to other samples. Both galena and sphalerite in malmi sample are oxidized. Ore 60 is oxidated more completely as compared to malmi sample. Sorter product is least oxidized. The sorter feed is slightly higher oxidized than sorter product. Good recoveries were achieved for sorter product, malmi and sorter feed samples. Ore 60 has the lowest galena recovery and highest pyrite recovery. Hence the flotation of ore 60 is complex due to oxidation and the presence of slimes (higher muscovite content). There was a good comparison between experimental flotation tests and simulation. The experimental and simulated recoveries of blends are close to each other. The blends of malmi and sorter product resulted in lower gangue grade and higher grade of ore minerals as compared to the simulated results. In contrast, the blends of ore 60 with malmi and sorter product resulted in higher experimental gangue grade and lower grade of ore minerals as compared to simulated blend's grades. The lower mass pull of concentrate (3-4%) and low grade of ore minerals resulted in slightly different experimental grades than simulated grades. In addition, oxidation and presence of slimes also affected blends flotation kinetics. The simulation results are close to the experimental results. Hence HSC simulation module can be used for the prediction of blend's flotation kinetics.

The recommendations include further investigation and recipe adjustment for the oxidized Ore 60 sample. Blends of more than two types of ores should be studied. The grindability tests for each blend should be conducted to investigate the blend's grindability. Multiple blends flotation tests should be undertaken to study the variance of flotation results. The cleaner flotation tests should be undertaken to study overall response of lead-silver flotation circuit along with rougher and scavenger flotation.

7 REFERENCES

Bond, F. C. (1961). *Crushing and grinding calculations*. Allis-Chalmers Manufacturiing Company.

Bulatovic, S. M. (2007). 14 - Flotation of Lead–Zinc Ores. In S. M. Bulatovic (Ed.), *Handbook of Flotation Reagents* (pp. 323–366). Elsevier. https://doi.org/https://doi.org/10.1016/B978-044453029-5/50023-X

Bulled, D., & McInnes, C. (2005). Flotation plant design and production planning through geometallurgical modelling. *Australasian Institute of Mining and Metallurgy Publication Series*, 809–814.

CUI, Y. Fang, JIAO, F., QIN, W. Qing, DONG, L. Yang, & WANG, X. (2020). Synergistic depression mechanism of zinc sulfate and sodium dimethyl dithiocarbamate on sphalerite in Pb−Zn flotation system. *Transactions of Nonferrous Metals Society of China (English Edition)*, *30*(9), 2547–2555. https://doi.org/10.1016/S1003-6326(20)65400-0

David, D. (2007). *The Importance of Geometallurgical Analysis in Plant Study, Design and Operational Phases*. The Australasian Institute of Mining and Metallurgy.

Dobby, G., Bennett, C., Bulled, D. and Kosick, G. (2004). *Geometallurgical modeling – The new approach to plant design and production forecasting/planning, and Mine/Mill Optimization*. Proceedings of 36th Annual Meeting of the Canadian Mineral Processors, January 20-22, 2004. Ottawa, Canada, Paper 15.

Dobby, G., Bennett, C., & Kosick, G. (2001). Advances in SAG circuit design and simulation applied: The mine block model. *Proceedings International Autogenous and Semiautogenous Grinding Technology*, *4*, 221–234.

Drzymala, J. (2007). *Mineral Processing, Foundations of theory and practice of minerallurgy*. https://doi.org/10.1017/CBO9781107415324.004

Duan, J., Fornasiero, D., & Ralston, J. (2003). Calculation of the flotation rate constant of chalcopyrite particles in an ore. *International Journal of Mineral Processing*, *72*(1), 227–237. https://doi.org/https://doi.org/10.1016/S0301-7516(03)00101-7

Foroutan, A., Abbas Zadeh Haji Abadi, M., Kianinia, Y., & Ghadiri, M. (2021). Critical importance of pH and collector type on the flotation of sphalerite and galena from a

low-grade lead–zinc ore. *Scientific Reports*, *11*(1), 3103. https://doi.org/10.1038/s41598-021-82759-3

Gharai, M., & Venugopal, R. (2016). *Modelling of flotation process- An overview of different approaches*.

Heiskari, H., Kurki, P., Luukkanen, S., Gonzalez, M. S., Lehto, H., & Liipo, J. (2019). Development of a comminution test method for small ore samples. *Minerals Engineering*, *130*(May 2018), 5–11. https://doi.org/10.1016/j.mineng.2018.10.005

Jameson, G. J., Nam, S., & Young, M. M. (1977). Physical factors affecting recovery rates in flotation. *Miner. Sci. Eng.; (South Africa)*.

Karimi, M., Akdogan, G., & Bradshaw, S. M. (2014). A computational fluid dynamics model for the flotation rate constant, Part I: Model development. *Minerals Engineering*, *69*, 214–222. https://doi.org/https://doi.org/10.1016/j.mineng.2014.03.028

Käyhkö, T. (2019). *The Validation of Predictive Geometallurgical Models for Concentrator Plant Process Design* (Issue August) [University of Oulu]. http://jultika.oulu.fi/Record/nbnfi-fe2021052030749

Kelly, E. G. (1982). *Introduction to mineral processing / Errol G. Kelly, David J. Spottiswood* (D. J. Spottiswood (ed.)). Wiley.

Lamberg, P. (2011). Particles–the bridge between geology and metallurgy. *Proceedings of the Conference in Minerals Engineering, Luleå, Sweden*, 8–9.

Laskowski, J. S., & Ralston, J. (1992). *Colloid Chemistry in Mineral Processing* (1st ed.).

Liipo, J., Hicks, M., Takalo, V., Remes, A., Talikka, M., Khizanishvili, S., & Natsvlishvili, M. (2019). *Geometallurgical characterization of South Georgian complex copper-gold ores*. *119*(April), 333–338.

Lindborg, T., Papunen, H., Parkkinen, J., & Tuokko, I. (2015). The Taivaljärvi Ag-Au-Zn deposit in the Archean TipasjÄrvi greenstone belt, eastern Finland. *Mineral Deposits of Finland*, *1999*, 633–657. https://doi.org/10.1016/B978-0-12-410438-9.00024-8

MacPherson, A. R., & Turner, R. R. (1978). Autogenous grinding from test work to purchase of a commercial unit. *Mineral Processing Plant Design*, 279–305.

Marcelo, L., & Kallemback, R. D. C. (2013). *Grindability of binary ore blends in ball mills*. *41*, 115–120. https://doi.org/10.1016/j.mineng.2012.11.001

Mcken, A., & Williams, S. (2005). An Overview of the Small-scale Tests Available to Characterize Ore Grindability for Design Purposes. *SGS Minerals Technical Bulleting*, *2005*(06), 8.

Meyer, L., & Davies, C. (2012). *SOTKAMO SILVER OY Taivaljärvi Mine Bankable Feasibility Study* (Issue May).

Mwanga, A., Lamberg, P., & Rosenkranz, J. (2015). Comminution test method using small drill core samples. *Minerals Engineering*. https://doi.org/10.1016/j.mineng.2014.12.009

Napier-Munn, T., & Wills, B. A. (2005). Wills' Mineral Processing Technology. In *Wills' Mineral Processing Technology* (Issue October). https://doi.org/10.1016/B978-0-7506-4450-1.X5000-0

Niitti, T. (1973). *Rapid evaluation of grindability by a simple batch test: This Paper was Presented at the IX International Mineral Processing Congress in Prague, June 1970*. Outokumpu. https://books.google.fi/books?id=OU4XHAAACAAJ

Niskanen, M. (2012). *Electromagnetic SAMPO soundings at Taivaljärvi 2011*.

Niskanen, M. (2013). *Electromagnetic SAMPO soundings at Taivaljärvi 2013*.

P. A, Mingione. (1991). *Performance characteristics and application of Aerophone 3418A promoter for base and precious metals flotation*. SME annual meeting Denver Colorado- February 25-28, 1991. https://www.911metallurgist.com/aerophine-3418a/

Papunen, H., Kopperoinen, T., Tuokko, I. (1989). Taivaljärvi Ag-Zn deposit in the Archean greenstone belt, eastern Finland. In *Economic Geology 84, 1262–1276*.

Pecina-Treviño, E. T., Uribe-Salas, A., Nava-Alonso, F., & Pérez-Garibay, R. (2003). On the sodium-diisobutyl dithiophosphinate (Aerophine 3418A) interaction with activated and unactivated galena and pyrite. *International Journal of Mineral Processing*, *71*(1), 201–217. https://doi.org/https://doi.org/10.1016/S0301-7516(03)00059-0

Runge, K. C., Alexander, D. J., Franzidis, J-P., Morrison, R. D., and Manlapig, E. (1998). *JKSimFloat - A tool for flotation modelling*.

Sargent, R. G. (1981). *An Assessment Procedure and a Set of Criteria for Use in the Evaluation of Computerized Models and Computer-Based Modeling Tools.*

Sargent, R. G. (2010). Verification and validation of simulation models. *Proceedings - Winter Simulation Conference*, *February*, 166–183. https://doi.org/10.1109/WSC.2010.5679166

Sherrell, I. M. (2004). Development of a Flotation Rate Equation from First Principles under Turbulent Flow Conditions. *Mining and Minerals Engineering*, 104.

Silver, S. (2021). *Mineral processing-Sotkamo silver*. https://www.silver.fi/en/silver-mine/mineral-processing

Singh, R., Banerjee, B., & Srivastava, J. P. (2004). Effects of process parameters on selective flotation of lead-Zinc Ore mineralogical characteristics of the sample. *International Seminar on Mineral Processing Technology*, 425–432.

Starkey, J., & Dobby, G. (1996). Application of the Minnovex Sag Power Index At Five Canadian Sag Plants. *Autogenous and Semi-Autogenous Grinding*, 345–360.

States, U., Efficiency, E., & Energy, R. (2004). Industrial Technologies Program — Boosting the Productivity and Competitiveness of U . S . Industry. *Program*.

Talikka, M., Remes, A., Hicks, M., Liipo, J., Takalo, V., & Copper, R. M. G. (2018). *Copper Ore Variability – Benefits of Advanced Simulation*. *July*, 10–12.

Tonder, E. Van, Deglon, D. A., & Napier-munn, T. J. (2010). lind. *Minerals Engineering*, *23*(8), 621–626. https://doi.org/10.1016/j.mineng.2010.02.008

Veras, M. M., Magalhães, C. A., & Baltar, J. B. de A. P. (2014). *Comparative study of the main flotation frothers using a new HYDROMESS adapted technique*. *67*(1), 87–92.

Wikedzi, A., Arinanda, M. A., Leißner, T., Peuker, U. A., & Mütze, T. (2018). Breakage and liberation characteristics of low grade sulfide gold ore blends. *Minerals Engineering*, *115*(October 2017), 33–40. https://doi.org/10.1016/j.mineng.2017.10.009

Wills, B. A., & Finch, J. A. (2016). Chapter 12 - Froth Flotation. In B. A. Wills & J. A. Finch (Eds.), *Wills' Mineral Processing Technology (Eighth Edition)* (Eighth Edi, pp. 265–380). Butterworth-Heinemann. https://doi.org/https://doi.org/10.1016/B978-0-08-097053-0.00012-1

Wills, B. A., & Napier-Munn, T. (2005). 12 - Froth flotation. In B. A. Wills & T. Napier-Munn (Eds.), *Wills' Mineral Processing Technology (Seventh Edition)* (Seventh Ed, pp. 267–352). Butterworth-Heinemann. https://doi.org/https://doi.org/10.1016/B978-075064450-1/50014-X

Woodburn, E. T., & Loveday, B. K. (1965). The effect of variable residence time on the performance of a flotation system. *Journal of the South African Institute of Mining and Metallurgy*, *65*(null), 612–628.

Yianatos, J., Bergh, L., Vinnett, L., Contreras, F., & Díaz, F. (2010). Flotation rate distribution in the collection zone of industrial cells. *Minerals Engineering*, *23*(11), 1030–1035. https://doi.org/https://doi.org/10.1016/j.mineng.2010.05.008

Yoon, R.-H., & Mao, L. (1996). Application of Extended DLVO Theory, IV: Derivation of Flotation Rate Equation from First Principles. *Journal of Colloid and Interface Science*, *181*(2), 613–626. https://doi.org/https://doi.org/10.1006/jcis.1996.0419

Zanin, M., Lambert, H., & du Plessis, C. A. (2019). Lime use and functionality in sulfide mineral flotation: A review. *Minerals Engineering*, *143*, 105922. https://doi.org/https://doi.org/10.1016/j.mineng.2019.105922

8 APPENDICES

Appendix A

Blends simulated and experimental flotation results over flotation time

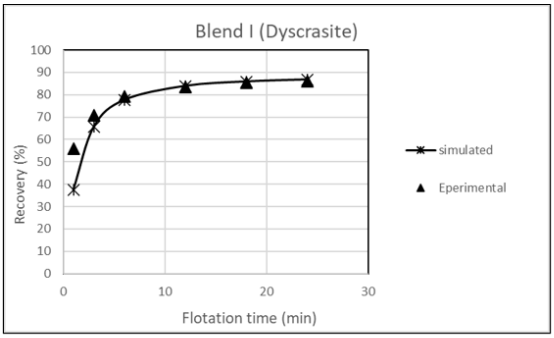

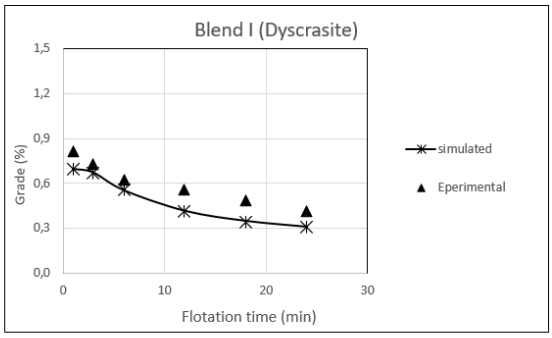

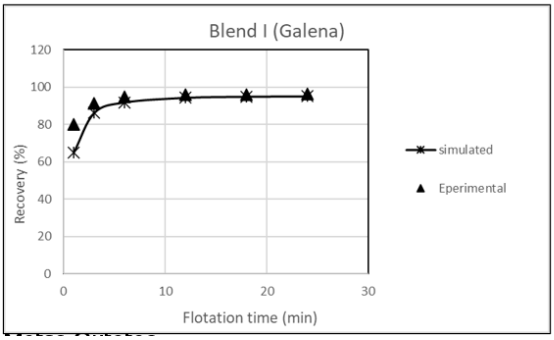

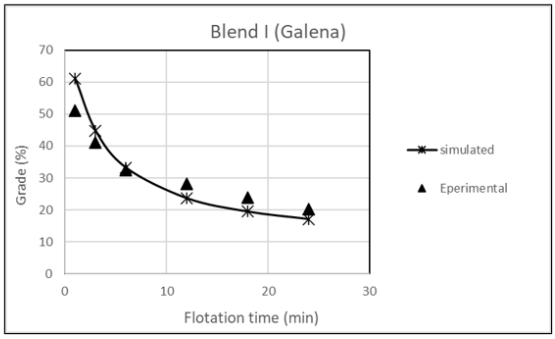

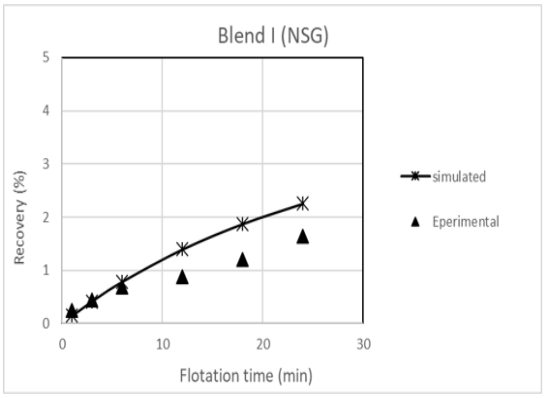

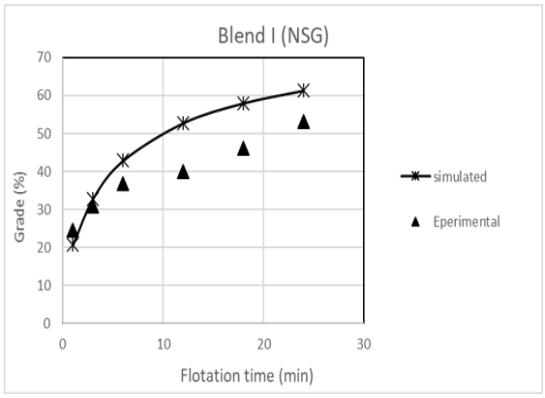

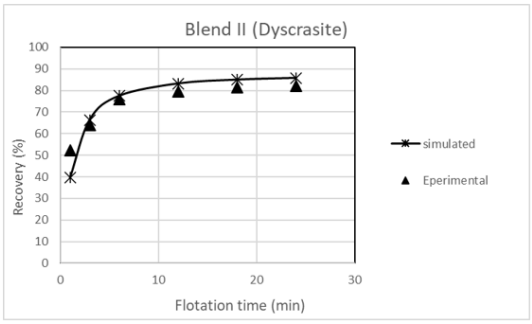
Blend II (Dyscrasite)
Recovery (%)
Flotation time (min)
simulated
Eperimental

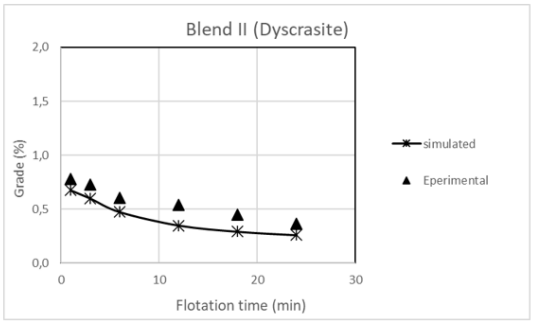
Blend II (Dyscrasite)
Grade (%)
Flotation time (min)
simulated
Eperimental

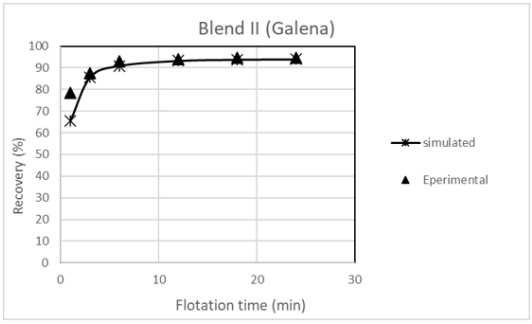
Blend II (Galena)
Recovery (%)
Flotation time (min)
simulated
Eperimental

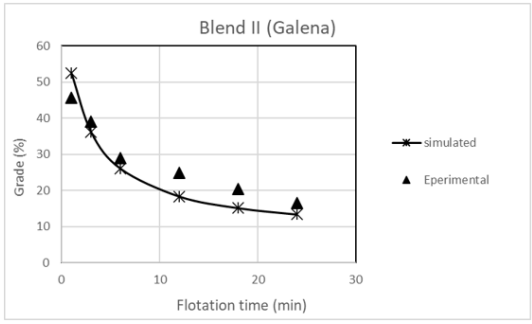
Blend II (Galena)
Grade (%)
Flotation time (min)
simulated
Eperimental

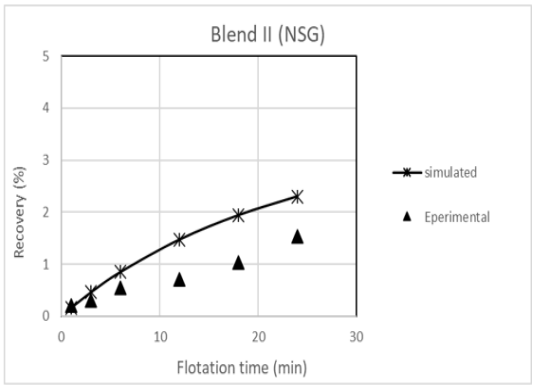
Blend II (NSG)
Recovery (%)
Flotation time (min)
simulated
Eperimental

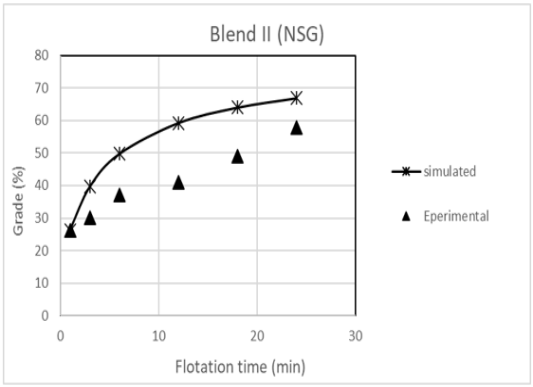
Blend II (NSG)
Grade (%)
Flotation time (min)
simulated
Eperimental

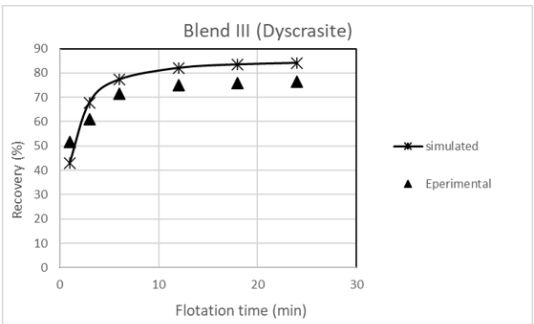
Blend III (Dyscrasite)
Recovery (%)
Flotation time (min)
simulated
Eperimental

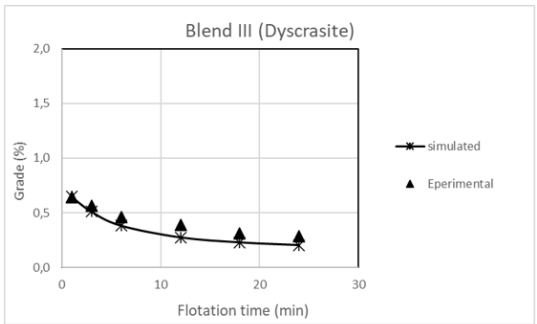
Blend III (Dyscrasite)
Grade (%)
Flotation time (min)
simulated
Eperimental

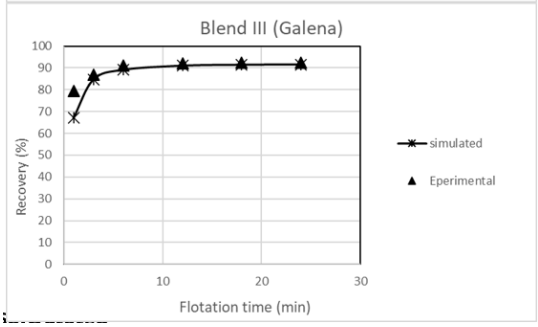
Blend III (Galena)
Recovery (%)
Flotation time (min)
simulated
Eperimental

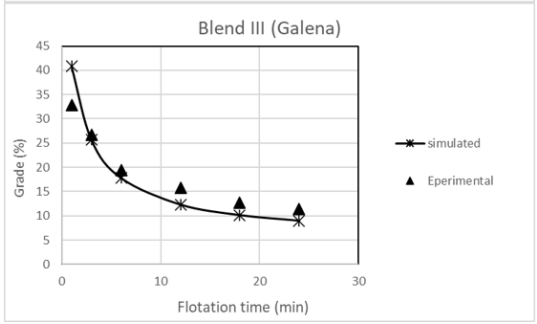
Blend III (Galena)
Grade (%)
Flotation time (min)
simulated
Eperimental

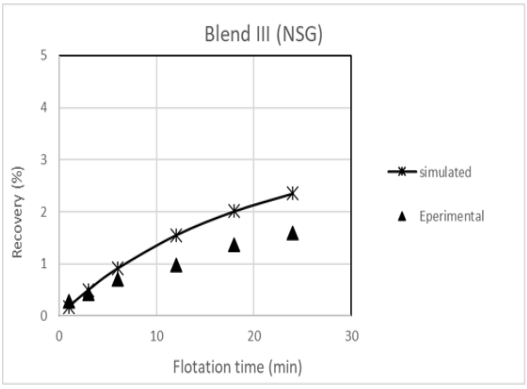
Blend III (NSG)
Recovery (%)
Flotation time (min)
simulated
Eperimental

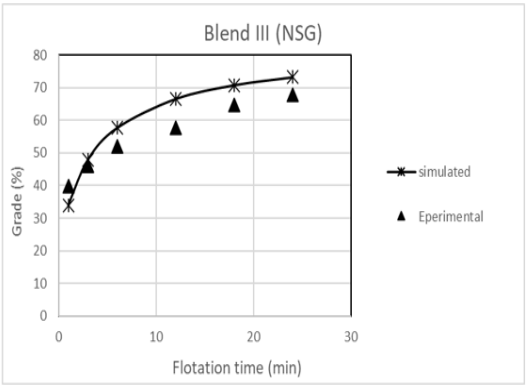
Blend III (NSG)
Grade (%)
Flotation time (min)
simulated
Eperimental

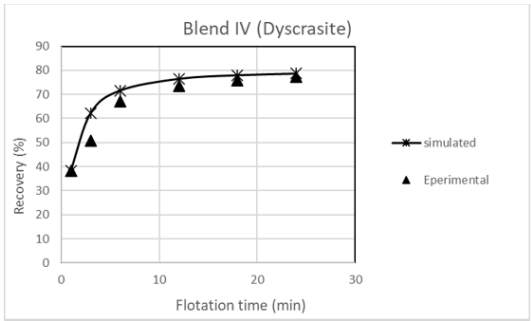
Blend IV (Dyscrasite)
Recovery (%)
Flotation time (min)
simulated
Eperimental

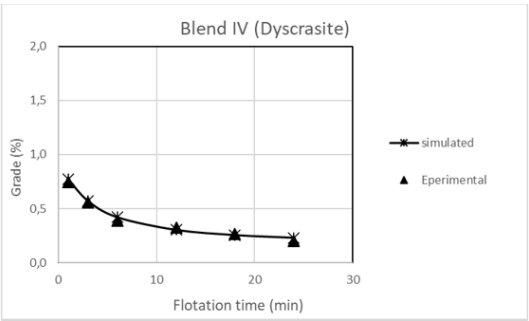
Blend IV (Dyscrasite)
Grade (%)
Flotation time (min)
simulated
Eperimental

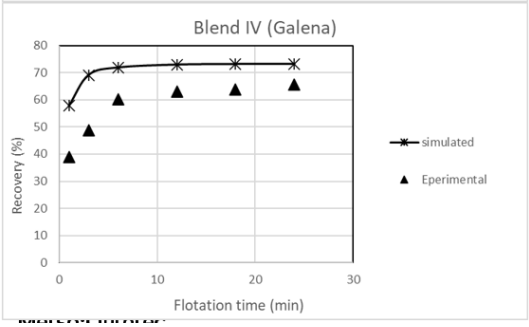
Blend IV (Galena)
Recovery (%)
Flotation time (min)
simulated
Eperimental

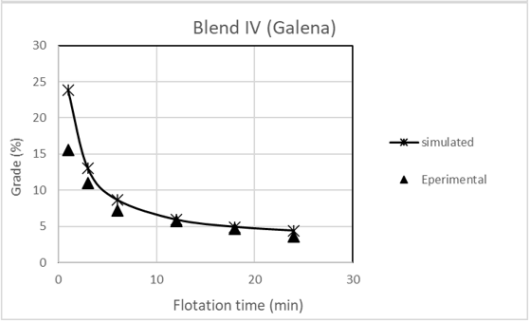
Blend IV (Galena)
Grade (%)
Flotation time (min)
simulated
Eperimental

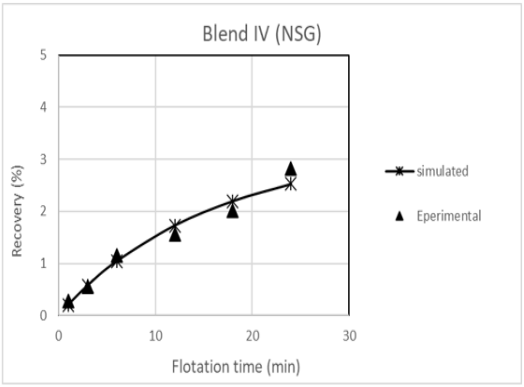
Blend IV (NSG)
Recovery (%)
Flotation time (min)
simulated
Eperimental

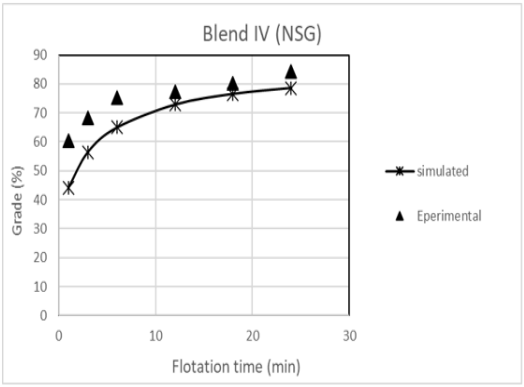
Blend IV (NSG)
Grade (%)
Flotation time (min)
simulated
Eperimental

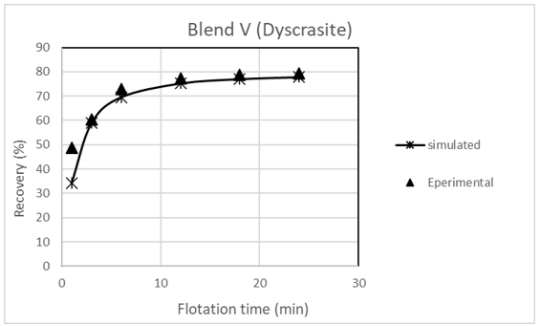
Blend V (Dyscrasite)
Recovery (%)
Flotation time (min)
simulated
Eperimental

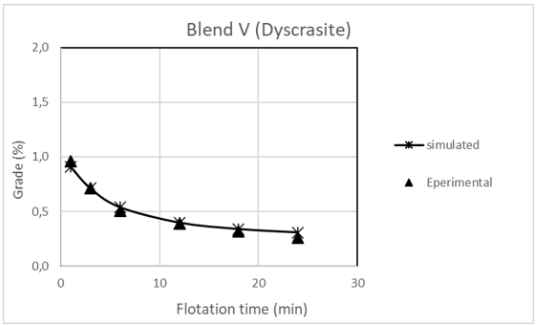
Blend V (Dyscrasite)
Grade (%)
Flotation time (min)
simulated
Eperimental

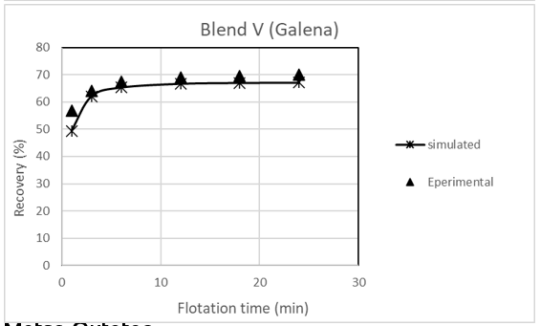
Blend V (Galena)
Recovery (%)
Flotation time (min)
simulated
Eperimental

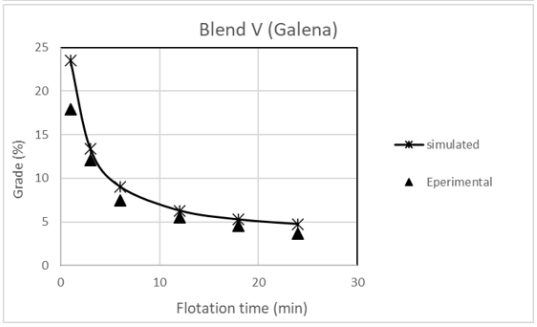
Blend V (Galena)
Grade (%)
Flotation time (min)
simulated
Eperimental

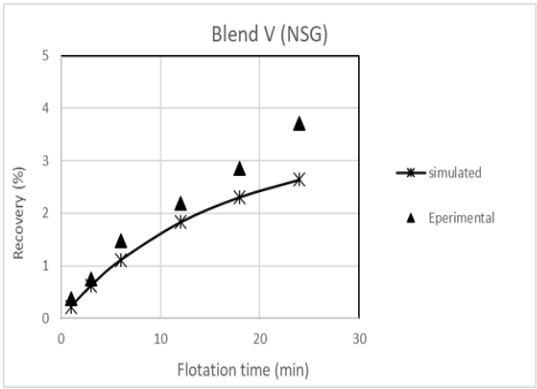
Blend V (NSG)
Recovery (%)
Flotation time (min)
simulated
Eperimental

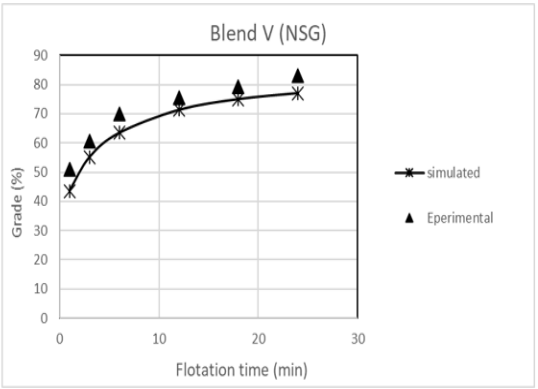
Blend V (NSG)
Grade (%)
Flotation time (min)
simulated
Eperimental

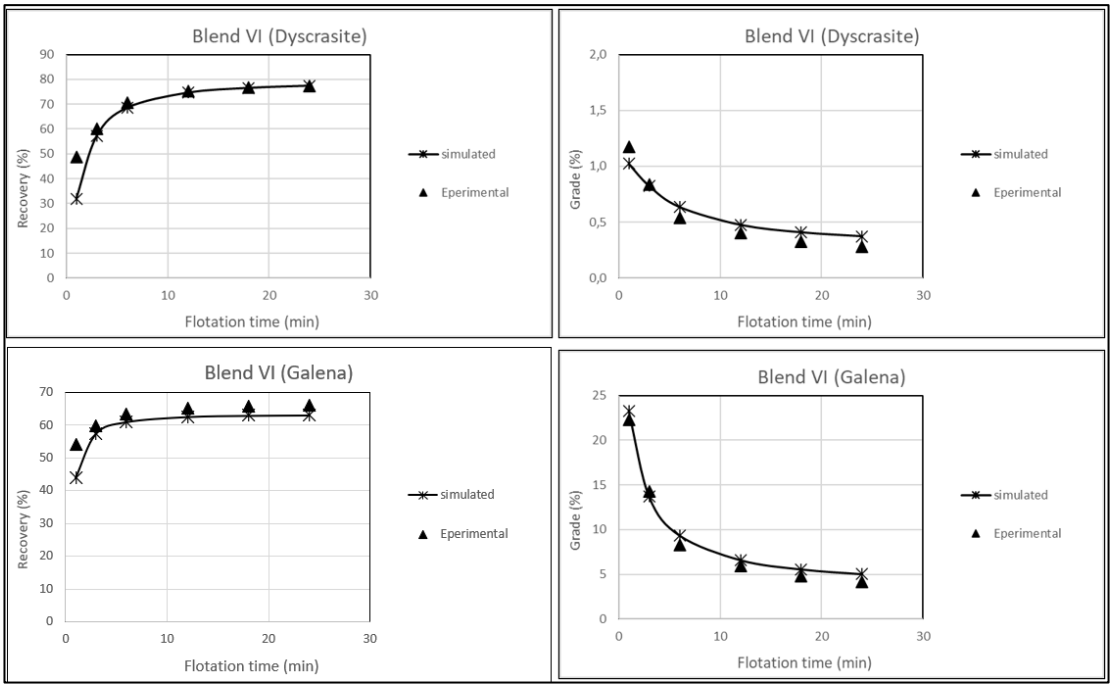
Blend VI (Dyscrasite)
Recovery (%)
Flotation time (min)
simulated
Eperimental
Blend VI (Dyscrasite)
Grade (%)
Flotation time (min)
simulated
Eperimental
Blend VI (Galena)
Recovery (%)
Flotation time (min)
simulated
Eperimental
Blend VI (Galena)
Grade (%)
Flotation time (min)
simulated
Eperimental

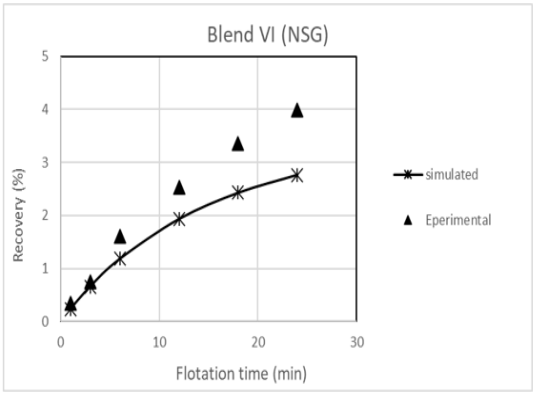
Blend VI (NSG)
Recovery (%)
Flotation time (min)
simulated
Eperimental

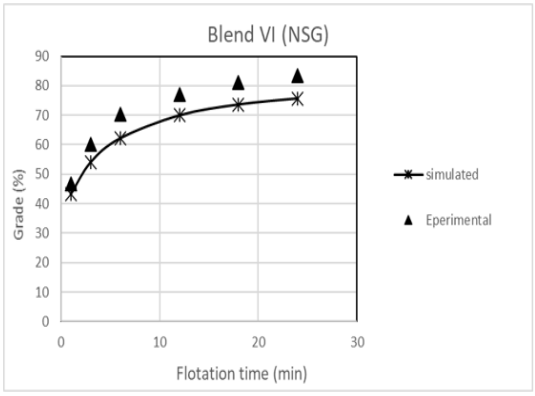
Blend VI (NSG)
Grade (%)
Flotation time (min)
simulated
Eperimental

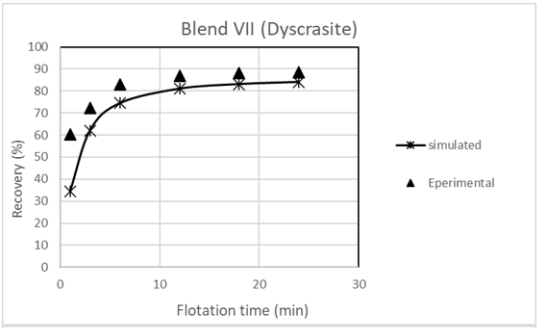
Blend VII (Dyscrasite)
Recovery (%)
Flotation time (min)
simulated
Eperimental

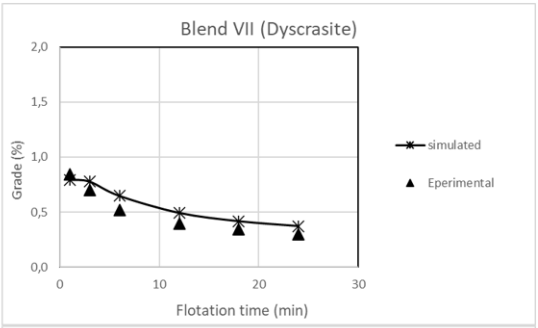
Blend VII (Dyscrasite)
Grade (%)
Flotation time (min)
simulated
Eperimental

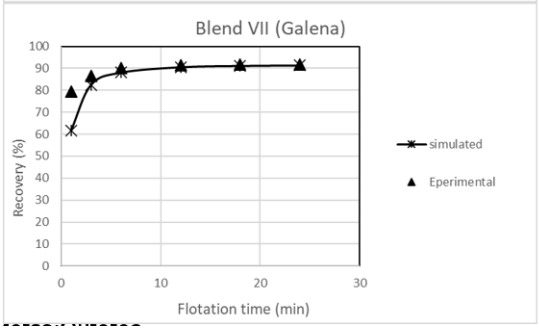
Blend VII (Galena)
Recovery (%)
Flotation time (min)
simulated
Eperimental

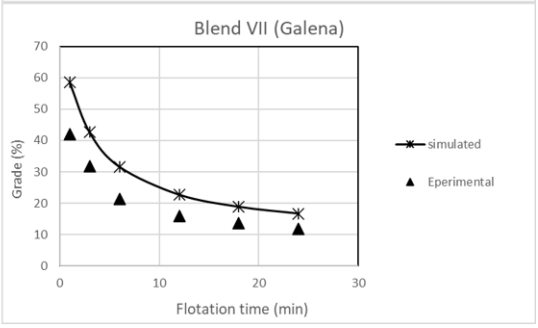
Blend VII (Galena)
Grade (%)
Flotation time (min)
simulated
Eperimental

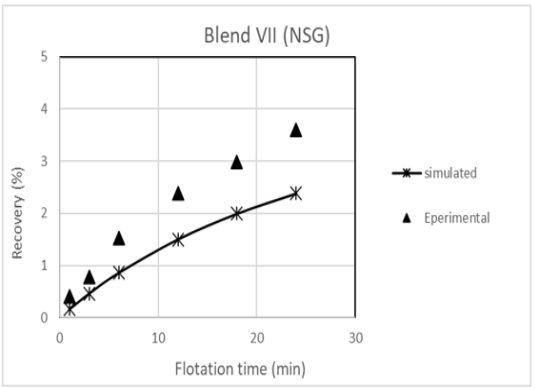
Blend VII (NSG)
Recovery (%)
Flotation time (min)
simulated
Eperimental

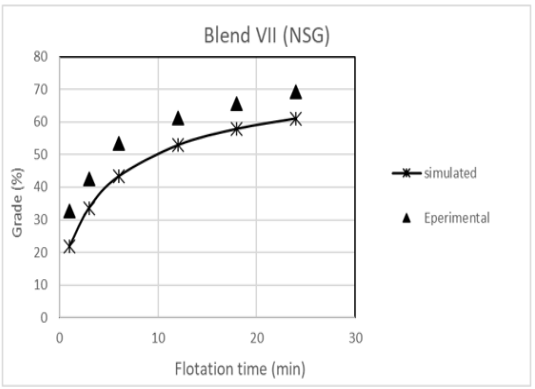
Blend VII (NSG)
Grade (%)
Flotation time (min)
simulated
Eperimental

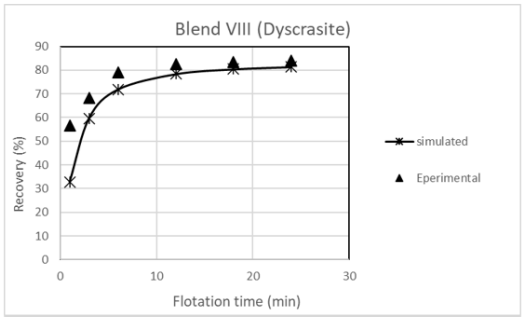
Blend VIII (Dyscrasite)
Recovery (%)
Flotation time (min)
simulated
Eperimental

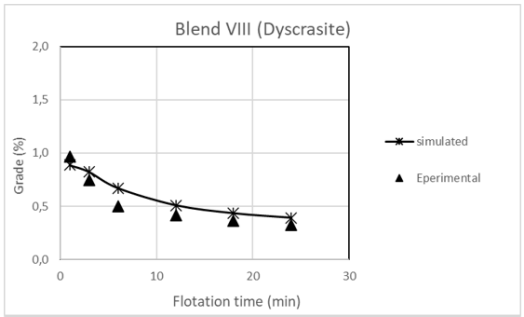
Blend VIII (Dyscrasite)
Grade (%)
Flotation time (min)
simulated
Eperimental

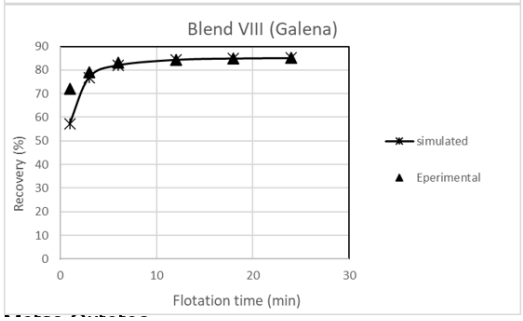
Blend VIII (Galena)
Recovery (%)
Flotation time (min)
simulated
Eperimental

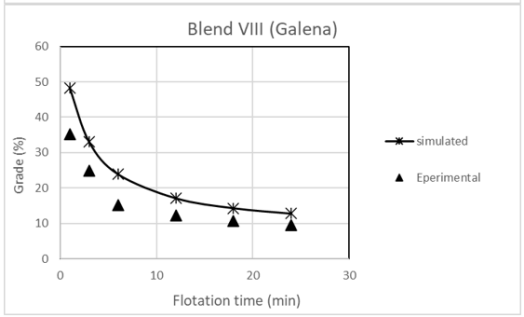
Blend VIII (Galena)
Grade (%)
Flotation time (min)
simulated
Eperimental

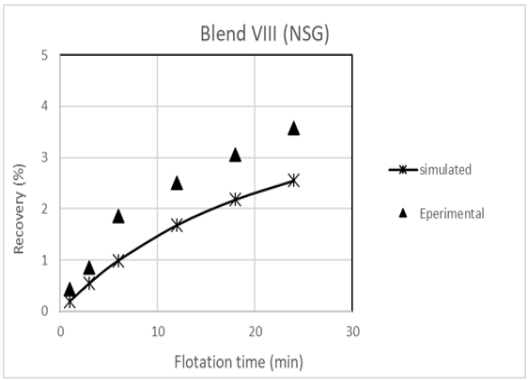
Blend VIII (NSG)
Recovery (%)
Flotation time (min)
simulated
Eperimental

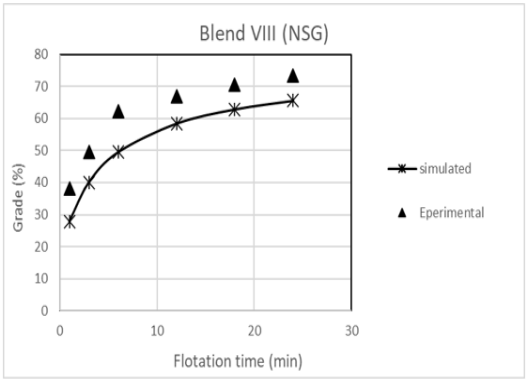
Blend VIII (NSG)
Grade (%)
Flotation time (min)
simulated
Eperimental

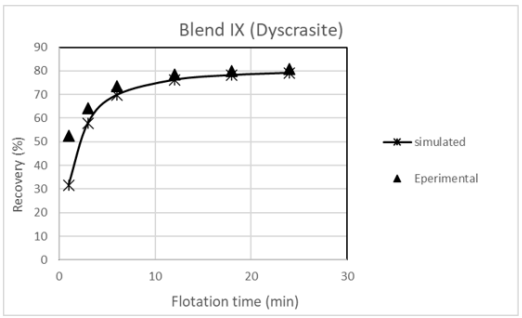
Blend IX (Dyscrasite)
Recovery (%)
Flotation time (min)
simulated
Eperimental

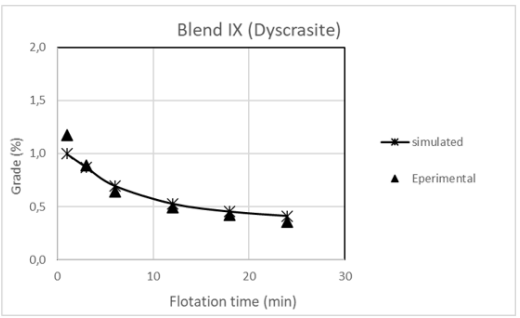
Blend IX (Dyscrasite)
Grade (%)
Flotation time (min)
simulated
Eperimental

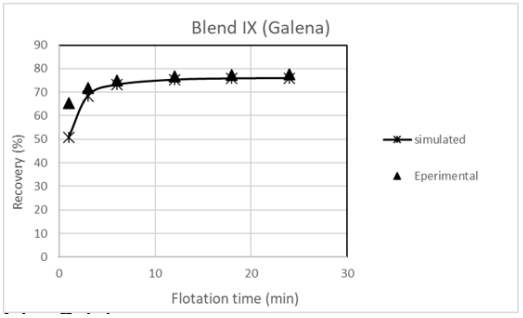
Blend IX (Galena)
Recovery (%)
Flotation time (min)
simulated
Eperimental

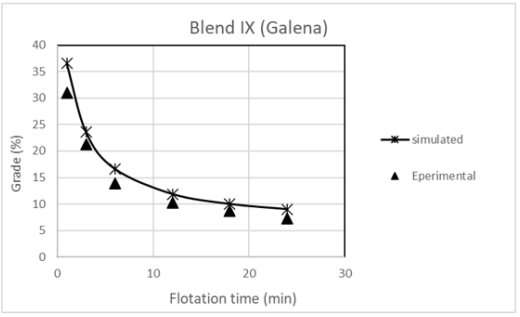
Blend IX (Galena)
Grade (%)
Flotation time (min)
simulated
Eperimental

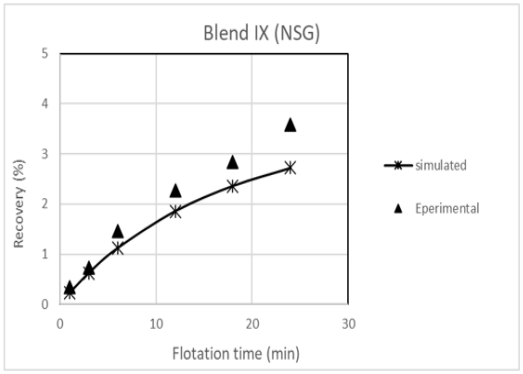
Blend IX (NSG)
Recovery (%)
Flotation time (min)
simulated
Eperimental

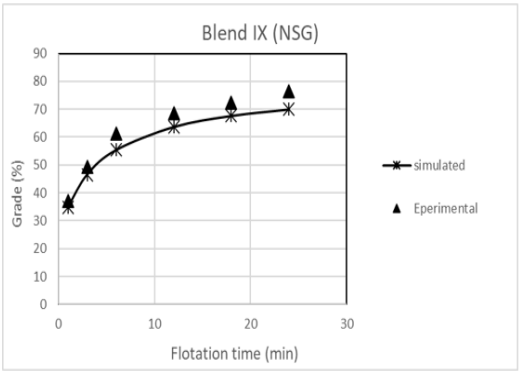
Blend IX (NSG)
Grade (%)
Flotation time (min)
simulated
Eperimental

Appendix B

Comparison of simulated and experimental grades and recoveries in blend series:

Blend series 1

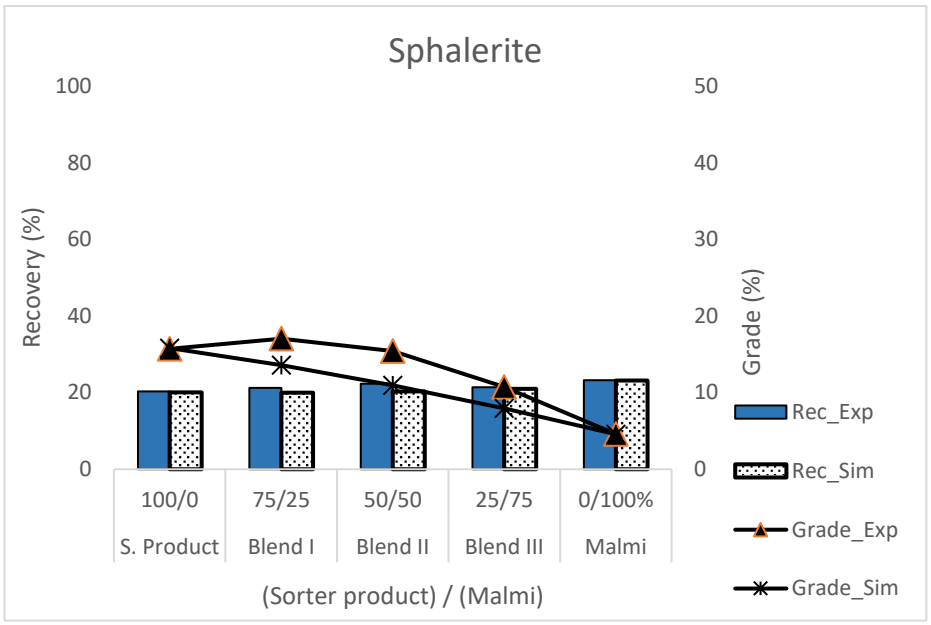

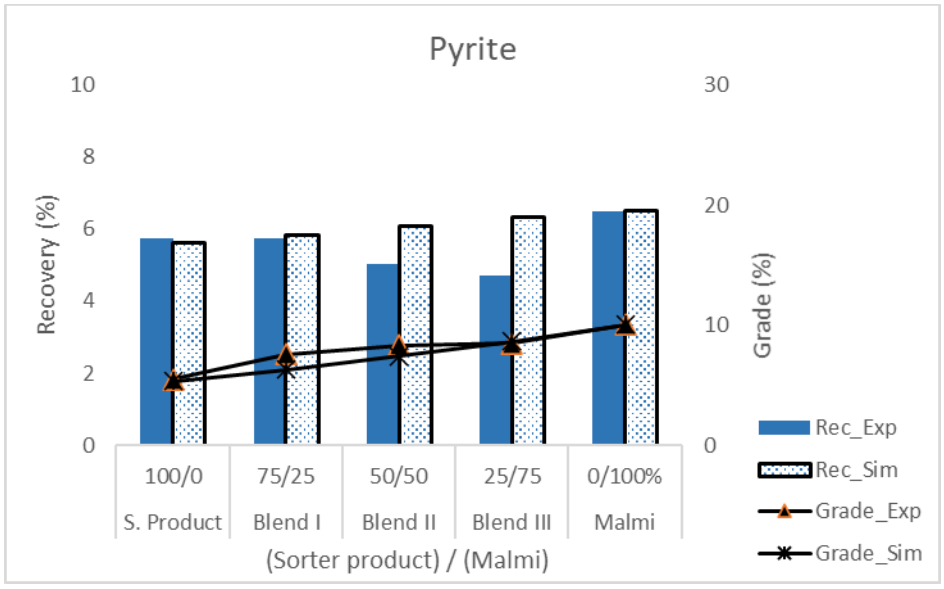

Blend series 2

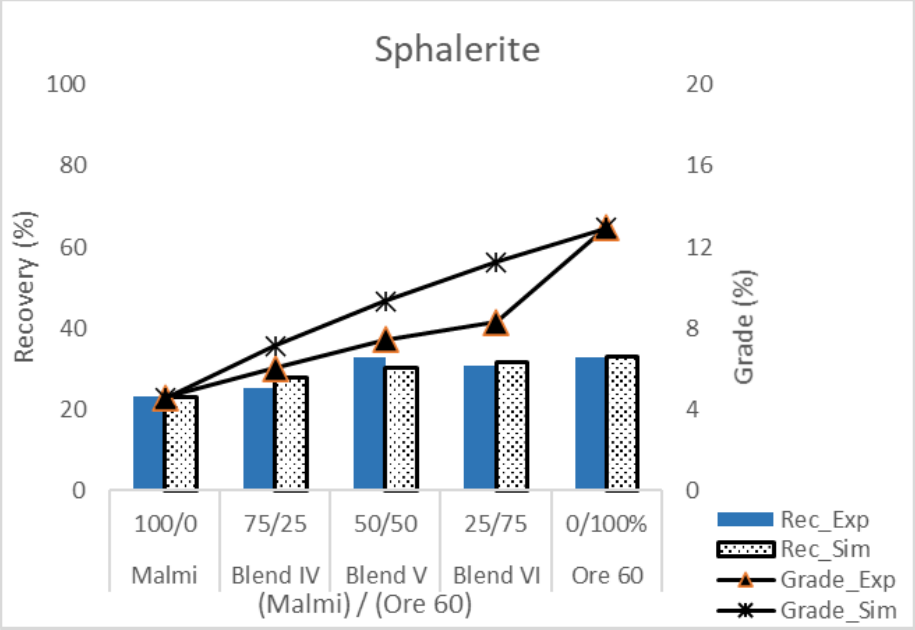
Sphalerite
Recovery (%)
Grade (%)
100
80
60
40
20
0
20
16
12
8
4
0
100/0
75/25
50/50
25/75
0/100%
Malmi
Blend IV
Blend V
Blend VI
Ore 60
(Malmi) / (Ore 60)
Rec_Exp
Rec_Sim
Grade_Exp
Grade_Sim

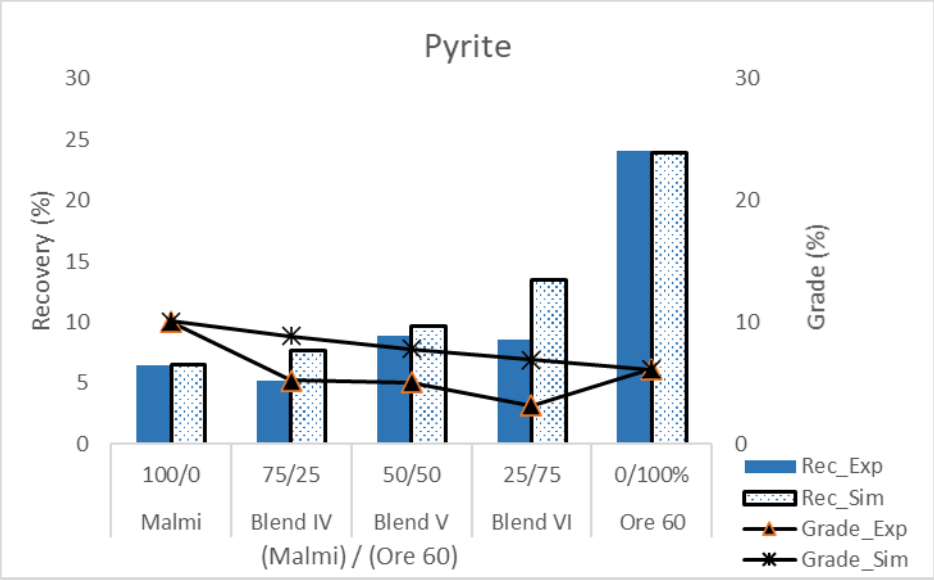
Pyrite
Recovery (%)
Grade (%)
30
25
20
15
10
5
0
30
20
10
0
100/0
75/25
50/50
25/75
0/100%
Malmi
Blend IV
Blend V
Blend VI
Ore 60
(Malmi) / (Ore 60)
Rec_Exp
Rec_Sim
Grade_Exp
Grade_Sim

Blend series 3

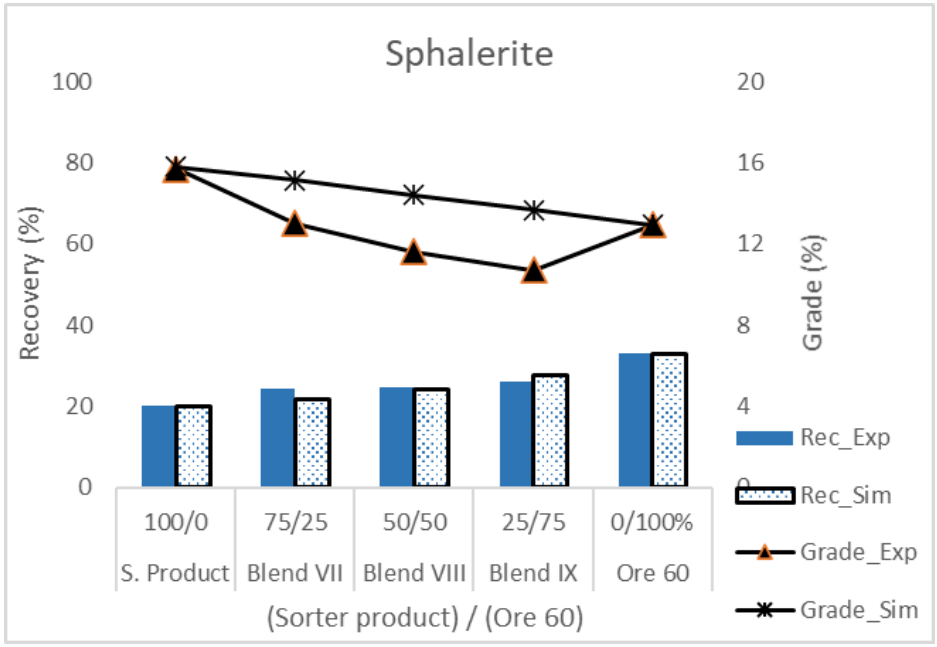

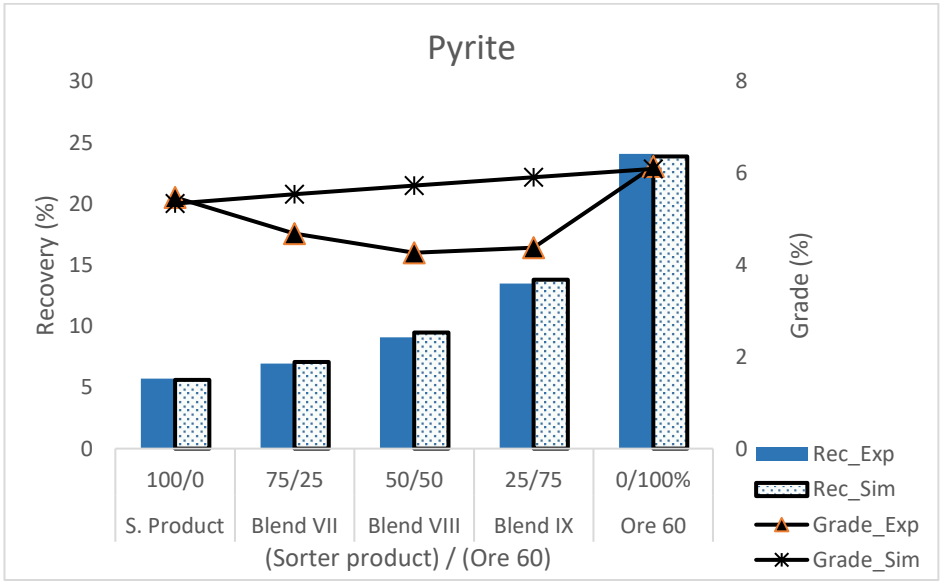

Appendix C

In this section the mass balance for experimental flotation tests is presented

Unit Name	Streams	Stream Type	Weight		Zn		Dys		Ccp		Sp		Py		Gn		Qtz	
			g	%	%	Rec%	%	Rec%	%	Rec%	%	Rec%	%	Rec%	%	Rec%	%	Rec%
Analyzed Feed	Analyzed Feed	Analyzed																
Test Feed	GFeed	Calculated	1787,30	100,00	0,34	100,0	0,00	100,0	0,05	100,0	0,56	100,0	4,36	100,0	0,14	100,0	94,89	100,0
Primary grinding	CFeed	Calculated	1787,30	100,00	0,34	100,0	0,00	100,0	0,05	100,0	0,56	100,0	4,36	100,0	0,14	100,0	94,89	100,0
Conditioner	RFeed	Calculated	1787,30	100,00	0,34	100,0	0,00	100,0	0,05	100,0	0,56	100,0	4,36	100,0	0,14	100,0	94,89	100,0
RF1	RC1	Analyzed	9,60	0,54	6,01	9,4	0,50	54,0	3,26	35,6	9,85	9,5	16,21	2,0	18,48	73,1	51,70	0,3
	RT1	Calculated	1777,70	99,46	0,31	90,6	0,00	46,0	0,03	64,4	0,51	90,5	4,30	98,0	0,04	26,9	95,12	99,7
RF2	RC2	Analyzed	4,80	0,27	4,61	3,6	0,19	9,9	0,58	3,2	7,55	3,6	12,65	0,8	2,72	5,4	76,30	0,2
	RT2	Calculated	1772,90	99,19	0,30	86,9	0,00	36,1	0,03	61,2	0,49	86,9	4,27	97,2	0,03	21,5	95,17	99,5
RF3	RC3	Analyzed	10,60	0,59	2,92	5,1	0,09	10,9	0,21	2,5	4,78	5,1	15,83	2,2	0,77	3,4	78,31	0,5
	RT3	Calculated	1762,30	98,60	0,28	81,9	0,00	25,2	0,03	58,7	0,46	81,9	4,20	95,1	0,02	18,1	95,28	99,0
RF4	RC4	Analyzed	11,40	0,64	1,82	3,4	0,03	4,3	0,07	0,9	2,98	3,4	7,23	1,1	0,25	1,2	89,42	0,6
	RT4	Calculated	1750,90	97,96	0,27	78,5	0,00	20,8	0,03	57,8	0,45	78,5	4,18	94,0	0,02	16,9	95,31	98,4
RF5	RC5	Analyzed	5,70	0,32	0,99	0,9	0,01	0,9	0,03	0,2	1,62	0,9	4,03	0,3	0,12	0,3	94,19	0,3
	RT5	Calculated	1745,20	97,64	0,27	77,5	0,00	19,9	0,03	57,5	0,44	77,5	4,18	93,7	0,02	16,7	95,32	98,1
RF6	RC6	Analyzed	8,50	0,48	0,56	0,8	0,01	0,5	0,03	0,3	0,92	0,8	2,04	0,2	0,06	0,2	96,95	0,5
	RT6	Analyzed	1736,70	97,17	0,27	76,8	0,00	19,5	0,03	57,3	0,44	76,7	4,20	93,5	0,02	16,5	95,31	97,6

Sorter product

Unit Name		Weight		Dys		Gn		Sp		Py		Ccp		Qtz	
		g	%	%	Rec%	%	Rec%	%	Rec%	%	Rec%	%	Rec%	%	Rec%
Analyzed Feed															
Test Feed		1797,20	100,00	0,02	100,0	0,75	100,0	2,93	100,0	3,61	100,0	0,08	100,0	92,60	100,0
		1797,20	100,00	0,02	100,0	0,75	100,0	2,93	100,0	3,61	100,0	0,08	100,0	92,60	100,0
Primary grinding															
		1797,20	100,00	0,02	100,0	0,75	100,0	2,93	100,0	3,61	100,0	0,08	100,0	92,60	100,0
Conditioner															
		30,10	1,67	0,75	76,4	41,30	91,7	16,55	9,5	5,17	2,4	3,12	62,9	33,10	0,6
RF1		1767,10	98,33	0,00	23,6	0,06	8,3	2,70	90,5	3,59	97,6	0,03	37,1	93,62	99,4
		8,90	0,50	0,10	3,0	2,32	1,5	16,55	2,8	3,94	0,5	0,21	1,3	76,90	0,4
RF2		1758,20	97,83	0,00	20,5	0,05	6,8	2,63	87,7	3,59	97,1	0,03	35,9	93,70	99,0
		14,50	0,81	0,13	6,3	1,95	2,1	17,04	4,7	7,68	1,7	0,19	1,8	73,00	0,6
		1743,70	97,02	0,00	14,2	0,04	4,7	2,51	83,0	3,55	95,3	0,03	34,1	93,87	98,4
RF3															
		5,80	0,32	0,07	1,4	0,86	0,4	18,03	2,0	5,15	0,5	0,11	0,4	75,80	0,3
RF4		1737,90	96,70	0,00	12,8	0,03	4,3	2,45	81,1	3,55	94,9	0,03	33,6	93,93	98,1
		8,70	0,48	0,03	0,8	0,26	0,2	8,16	1,3	4,65	0,6	0,04	0,2	86,90	0,5
RF5		1729,20	96,22	0,00	12,0	0,03	4,2	2,43	79,7	3,54	94,3	0,03	33,4	93,97	97,6

Sorter feed

Unit Name		Streams	Stream Type	Weight		Dys		Sp		Gn		Py		Ccp		Qtz	
				g	%	%	Rec%	%	Rec%	%	Rec%	%	Rec%	%	Rec%	%	Rec%
Analyzed Feed		Analyzed Feed	Analyzed														
Test Feed		GFeed	Calculated	1796,50	100,00	0,01	100,0	1,11	100,0	0,24	100,0	2,67	100,0	0,06	100,0	95,91	100,0
Primary grinding		CFeed	Calculated	1796,50	100,00	0,01	100,0	1,11	100,0	0,24	100,0	2,67	100,0	0,06	100,0	95,91	100,0
		RFeed	Calculated	1796,50	100,00	0,01	100,0	1,11	100,0	0,24	100,0	2,67	100,0	0,06	100,0	95,91	100,0
Conditioner		RC1	Analyzed	10,60	0,59	0,46	50,8	17,92	9,5	31,18	76,0	9,81	2,2	3,41	36,1	37,20	0,2
RF1		RT1	Calculated	1785,90	99,41	0,00	49,2	1,01	90,5	0,06	24,0	2,63	97,8	0,04	63,9	96,26	99,8
RF2		RC2	Analyzed	7,50	0,42	0,23	17,6	20,03	7,5	7,62	13,1	9,49	1,5	0,92	6,9	61,70	0,3
		RT2	Calculated	1778,40	98,99	0,00	31,6	0,93	82,9	0,03	10,9	2,60	96,4	0,03	56,9	96,40	99,5
RF3		RC3	Analyzed	17,00	0,95	0,08	14,2	13,19	11,2	1,25	4,9	9,19	3,3	0,25	4,2	76,00	0,7
		RT3	Calculated	1761,40	98,05	0,00	17,4	0,81	71,7	0,01	6,0	2,54	93,1	0,03	52,7	96,60	98,8
RF4		RC4	Analyzed	10,80	0,60	0,03	3,2	9,28	5,0	0,38	0,9	6,40	1,4	0,23	2,4	83,70	0,5
		RT4	Calculated	1750,60	97,45	0,00	14,2	0,76	66,7	0,01	5,1	2,52	91,7	0,03	50,3	96,68	98,2
RF5		RC5	Analyzed	23,70	1,32	0,01	1,5	2,66	3,2	0,09	0,5	2,17	1,1	0,02	0,4	95,10	1,3
		RT5	Analyzed	1726,90	96,13	0,00	12,7	0,73	63,5	0,01	4,6	2,52	90,6	0,03	49,9	96,70	96,9

Ore 60

Unit Name	Streams	Stream Type	Weight		Zn		Dys		Sp		Gn		Py		Ccp		Qtz	
			g	%	%	Rec%	%	Rec%	%	Rec%	%	Rec%	%	Rec%	%	Rec%	%	Rec%
Analyzed Feed	Analyzed Feed	Analyzed																
Test Feed	GFeed	Calculated	1773,80	100,00	0,90	100,0	0,02	100,0	1,48	100,0	0,33	100,0	0,96	100,0	0,06	100,0	97,15	100,0
	CFeed	Calculated	1773,80	100,00	0,90	100,0	0,02	100,0	1,48	100,0	0,33	100,0	0,96	100,0	0,06	100,0	97,15	100,0
Primary grinding																		
	RFeed	Calculated	1773,80	100,00	0,90	100,0	0,02	100,0	1,48	100,0	0,33	100,0	0,96	100,0	0,06	100,0	97,15	100,0
Conditioner																		
RF1	RC1	Analyzed	14,60	0,82	12,10	11,0	1,13	44,3	19,83	11,0	17,67	44,2	9,76	8,4	2,40	34,3	49,22	0,4
	RT1	Calculated	1759,20	99,18	0,81	89,0	0,01	55,7	1,33	89,0	0,19	55,8	0,89	91,6	0,04	65,7	97,55	99,6
RF2	RC2	Analyzed	9,40	0,53	11,00	6,4	0,52	13,0	18,03	6,5	5,31	8,5	6,31	3,5	0,92	8,5	68,91	0,4
	RT2	Calculated	1749,80	98,65	0,76	82,5	0,01	42,7	1,24	82,5	0,16	47,3	0,86	88,1	0,03	57,2	97,70	99,2
RF3	RC3	Analyzed	14,80	0,83	8,30	7,7	0,27	10,6	13,60	7,7	1,73	4,4	5,92	5,1	0,33	4,9	78,14	0,7
	RT3	Calculated	1735,00	97,81	0,69	74,9	0,01	32,2	1,13	74,9	0,14	42,9	0,81	83,0	0,03	52,4	97,87	98,5
RF4	RC4	Analyzed	10,10	0,57	7,10	4,5	0,20	5,4	11,64	4,5	1,11	1,9	6,31	3,7	0,22	2,2	80,53	0,5
	RT4	Calculated	1724,90	97,24	0,65	70,4	0,01	26,8	1,07	70,4	0,14	41,0	0,78	79,3	0,03	50,2	97,97	98,1
RF5	RC5	Analyzed	9,10	0,51	3,70	2,1	0,10	2,5	6,06	2,1	0,61	1,0	3,54	1,9	0,13	1,1	89,55	0,5
	RT5	Calculated	1715,80	96,73	0,64	68,3	0,01	24,3	1,05	68,3	0,14	40,0	0,77	77,4	0,03	49,1	98,02	97,6
RF6	RC6	Analyzed	8,70	0,49	2,24	1,2	0,06	1,4	3,67	1,2	0,38	0,6	2,85	1,5	0,07	0,6	92,97	0,5
	RT6	Analyzed	1707,10	96,24	0,63	67,1	0,00	22,9	1,03	67,1	0,13	39,5	0,76	75,9	0,03	48,5	98,04	97,1

Blend I

Unit Name	Weight		Dys		Gn		Sp		Py		Ccp		Qtz	
	g	%	%	Rec%	%	Rec%	%	Rec%	%	Rec%	%	Rec%	%	Rec%
Analyzed Feed														
Test Feed	1799,50	100,00	0,01	100,0	0,60	100,0	2,30	100,0	3,81	100,0	0,07	100,0	93,20	100,0
Primary grinding	1799,50	100,00	0,01	100,0	0,60	100,0	2,30	100,0	3,81	100,0	0,07	100,0	93,20	100,0
Conditioner	1799,50	100,00	0,01	100,0	0,60	100,0	2,30	100,0	3,81	100,0	0,07	100,0	93,20	100,0
RF1	17,00	0,94	0,82	55,9	51,16	80,3	13,44	5,5	6,25	1,6	3,75	48,7	24,58	0,2
	1782,50	99,06	0,01	44,1	0,12	19,7	2,20	94,5	3,79	98,4	0,04	51,3	93,85	99,8
RF2	7,10	0,39	0,52	14,9	16,74	11,0	25,24	4,3	9,92	1,0	1,44	7,8	46,13	0,2
	1775,40	98,66	0,00	29,2	0,05	8,7	2,11	90,2	3,76	97,4	0,03	43,4	94,04	99,6
RF3	7,60	0,42	0,28	8,6	5,20	3,6	27,04	5,0	11,57	1,3	0,53	3,1	55,39	0,3
	1767,80	98,24	0,00	20,6	0,03	5,1	2,00	85,2	3,73	96,1	0,03	40,4	94,21	99,3
RF4	5,30	0,29	0,19	4,1	1,99	1,0	26,55	3,4	11,16	0,9	0,27	1,1	59,85	0,2
	1762,50	97,94	0,00	16,6	0,03	4,1	1,92	81,8	3,71	95,3	0,03	39,3	94,31	99,1
RF5	6,70	0,37	0,07	1,8	0,49	0,3	12,50	2,0	6,96	0,7	0,08	0,4	79,90	0,3
	1755,80	97,57	0,00	14,7	0,02	3,8	1,88	79,8	3,69	94,6	0,03	38,8	94,37	98,8
RF6	8,00	0,44	0,02	0,7	0,15	0,1	5,42	1,0	2,80	0,3	0,02	0,1	91,57	0,4
	1747,80	97,13	0,00	14,1	0,02	3,7	1,87	78,8	3,70	94,3	0,03	38,7	94,38	98,4

Blend II

Unit Name	Weight		Zn		Dys		Gn		Sp		Py		Ccp		Qtz	
	g	%	%	Rec%	%	Rec%	%	Rec%	%	Rec%	%	Rec%	%	Rec%	%	Rec%
Analyzed Feed																
Test Feed	1799,20	100,00	1,04	100,0	0,01	100,0	0,43	100,0	1,71	100,0	4,12	100,0	0,06	100,0	93,67	100,0
Primary grinding	1799,20	100,00	1,04	100,0	0,01	100,0	0,43	100,0	1,71	100,0	4,12	100,0	0,06	100,0	93,67	100,0
Conditioner	1799,20	100,00	1,04	100,0	0,01	100,0	0,43	100,0	1,71	100,0	4,12	100,0	0,06	100,0	93,67	100,0
RF1	13,30	0,74	9,51	6,7	0,78	52,4	45,61	78,4	15,58	6,7	7,94	1,4	3,87	44,4	26,22	0,2
	1785,90	99,26	0,98	93,3	0,01	47,6	0,09	21,6	1,60	93,3	4,09	98,6	0,04	55,6	94,17	99,8
RF2	4,00	0,22	15,90	3,4	0,57	11,5	17,67	9,1	26,06	3,4	11,10	0,6	1,68	5,8	42,93	0,1
	1781,90	99,04	0,95	89,9	0,00	36,1	0,05	12,4	1,55	89,9	4,07	98,0	0,03	49,8	94,29	99,7
RF3	7,50	0,42	15,40	6,2	0,32	12,2	5,68	5,5	25,24	6,2	14,54	1,5	0,64	4,1	53,59	0,2
	1774,40	98,62	0,88	83,7	0,00	23,9	0,03	6,9	1,45	83,7	4,03	96,5	0,03	45,7	94,46	99,5
RF4	4,40	0,24	14,00	3,3	0,16	3,5	1,88	1,1	22,94	3,3	12,08	0,7	0,27	1,0	62,67	0,2
	1770,00	98,38	0,85	80,4	0,00	20,3	0,03	5,9	1,40	80,4	4,01	95,8	0,03	44,6	94,54	99,3
RF5	6,50	0,36	5,24	1,8	0,06	1,9	0,55	0,5	8,59	1,8	5,59	0,5	0,08	0,5	85,12	0,3
	1763,50	98,02	0,84	78,6	0,00	18,4	0,02	5,4	1,37	78,6	4,00	95,3	0,03	44,2	94,57	99,0
RF6	8,80	0,49	2,00	0,9	0,02	0,7	0,15	0,2	3,28	0,9	2,62	0,3	0,03	0,2	93,91	0,5
	1754,70	97,53	0,83	77,7	0,00	17,7	0,02	5,2	1,36	77,7	4,01	95,0	0,03	43,9	94,58	98,5

Blend III

Unit Name	Weight		Dys		Gn		Sp		Py		Ccp		Qtz	
	g	%	%	Rec%	%	Rec%	%	Rec%	%	Rec%	%	Rec%	%	Rec%
Analyzed Feed														
Test Feed	1796,90	100,00	0,01	100,0	0,27	100,0	1,12	100,0	4,02	100,0	0,06	100,0	94,52	100,0
Primary grinding	1796,90	100,00	0,01	100,0	0,27	100,0	1,12	100,0	4,02	100,0	0,06	100,0	94,52	100,0
Conditioner	1796,90	100,00	0,01	100,0	0,27	100,0	1,12	100,0	4,02	100,0	0,06	100,0	94,52	100,0
RF1	11,90	0,66	0,65	51,6	32,91	79,5	13,31	7,9	9,86	1,6	3,35	40,0	39,93	0,3
	1785,00	99,34	0,00	48,4	0,06	20,5	1,04	92,1	3,98	98,4	0,03	60,0	94,89	99,7
RF2	4,10	0,23	0,34	9,3	8,95	7,4	17,37	3,5	8,72	0,5	1,04	4,3	63,58	0,2
	1780,90	99,11	0,00	39,1	0,04	13,0	1,00	88,6	3,97	97,9	0,03	55,7	94,96	99,6
RF3	7,00	0,39	0,23	10,6	2,84	4,0	15,35	5,3	15,42	1,5	0,46	3,2	65,70	0,3
	1773,90	98,72	0,00	28,4	0,02	9,0	0,94	83,3	3,92	96,4	0,03	52,5	95,08	99,3
RF4	5,70	0,32	0,09	3,3	0,92	1,1	9,88	2,8	8,59	0,7	0,16	0,9	80,36	0,3
	1768,20	98,40	0,00	25,1	0,02	7,9	0,92	80,5	3,91	95,7	0,03	51,5	95,12	99,0
RF5	7,20	0,40	0,02	1,1	0,22	0,3	3,69	1,3	2,90	0,3	0,04	0,3	93,13	0,4
	1761,00	98,00	0,00	24,0	0,02	7,6	0,90	79,1	3,91	95,4	0,03	51,3	95,13	98,6
RF6	4,10	0,23	0,02	0,4	0,14	0,1	2,52	0,5	2,33	0,1	0,03	0,1	94,96	0,2
	1756,90	97,77	0,00	23,6	0,02	7,5	0,90	78,6	3,92	95,3	0,03	51,1	95,13	98,4

Blend IV

Unit Name	Weight		Dys		Gn		Sp		Py		Ccp		Qtz	
	g	%	%	Rec%	%	Rec%	%	Rec%	%	Rec%	%	Rec%	%	Rec%
Analyzed Feed														
Test Feed	1782,30	100,00	0,01	100,0	0,17	100,0	0,76	100,0	3,23	100,0	0,05	100,0	95,78	100,0
Primary grinding	1782,30	100,00	0,01	100,0	0,17	100,0	0,76	100,0	3,23	100,0	0,05	100,0	95,78	100,0
Conditioner	1782,30	100,00	0,01	100,0	0,17	100,0	0,76	100,0	3,23	100,0	0,05	100,0	95,78	100,0
RF1	7,80	0,44	0,74	38,2	15,59	39,0	12,64	7,2	7,43	1,0	3,18	28,6	60,42	0,3
	1774,50	99,56	0,01	61,8	0,11	61,0	0,71	92,8	3,21	99,0	0,03	71,4	95,93	99,7
RF2	6,00	0,34	0,31	12,4	5,08	9,8	9,08	4,0	6,25	0,7	0,90	6,2	78,38	0,3
	1768,50	99,23	0,00	49,3	0,09	51,2	0,68	88,8	3,20	98,3	0,03	65,2	95,99	99,4
RF3	12,20	0,68	0,20	16,4	2,93	11,5	6,87	6,1	6,43	1,4	0,36	5,0	83,21	0,6
	1756,30	98,54	0,00	32,9	0,07	39,8	0,64	82,6	3,17	97,0	0,03	60,2	96,08	98,9
RF4	8,20	0,46	0,12	6,4	1,03	2,7	7,39	4,4	6,90	1,0	0,17	1,6	84,39	0,4
	1748,10	98,08	0,00	26,6	0,07	37,1	0,61	78,2	3,16	96,0	0,03	58,6	96,14	98,4
RF5	8,50	0,48	0,04	2,5	0,36	1,0	3,29	2,1	4,22	0,6	0,06	0,5	92,03	0,5
	1739,60	97,60	0,00	24,1	0,06	36,1	0,60	76,1	3,15	95,4	0,03	58,0	96,16	98,0
RF6	14,60	0,82	0,01	1,3	0,38	1,8	1,38	1,5	2,23	0,6	0,02	0,3	95,98	0,8
	1725,00	96,79	0,00	22,7	0,06	34,3	0,59	74,7	3,16	94,8	0,03	57,7	96,16	97,2

Blend V

Unit Name	Weight		Dys		Gn		Sp		Py		Ccp		Qtz	
	g	%	%	Rec%	%	Rec%	%	Rec%	%	Rec%	%	Rec%	%	Rec%
Analyzed Feed														
Test Feed	1797,40	100,00	0,01	100,0	0,22	100,0	0,98	100,0	2,47	100,0	0,05	100,0	96,27	100,0
Primary grinding	1797,40	100,00	0,01	100,0	0,22	100,0	0,98	100,0	2,47	100,0	0,05	100,0	96,27	100,0
Conditioner	1797,40	100,00	0,01	100,0	0,22	100,0	0,98	100,0	2,47	100,0	0,05	100,0	96,27	100,0
RF1	12,80	0,71	0,96	48,9	17,90	56,9	16,72	12,2	10,69	3,1	2,65	36,1	51,08	0,4
	1784,60	99,29	0,01	51,1	0,10	43,1	0,87	87,8	2,41	96,9	0,03	63,9	96,59	99,6
RF2	8,50	0,47	0,34	11,6	3,39	7,2	15,16	7,3	5,56	1,1	0,63	5,7	74,91	0,4
	1776,10	98,81	0,01	39,5	0,08	36,0	0,80	80,5	2,39	95,8	0,03	58,2	96,69	99,3
RF3	15,10	0,84	0,21	12,6	0,89	3,3	7,67	6,6	7,87	2,7	0,19	3,1	83,17	0,7
	1761,00	97,97	0,00	27,0	0,07	32,7	0,74	73,9	2,34	93,2	0,03	55,1	96,81	98,5
RF4	13,90	0,77	0,08	4,4	0,47	1,6	5,28	4,2	3,89	1,2	0,10	1,4	90,19	0,7
	1747,10	97,20	0,00	22,5	0,07	31,0	0,70	69,8	2,33	91,9	0,03	53,7	96,86	97,8
RF5	11,80	0,66	0,03	1,4	0,23	0,7	2,26	1,5	1,90	0,5	0,04	0,4	95,54	0,7
	1735,30	96,55	0,00	21,1	0,07	30,3	0,69	68,2	2,34	91,4	0,03	53,3	96,87	97,2
RF6	15,30	0,85	0,01	0,7	0,12	0,5	1,08	0,9	0,79	0,3	0,02	0,3	97,98	0,9
	1720,00	95,69	0,00	20,5	0,07	29,9	0,69	67,3	2,35	91,2	0,03	53,0	96,86	96,3

Blend VI

Unit Name	Weight		Dys		Gn		Sp		Py		Ccp		Qtz	
	g	%	%	Rec%	%	Rec%	%	Rec%	%	Rec%	%	Rec%	%	Rec%
Analyzed Feed														
Test Feed	1793,50	100,00	0,02	100,0	0,29	100,0	1,24	100,0	1,72	100,0	0,06	100,0	96,67	100,0
Primary grinding	1793,50	100,00	0,02	100,0	0,29	100,0	1,24	100,0	1,72	100,0	0,06	100,0	96,67	100,0
Conditioner	1793,50	100,00	0,02	100,0	0,29	100,0	1,24	100,0	1,72	100,0	0,06	100,0	96,67	100,0
RF1	12,60	0,70	1,18	48,8	22,29	54,0	21,30	12,0	5,43	2,2	3,00	38,2	46,80	0,3
	1780,90	99,30	0,01	51,2	0,13	46,0	1,10	88,0	1,69	97,8	0,03	61,8	97,03	99,7
RF2	9,20	0,51	0,37	11,3	3,24	5,7	13,81	5,7	3,62	1,1	0,61	5,7	78,33	0,4
	1771,70	98,78	0,01	39,9	0,12	40,2	1,04	82,3	1,68	96,7	0,03	56,1	97,12	99,2
RF3	17,90	1,00	0,18	10,7	1,06	3,7	9,68	7,8	5,83	3,4	0,21	3,8	83,03	0,9
	1753,80	97,79	0,01	29,2	0,11	36,6	0,95	74,5	1,64	93,3	0,03	52,3	97,27	98,4
RF4	17,20	0,96	0,08	4,5	0,49	1,6	4,47	3,4	2,33	1,3	0,08	1,5	92,55	0,9
	1736,60	96,83	0,00	24,8	0,10	35,0	0,91	71,1	1,63	92,0	0,03	50,9	97,31	97,5
RF5	14,80	0,83	0,03	1,4	0,23	0,7	1,97	1,3	0,78	0,4	0,04	0,5	96,96	0,8
	1721,80	96,00	0,00	23,3	0,10	34,3	0,90	69,8	1,64	91,6	0,03	50,3	97,32	96,6
RF6	11,30	0,63	0,02	0,8	0,18	0,4	1,39	0,7	0,58	0,2	0,03	0,3	97,80	0,6
	1710,50	95,37	0,00	22,6	0,10	33,9	0,90	69,1	1,65	91,4	0,03	50,1	97,31	96,0

Blend VII

Unit Name	Weight		Dys		Gn		Sp		Py		Ccp		Qtz	
	g	%	%	Rec%	%	Rec%	%	Rec%	%	Rec%	%	Rec%	%	Rec%
Analyzed Feed														
Test Feed	1796,60	100,00	0,02	100,0	0,63	100,0	2,60	100,0	3,27	100,0	0,08	100,0	93,43	100,0
Primary grinding	1796,60	100,00	0,02	100,0	0,63	100,0	2,60	100,0	3,27	100,0	0,08	100,0	93,43	100,0
Conditioner	1796,60	100,00	0,02	100,0	0,63	100,0	2,60	100,0	3,27	100,0	0,08	100,0	93,43	100,0
RF1	21,30	1,19	0,84	60,2	42,03	79,3	15,13	6,9	6,61	2,4	3,41	53,1	32,78	0,4
	1775,30	98,81	0,01	39,8	0,13	20,7	2,44	93,1	3,23	97,6	0,04	46,9	94,15	99,6
RF2	9,50	0,53	0,38	12,1	8,64	7,3	21,30	4,3	4,32	0,7	0,78	5,4	64,58	0,4
	1765,80	98,29	0,00	27,7	0,09	13,4	2,34	88,7	3,22	96,9	0,03	41,4	94,31	99,2
RF3	16,90	0,94	0,19	10,6	2,41	3,6	17,37	6,3	6,37	1,8	0,27	3,4	73,39	0,7
	1748,90	97,34	0,00	17,1	0,06	9,8	2,20	82,5	3,19	95,1	0,03	38,0	94,52	98,5
RF4	17,50	0,97	0,07	4,1	0,76	1,2	11,85	4,4	4,47	1,3	0,10	1,3	82,75	0,9
	1731,40	96,37	0,00	12,9	0,06	8,6	2,10	78,0	3,18	93,7	0,03	36,7	94,63	97,6
RF5	11,00	0,61	0,03	1,1	0,30	0,3	6,39	1,5	2,16	0,4	0,04	0,3	91,07	0,6
	1720,40	95,76	0,00	11,8	0,05	8,3	2,07	76,5	3,18	93,3	0,03	36,4	94,66	97,0
RF6	10,90	0,61	0,01	0,4	0,14	0,1	3,38	0,8	1,52	0,3	0,02	0,1	94,93	0,6
	1709,50	95,15	0,00	11,5	0,05	8,2	2,07	75,7	3,19	93,0	0,03	36,3	94,65	96,4

Blend VIII

Unit Name	Weight		Dys		Ccp		Sp		Py		Gn		Qtz	
	g	%	%	Rec%	%	Rec%	%	Rec%	%	Rec%	%	Rec%	%	Rec%
Analyzed Feed														
Test Feed	1805,30	100,00	0,02	100,0	0,07	100,0	2,18	100,0	2,17	100,0	0,52	100,0	95,04	100,0
Primary grinding	1805,30	100,00	0,02	100,0	0,07	100,0	2,18	100,0	2,17	100,0	0,52	100,0	95,04	100,0
Conditioner	1805,30	100,00	0,02	100,0	0,07	100,0	2,18	100,0	2,17	100,0	0,52	100,0	95,04	100,0
RF1	19,10	1,06	0,96	56,5	3,12	48,3	16,55	8,0	5,95	2,9	35,22	72,0	38,19	0,4
	1786,20	98,94	0,01	43,5	0,04	51,7	2,03	92,0	2,13	97,1	0,15	28,0	95,65	99,6
RF2	10,60	0,59	0,36	11,8	0,64	5,5	17,04	4,6	5,44	1,5	6,34	7,2	70,18	0,4
	1775,60	98,35	0,01	31,7	0,03	46,3	1,94	87,4	2,11	95,6	0,11	20,8	95,80	99,1
RF3	21,50	1,19	0,16	10,8	0,23	4,0	12,63	6,9	5,67	3,1	1,80	4,1	79,50	1,0
	1754,10	97,16	0,00	20,9	0,03	42,3	1,80	80,5	2,07	92,5	0,09	16,7	96,00	98,1
RF4	13,10	0,73	0,09	3,4	0,11	1,2	9,90	3,3	3,17	1,1	0,82	1,2	85,91	0,7
	1741,00	96,44	0,00	17,5	0,03	41,1	1,74	77,2	2,06	91,5	0,08	15,5	96,08	97,5
RF5	10,10	0,56	0,03	1,0	0,05	0,4	4,43	1,1	1,35	0,3	0,34	0,4	93,81	0,6
	1730,90	95,88	0,00	16,5	0,03	40,7	1,73	76,0	2,07	91,1	0,08	15,2	96,09	96,9
RF6	9,30	0,52	0,02	0,6	0,03	0,2	3,10	0,7	0,96	0,2	0,26	0,3	95,63	0,5
	1721,60	95,36	0,00	15,9	0,03	40,4	1,72	75,3	2,07	90,9	0,08	14,9	96,10	96,4

Blend IX

Unit Name	Weight		Dys		Ccp		Sp		Py		Gn		Qtz	
	g	%	%	Rec%	%	Rec%	%	Rec%	%	Rec%	%	Rec%	%	Rec%
Analyzed Feed														
Test Feed	1796,80	100,00	0,02	100,0	0,06	100,0	1,85	100,0	1,47	100,0	0,43	100,0	96,18	100,0
Primary grinding	1796,80	100,00	0,02	100,0	0,06	100,0	1,85	100,0	1,47	100,0	0,43	100,0	96,18	100,0
Conditioner	1796,80	100,00	0,02	100,0	0,06	100,0	1,85	100,0	1,47	100,0	0,43	100,0	96,18	100,0
RF1	16,10	0,90	1,17	52,5	3,12	44,4	19,99	9,7	7,51	4,6	31,06	65,3	37,14	0,3
	1780,70	99,10	0,01	47,5	0,04	55,6	1,68	90,3	1,41	95,4	0,15	34,7	96,71	99,7
RF2	9,80	0,55	0,43	11,8	0,66	5,8	17,86	5,3	6,23	2,3	5,22	6,7	69,59	0,4
	1770,90	98,56	0,01	35,7	0,03	49,8	1,59	85,0	1,39	93,1	0,12	28,1	96,86	99,3
RF3	15,30	0,85	0,22	9,2	0,24	3,3	11,16	5,1	5,53	3,2	1,57	3,1	81,28	0,7
	1755,60	97,71	0,01	26,5	0,03	46,5	1,51	79,9	1,35	89,9	0,11	24,9	97,00	98,5
RF4	15,90	0,88	0,12	5,1	0,11	1,6	7,16	3,4	3,97	2,4	0,75	1,6	87,89	0,8
	1739,70	96,82	0,00	21,4	0,03	44,9	1,46	76,4	1,33	87,5	0,10	23,4	97,08	97,7
RF5	10,60	0,59	0,05	1,5	0,06	0,5	5,19	1,7	1,92	0,8	0,43	0,6	92,35	0,6
	1729,10	96,23	0,00	19,9	0,03	44,4	1,43	74,8	1,32	86,7	0,10	22,8	97,11	97,2
RF6	13,50	0,75	0,02	0,8	0,03	0,3	2,54	1,0	0,43	0,2	0,22	0,4	96,76	0,8
	1715,60	95,48	0,00	19,1	0,03	44,0	1,43	73,7	1,33	86,5	0,10	22,4	97,11	96,4

Appendix D

The modelling of flotation kinetic parameters for minerals in each sample are presented here.

- **Malmi**

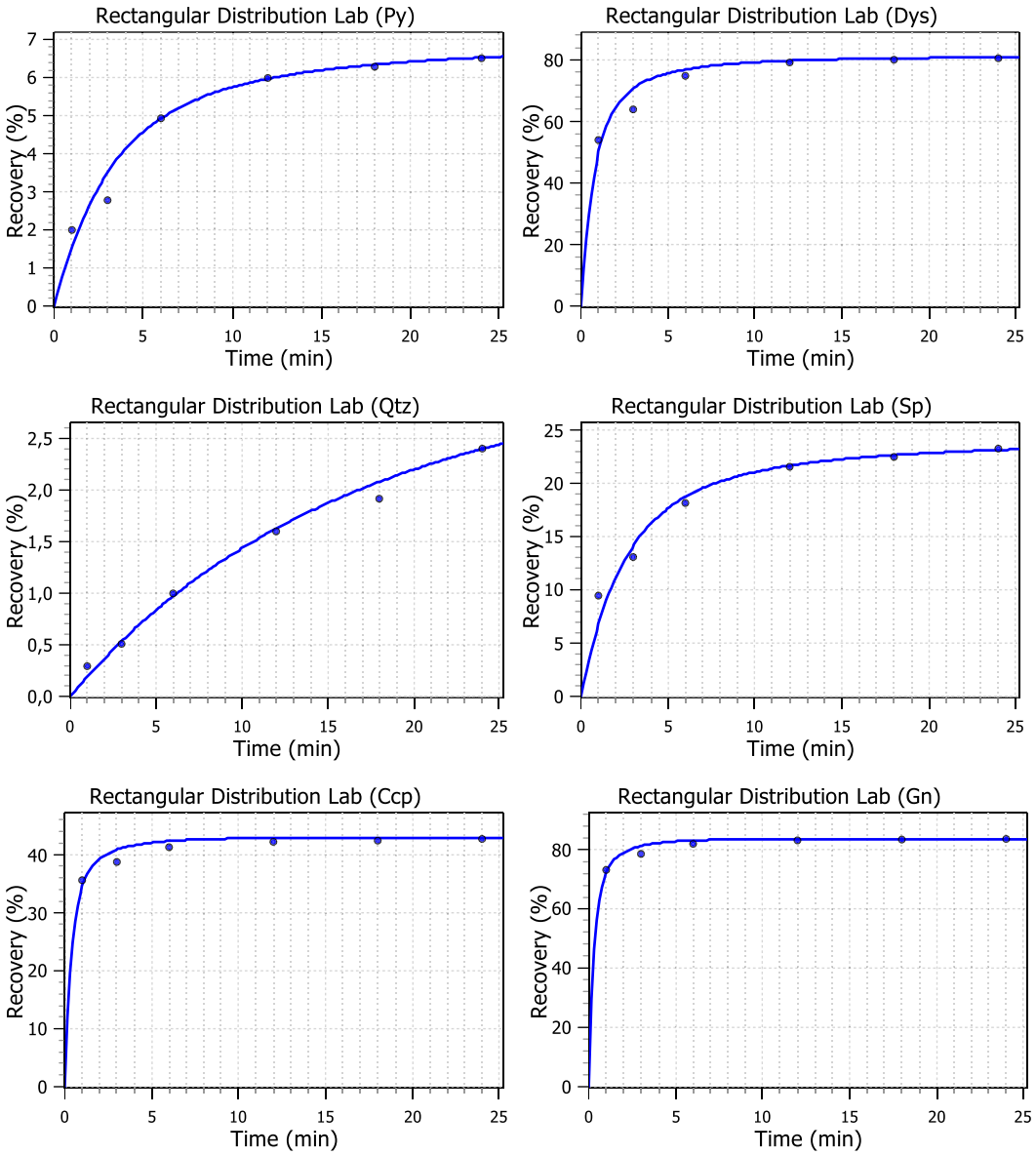

- **Sorter feed**

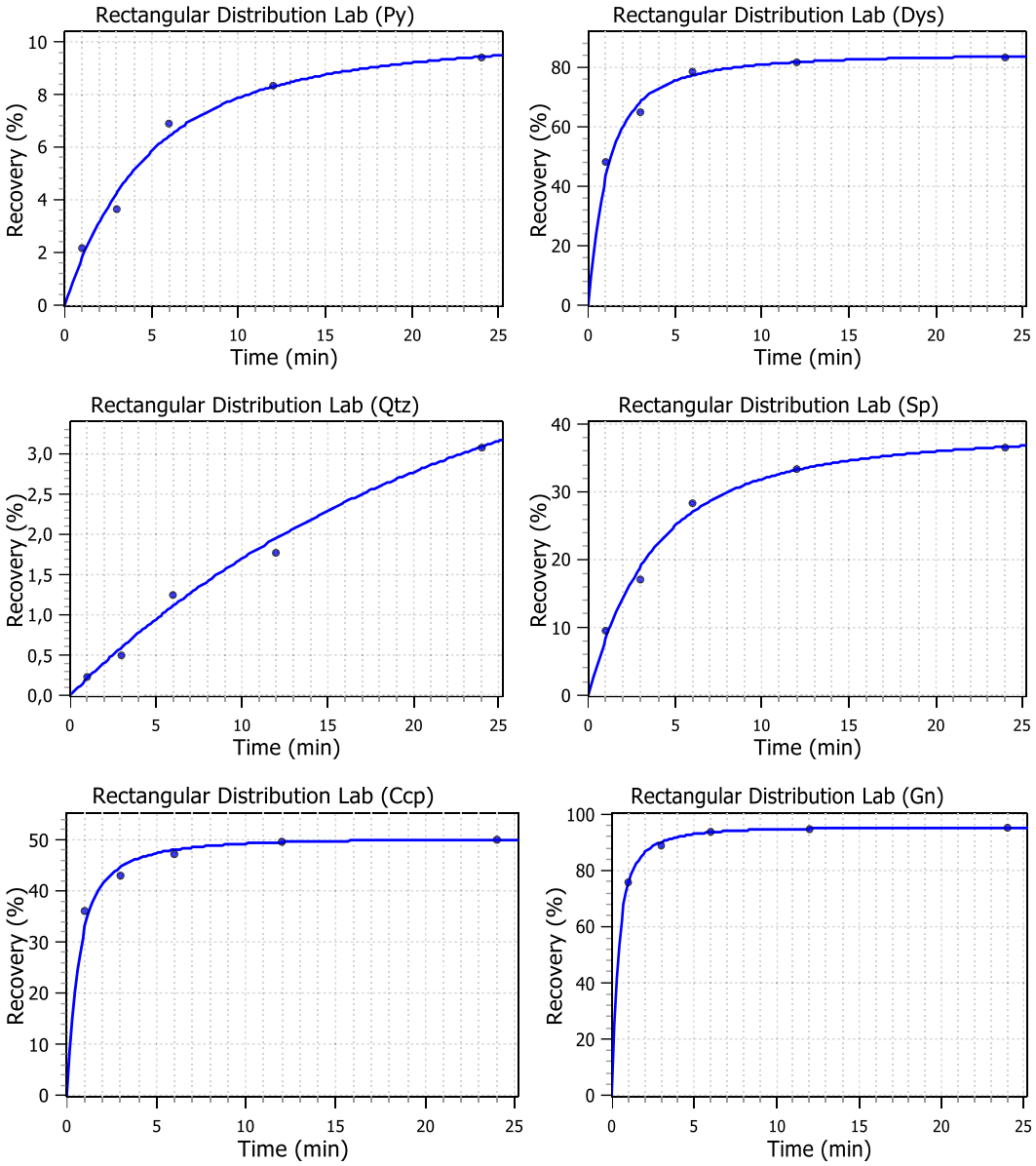
Rectangular Distribution Lab (Py)
Recovery (%)
Time (min)
Rectangular Distribution Lab (Dys)
Recovery (%)
Time (min)
Rectangular Distribution Lab (Qtz)
Recovery (%)
Time (min)
Rectangular Distribution Lab (Sp)
Recovery (%)
Time (min)
Rectangular Distribution Lab (Ccp)
Recovery (%)
Time (min)
Rectangular Distribution Lab (Gn)
Recovery (%)
Time (min)

- **Sorter product**

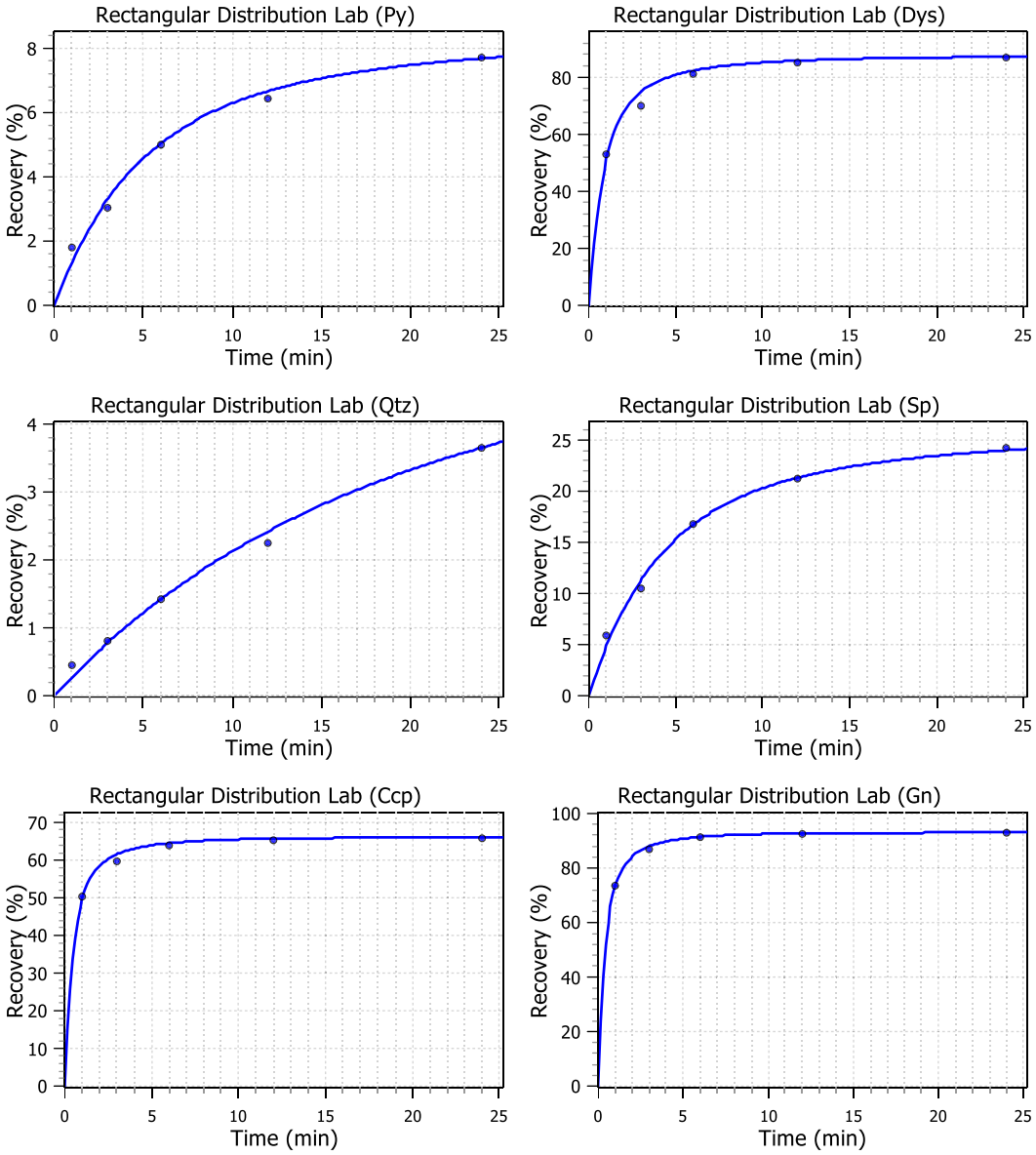

- **Ore 60**

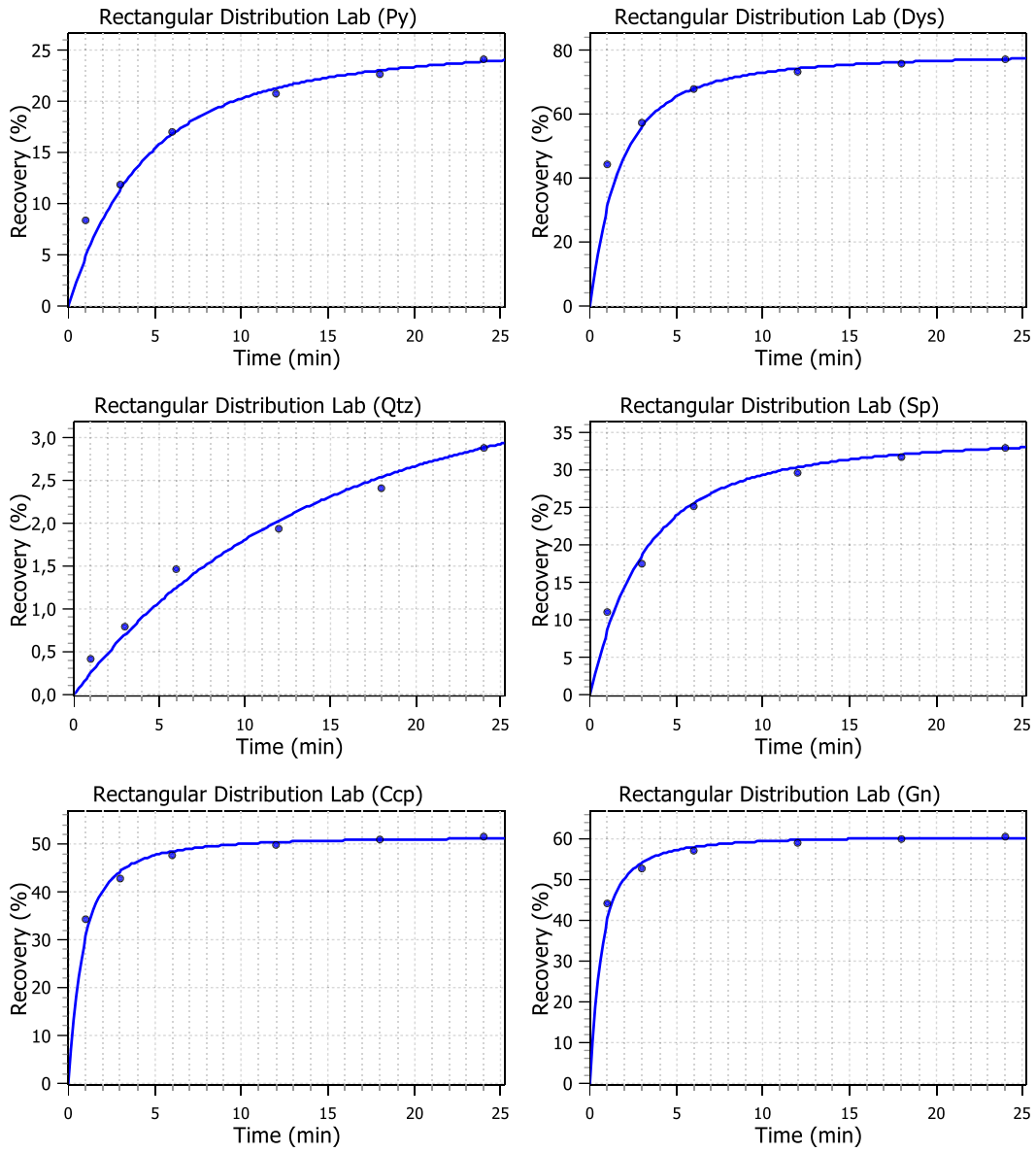

Appendix E

In this section the simulation results are presented.

		Grade						Recovery					
Stream Name	mass pull (%)	Ccp	Dys	Gn	Py	Qtz	Sp	Ccp	Dys	Gn	Py	Qtz	Sp
Malmi													
RC1	0,40	4,20	0,61	24,27	16,86	44,72	9,34	34,48	49,47	72,13	1,56	0,19	6,73
RC1+RC2	0,87	2,31	0,40	12,63	17,51	58,09	9,06	40,90	70,67	81,15	3,50	0,53	14,11
RC1+RC2+RC3	1,38	1,51	0,28	8,18	15,59	66,83	7,60	42,37	76,90	83,03	4,93	0,97	18,72
RC1+RC2+RC3+RC4	2,06	1,02	0,19	5,50	12,61	74,80	5,87	42,91	79,76	83,55	5,97	1,63	21,66
RC1+RC2+RC3+RC4+RC5	2,52	0,84	0,16	4,51	10,99	78,46	5,04	42,98	80,53	83,60	6,34	2,08	22,65
RC1+RC2+RC3+RC4+RC5+RC6	2,83	0,75	0,14	4,01	10,05	80,48	4,57	43,00	80,81	83,60	6,52	2,40	23,13
Sorter feed													
RC1	0,54	3,35	0,45	33,68	8,73	36,74	17,03	32,59	42,73	75,27	1,77	0,21	8,28
RC1+RC2	1,14	2,18	0,34	19,14	9,97	49,90	18,47	44,68	68,32	90,15	4,26	0,59	18,91
RC1+RC2+RC3	1,80	1,49	0,25	12,64	9,55	59,28	16,79	48,02	77,36	93,63	6,41	1,11	27,04
RC1+RC2+RC3+RC4	2,73	1,01	0,17	8,45	8,14	68,62	13,61	49,52	81,77	94,91	8,29	1,95	33,24
RC1+RC2+RC3+RC4+RC5	3,89	0,72	0,12	5,94	6,49	76,22	10,51	50,02	83,62	95,15	9,43	3,09	36,64
Sorter product													
RC1	1,66	3,02	0,66	42,82	4,34	34,20	14,97	62,47	74,99	91,18	2,06	0,61	8,54
RC1+RC2	2,37	2,21	0,51	31,15	5,12	44,30	16,71	65,12	83,04	94,46	3,46	1,13	13,57
RC1+RC2+RC3	2,91	1,82	0,43	25,59	5,34	50,09	16,72	65,85	85,64	95,32	4,43	1,57	16,68
RC1+RC2+RC3+RC4	3,34	1,59	0,38	22,35	5,38	53,99	16,31	66,13	86,86	95,63	5,12	1,94	18,68
RC1+RC2+RC3+RC4+RC5	3,69	1,44	0,34	20,23	5,34	56,83	15,81	66,25	87,53	95,75	5,63	2,26	20,04
Ore 60													
RC1	0,57	3,07	1,12	23,01	8,08	42,76	21,96	30,52	30,51	39,98	4,82	0,25	8,48
RC1+RC2	1,28	2,00	0,92	13,95	8,54	53,07	21,53	44,30	56,04	54,14	11,37	0,70	18,58
RC1+RC2+RC3	1,98	1,41	0,72	9,63	8,12	61,06	19,07	48,44	67,89	58,00	16,79	1,25	25,55
RC1+RC2+RC3+RC4	2,87	1,01	0,54	6,86	7,12	68,78	15,69	50,36	74,23	59,71	21,28	2,03	30,37
RC1+RC2+RC3+RC4+RC5	3,41	0,86	0,47	5,81	6,49	72,43	13,94	50,89	76,24	60,13	23,01	2,54	32,06
RC1+RC2+RC3+RC4+RC5+RC6	3,76	0,78	0,43	5,28	6,10	74,46	12,95	51,08	77,18	60,26	23,88	2,88	32,88

Blend I			Grade						Recovery					
Streams ID	Solids Flow (t/h)	Streams	Ccp	Dys	Gn	Py	Qtz	Sp	Ccp	Dys	Gn	Py	Qtz	Sp
RC1	0,66	RC1	4,51	0,69	61,14	4,50	20,72	8,42	40,87	37,53	64,94	0,80	0,15	2,38
RC2	0,53	RC1+RC2	3,40	0,67	44,84	6,15	32,87	12,07	55,69	65,53	86,15	1,97	0,42	6,18
RC3	0,52	RC1+RC2+RC3	2,54	0,55	33,24	6,80	42,87	14,00	59,83	77,59	91,82	3,13	0,79	10,30
RC4	0,75	RC1+RC2+RC3+RC4	1,82	0,41	23,69	6,79	52,77	14,52	61,68	83,89	94,29	4,50	1,39	15,39
RC5	0,55	RC1+RC2+RC3+RC4+RC5	1,50	0,35	19,51	6,55	57,99	14,10	62,14	85,85	94,88	5,30	1,87	18,26
RC6	0,42	RC1+RC2+RC3+RC4+RC5+RC6	1,32	0,31	17,17	6,32	61,31	13,57	62,30	86,74	95,07	5,83	2,25	20,01
Blend II														
RC1	0,57	RC1	4,44	0,67	52,48	7,40	26,36	8,64	39,25	39,57	65,65	1,08	0,16	2,85
RC2	0,51	RC1+RC2	3,11	0,60	36,20	9,20	39,63	11,26	51,95	66,41	85,66	2,54	0,46	7,03
RC3	0,52	RC1+RC2+RC3	2,25	0,47	26,04	9,32	49,75	12,16	55,41	77,47	90,95	3,79	0,85	11,20
RC4	0,73	RC1+RC2+RC3+RC4	1,58	0,35	18,32	8,51	59,27	11,97	56,92	83,18	93,23	5,04	1,47	16,06
RC5	0,52	RC1+RC2+RC3+RC4+RC5	1,30	0,29	15,09	7,86	64,02	11,43	57,29	84,94	93,77	5,69	1,94	18,73
RC6	0,38	RC1+RC2+RC3+RC4+RC5+RC6	1,15	0,26	13,32	7,41	66,91	10,94	57,41	85,73	93,93	6,09	2,30	20,34
Blend III														
RC1	0,49	RC1	4,34	0,65	40,82	11,31	33,95	8,93	37,19	42,92	67,13	1,33	0,18	3,80
RC2	0,49	RC1+RC2	2,75	0,51	25,69	12,90	47,86	10,28	47,18	67,85	84,63	3,04	0,50	8,76
RC3	0,51	RC1+RC2+RC3	1,91	0,38	17,78	12,22	57,66	10,05	49,78	77,28	89,14	4,39	0,91	13,03
RC4	0,71	RC1+RC2+RC3+RC4	1,32	0,28	12,30	10,43	66,56	9,11	50,87	82,03	91,02	5,53	1,55	17,42
RC5	0,48	RC1+RC2+RC3+RC4+RC5	1,09	0,23	10,13	9,33	70,79	8,43	51,12	83,45	91,44	6,03	2,01	19,69
RC6	0,35	RC1+RC2+RC3+RC4+RC5+RC6	0,96	0,20	8,97	8,64	73,25	7,97	51,19	84,06	91,57	6,32	2,35	21,02

Blend IV			Grade						Recovery					
Streams ID	Solids Flow (t/h)	Streams	Ccp	Dys	Gn	Py	Qtz	Sp	Ccp	Dys	Gn	Py	Qtz	Sp
RC1	0,45	RC1	3,84	0,78	23,86	14,04	44,10	13,39	33,37	38,40	57,76	1,78	0,21	7,55
RC2	0,53	RC1+RC2	2,21	0,57	13,06	14,57	56,44	13,15	41,85	62,13	69,07	4,04	0,58	16,21
RC3	0,56	RC1+RC2+RC3	1,48	0,42	8,65	13,17	64,96	11,32	44,08	71,64	71,84	5,74	1,04	21,92
RC4	0,73	RC1+RC2+RC3+RC4	1,02	0,30	5,93	10,87	72,89	8,98	45,00	76,53	72,89	7,01	1,73	25,74
RC5	0,47	RC1+RC2+RC3+RC4+RC5	0,85	0,26	4,92	9,59	76,58	7,81	45,20	78,03	73,10	7,48	2,20	27,06
RC6	0,33	RC1+RC2+RC3+RC4+RC5+RC6	0,76	0,23	4,40	8,84	78,63	7,14	45,27	78,69	73,17	7,71	2,52	27,70
blend V														
Streams ID	Solids Flow (t/h)		Ccp	Dys	Gn	Py	Qtz	Sp	Ccp	Dys	Gn	Py	Qtz	Sp
RC1	0,49	RC1	3,54	0,91	23,53	11,71	43,58	16,74	32,35	34,15	49,36	2,15	0,22	8,00
RC2	0,59	RC1+RC2	2,12	0,71	13,42	12,18	55,10	16,47	42,73	58,85	62,03	4,92	0,62	17,35
RC3	0,61	RC1+RC2+RC3	1,45	0,54	9,03	11,18	63,43	14,37	45,64	69,62	65,31	7,07	1,11	23,67
RC4	0,78	RC1+RC2+RC3+RC4	1,02	0,40	6,29	9,42	71,30	11,58	46,93	75,29	66,67	8,73	1,83	27,98
RC5	0,50	RC1+RC2+RC3+RC4+RC5	0,85	0,34	5,26	8,40	74,99	10,16	47,24	77,07	66,98	9,35	2,31	29,48
RC6	0,33	RC1+RC2+RC3+RC4+RC5+RC6	0,77	0,31	4,73	7,79	77,04	9,35	47,36	77,87	67,08	9,66	2,64	30,21
blend VI														
Streams ID	Solids Flow (t/h)		Ccp	Dys	Gn	Py	Qtz	Sp	Ccp	Dys	Gn	Py	Qtz	Sp
RC1	0,53	RC1	3,29	1,02	23,25	9,75	43,14	19,56	31,40	31,91	43,86	2,86	0,24	8,29
RC2	0,65	RC1+RC2	2,05	0,83	13,71	10,20	54,00	19,22	43,55	57,11	57,41	6,63	0,66	18,08
RC3	0,66	RC1+RC2+RC3	1,43	0,64	9,35	9,52	62,15	16,91	47,09	68,55	61,02	9,64	1,18	24,78
RC4	0,83	RC1+RC2+RC3+RC4	1,01	0,48	6,59	8,18	69,94	13,79	48,71	74,64	62,59	12,06	1,93	29,40
RC5	0,52	RC1+RC2+RC3+RC4+RC5	0,86	0,41	5,56	7,38	73,62	12,18	49,13	76,56	62,96	12,97	2,43	31,00
RC6	0,34	RC1+RC2+RC3+RC4+RC5+RC6	0,78	0,37	5,02	6,89	75,67	11,27	49,29	77,44	63,08	13,43	2,76	31,79

Blend VII			Grade						Recovery					
Streams ID	Solids Flow (t/h)	Streams	Ccp	Dys	Gn	Py	Qtz	Sp	Ccp	Dys	Gn	Py	Qtz	Sp
Streams ID	Minerals (t/h)		Ccp	Dys	Gn	Py	Qtz	Sp	Ccp	Dys	Gn	Py	Qtz	Sp
RC1	0,70	RC1	4,26	0,79	58,66	3,45	21,77	11,06	39,93	34,33	61,49	0,84	0,16	3,03
RC2	0,59	RC1+RC2	3,24	0,78	42,63	4,82	33,61	14,92	55,93	62,04	82,46	2,17	0,46	7,54
RC3	0,57	RC1+RC2+RC3	2,43	0,65	31,58	5,53	43,29	16,53	60,51	74,49	88,09	3,59	0,86	12,04
RC4	0,80	RC1+RC2+RC3+RC4	1,75	0,49	22,69	5,75	52,81	16,51	62,59	81,06	90,57	5,34	1,50	17,22
RC5	0,57	RC1+RC2+RC3+RC4+RC5	1,46	0,42	18,82	5,67	57,81	15,82	63,13	83,14	91,17	6,39	1,99	20,02
RC6	0,43	RC1+RC2+RC3+RC4+RC5+RC6	1,29	0,37	16,66	5,54	60,98	15,15	63,32	84,09	91,36	7,08	2,38	21,70
Blend IX														
Streams ID	Solids Flow (t/h)		Ccp	Dys	Gn	Py	Qtz	Sp	Ccp	Dys	Gn	Py	Qtz	Sp
RC1	0,66	RC1	3,92	0,89	48,31	4,80	27,86	14,22	37,31	32,83	57,24	1,41	0,19	4,25
RC2	0,63	RC1+RC2	2,83	0,82	33,14	6,05	40,05	17,11	52,70	59,68	76,86	3,49	0,54	10,02
RC3	0,62	RC1+RC2+RC3	2,07	0,67	23,95	6,43	49,47	17,41	57,15	71,89	82,14	5,48	0,99	15,08
RC4	0,83	RC1+RC2+RC3+RC4	1,49	0,51	17,15	6,23	58,40	16,22	59,19	78,37	84,47	7,63	1,68	20,17
RC5	0,56	RC1+RC2+RC3+RC4+RC5	1,25	0,43	14,33	5,95	62,86	15,17	59,72	80,42	85,03	8,78	2,18	22,72
RC6	0,40	RC1+RC2+RC3+RC4+RC5+RC6	1,12	0,39	12,80	5,73	65,55	14,41	59,91	81,37	85,20	9,49	2,55	24,22
Blend X														
Streams ID	Solids Flow (t/h)		Ccp	Dys	Gn	Py	Qtz	Sp	Ccp	Dys	Gn	Py	Qtz	Sp
RC1	0,61	RC1	3,52	1,00	36,53	6,33	34,80	17,82	34,22	31,57	50,81	2,44	0,22	5,96
RC2	0,67	RC1+RC2	2,41	0,87	23,58	7,29	46,54	19,31	48,88	57,71	68,39	5,86	0,62	13,46
RC3	0,66	RC1+RC2+RC3	1,73	0,70	16,64	7,29	55,38	18,26	53,19	69,72	73,15	8,88	1,12	19,29
RC4	0,86	RC1+RC2+RC3+RC4	1,25	0,53	11,88	6,69	63,71	15,95	55,17	76,13	75,25	11,73	1,86	24,28
RC5	0,55	RC1+RC2+RC3+RC4+RC5	1,05	0,45	10,00	6,22	67,72	14,55	55,70	78,16	75,75	13,06	2,36	26,48
RC6	0,38	RC1+RC2+RC3+RC4+RC5+RC6	0,95	0,41	9,00	5,92	70,05	13,67	55,90	79,10	75,91	13,82	2,72	27,71